



*International Student Workshop on Laser
Applications 2011*

Program and Abstracts

*May 31-June 4, 2011
Bran
Romania*

Welcome to “ISWLA’11”

It is a great pleasure to welcome you at the second edition of the workshop ISWLA '11 – International Student Workshop for Laser Applications, 2011 <http://iswla.inflpr.ro> organized by students, mainly for young researchers.

This edition is dedicated to the 10th anniversary since the IAP (Institute for Atomic Physics) SPIE Student Chapter was organized in Romania. This membership represented a challenge and an important opportunity for students to attend scientific events and enhance the experience by international contacts.

The organizing body consists of members of SPIE Romanian Student Chapter <http://spie.inflpr.ro/>. In this second edition of the conference we are glad to have guests from Armenia and Poland who attended, as well the previous edition and welcome the participation of students from Bulgaria, Germany and Greece.

The purpose of ISWLA '11 is to continue and valorise the experience of the first edition, to promote recent results obtained by the attendees, to enhance the knowledge in laser physics, material science and laser applications, mainly the new project supported by EU the pan - European ELI – Extreme Light Infrastructure, to be developed on Magurele Physics Platform. By promoting new interdisciplinary activities, by stimulating innovation, we hope to enhance the interest of young scientists to be better connected to the society needs and transfer the scientific knowledge in business.

The youth spirit, the innovation thinking will be promoted by bridging the research and business sector, research and industry, research and university, research and SMEs sector. The direct contacts with students from other chapters will favour to promote the best practices, the innovative thinking among young scientists – research capitalization .

Undergraduate students from Faculty of Physics, University of Bucharest and “Politehnica” University joint the SPIE Chapter, as well, a benefit for future career decisions, as thinking at the opportunity to participate in projects funded by the international bodies. In the last years, since 2004 the investment in research allowed to improve the endowment in the laboratories and using mobility to enhance the professional level of young scientists.

The organization of the conference was possible due to the moral and material support offered by SPIE and OSA Chapter Directorate for developing Chapter activities, to the support of the main research institutes from the Physics Platform Magurele: the National Institute for Laser, Plasma and Radiation Physics, National Institute for Nuclear Engineering, Faculty of Physics - University Bucharest and the National Authority for Scientific Research of the Ministry of Education and Research. We are grateful as well, for support to ARFO-Romanian Association for Photonics, SRF (Romanian Society for Physics) “Radiatia Trade Union” as well, to Appel Laser and European Physics Society. We would like to mention the support offered by the laboratories heads, which encouraged students to present the results of their research and surveyed the preparation of the manuscripts and presentations.

This is a pleasant duty to mention the hard work of Viorel Nastasa the leader of the organizing committee and former SPIE Romanian Chapter president, who coordinated the distribution of responsibilities among the members of the team: Mihai Boni , president of SPIE Romanian Chapter , Silviu Popescu, who organized the web site, Andra Militaru , Gabriela Salamu, Ana Maria Voiculescu and Radu Stancu, involved in all the steps of the organization.

As advisor of the student chapter it is an interesting work to share my experience, advise students but ask their opinion and try to find together the best solution, encourage them to overpass bottlenecks and note with high satisfaction their initiative spirit, the ability to manage and control situations, the large disposal to cooperate. I think that working in the organization of a conference is developing new dimensions of the personality by inter human relations and contacts with the administrative bodies. This means that this new experience of a scientist is useful to develop capabilities in the scientific career, as well.

Finally I hope that the attendees will enjoy this conference both for the opportunity to present their results and also for the social program and surprises of the organizers.

Welcome and enjoy this participation in a very special place of Romania – Bran – because of the marvelous landscape and also for the historical and cultural significance.

Dr. Clementina Timus
Conference Advisor



Table of contents

<i>Conference program</i>	5
<i>Location</i>	14
<i>Oral presentations</i>	15
<i>Posters</i>	63
<i>Participants list</i>	92

Organizing Committee:

Advisor: *Clementina Timus*

Coordinator: *Viorel Nastasa*

Organizing Chapters:

- *SPIE Institute for Atomic Physics Student Chapter*
- *INFLPR OSA Student Chapter – Romania*

Co-Organizing Chapters:

- *Munich Student Chapter - Germany*
- *Nicolaus Copernicus Univ. SPIE Chapter - Poland*
- *Gdansk Univ. of Technology SPIE Chapter - Poland*
- *Institute of Radiophysics and Electronics NASU - OSA Student Chapter - Ukraine*
- *Yerevan State Univ. SPIE Chapter- Armenia*
- *Taras Shevchenko National University of Kyiv student chapter of OSA – Ukraine*

Local Organizing Committee:

- *Cristina Achim*
- *Ionut Relu Andrei*
- *Mihai Boni*
- *Catalin Constantinescu*
- *Andra Militaru*
- *Iulian Pana*
- *Silviu Teodor Popescu*
- *Radu Stancu*
- *Ana Maria Voiculescu*
- *Gabriela Salamu*

Co-Organizing Centres :



Scientific Committee:

- *Prof. Dr. Jean-luc Doumont* - Founding partner Principiae/SPIE trainer
- *Dr. Eng. Ion Morjan* - NILPRP General Manager
- *Dr. Traian Dascalu* - NILPRP Vice -Director
- *Prof. Dr. Nicolae Zamfir* - IFIN-HH General Manager
- *Dr. Lucian Pintilie* - IFTM General Manager
- *Prof. Dr. Alexandru Jipa* - Dean Faculty of Physics Bucharest University
- *Prof. Dr. Stefan Antohe* - Vice Dean Faculty of Physics Bucharest University
- *Prof. Dr. Sabina Stefan* - Prof. Faculty of Physics Bucharest University
- *Dr. Viorica Stancalie* - NILPRP Head of Laser Department
- *Prof. Dr. Mihail Lucian Pascu* - NILPRP Laser Spectroscopy
- *Prof. Dr. Dan Dumitras* - NILPRP
- *Dr. Cristian Ruset* - Head of Plasma Surface Engineering Laboratory
- *Dr. Maria Dinescu* - NILPRP Photonic Processing of Advanced Materials
- *Dr. Serban Georgescu* - Head of ECS / NILPRP
- *Dr. George Nemes* - President ASTiGMAT™, Santa Clara, CA
- *Dr. Clementina Timus* - SPIE Student Advisor
- *Dr. Daniel Ursescu* - NILPRP
- *Dr. Mircea Udrea* - NILPRP/ General Manager of Apel Laser
- *Dr. Eng. Dan Sporea* - Head of CSET -Center for Science and Education/ Head of LMSL - NILPRP

Conference program

Monday May 30, 2011		
	16.00	Registration Desk Open
	19.30	Welcome Party

Tuesday May 31, 2011		
	08.00	Breakfast
	09.00	<i>Conference Opening</i> Dr. Ing. Ion Morjan Director of the National Institute for Laser, Plasma and Radiation Physics, Bucharest-Magurele, Romania
INVITED LECTURE	09.15	<i>"ELI Nuclear Physics"</i> Prof. Dr. Nicolae Zamfir Horia Hulubei National Institute of Physics and Nuclear Engineering - IFIN HH, Romanian Academy Bucharest-Magurele, Romania
INVITED LECTURE	10.00	<i>"Laser 50: From the First Laser to ELI - Unfolding History"</i> Prof. Dr. Dan C. Dumitras Laser Department, National Institute for Laser, Plasma and Radiation Physics, Bucharest-Magurele, Romania
	11.00	Coffee break
INVITED LECTURE	11.30	<i>"Matrix treatment of optical systems and laser beams: first-order design of laser optics"</i> Prof. Dr. George Nemes ASTiGMAT™, Santa Clara, CA 95050, USA
	12.15	<i>"Modern Laser Applications in Industry: innovation and efficiency"</i> V. Sava ^{1,2} , M. Udrea ^{1,3} ¹ Apel Laser S.R.L. Str. Fabricii, Nr 47, Corp Z et3 Bucharest, Romania ² Faculty of Physics, University of Bucharest, Romania ³ Laser Department, National Institute for Laser, Plasma and Radiation Physics, Bucharest-Magurele, Romania
	12.30	<i>"Optical emission by micro- and nano-droplets"</i> M. Boni, V. Nastasa, I.R. Andrei, G.V. Popescu, M.L. Pascu Laser Department, National Institute for Laser, Plasma and Radiation Physics, Bucharest-Magurele, Romania

	12.45	<p><i>“Stability properties of medicines solutions: spectral evidence and wire like formation”</i></p> <p>A. Militaru¹, A. Smarandache¹, L. Frunza², J.M. Pages³, M.L. Pascu¹</p> <p>¹Laser Department, National Institute for Laser, Plasma and Radiation Physics, Bucharest-Magurele, Romania</p> <p>²National Institute of Material Physics, Magurele, Romania</p> <p>³UMR-MD1, Faculté de Pharmacie, Université Méditerranée, IFR88, Marseille, France</p>
	13.00	Lunch
INVITED LECTURE	14.30	<p><i>“Photophysical studies on amino acids and proteins oxidation”</i></p> <p>A. Staicu¹, M. Enescu², A. Pascu¹, S. Foley², M. Boni¹, M.L. Pascu¹</p> <p>¹Laser Department, National Institute for Laser, Plasma and Radiation Physics, Bucharest-Magurele, Romania</p> <p>²Laboratoire de Chimie Physique et Rayonnement Alain Chabaudet UMR EA, Université de Franche-Comté, 16 Route de Gray, 25030, Besancon, France</p>
	15.00	<p><i>“IR Stimulated Raman-Spectroscopy for Advanced Gear-Oil Analysis”</i></p> <p>D. G. Dorigo, B. R. Wiesent, Ö. Şimşek, G. Pérez, C. Ana, A. W. Koch</p> <p>Institute for Measurement Systems and Sensor Technology, Technische Universität München, Theresienstr. 90 / N5, D-80333, Munich</p>
	15.15	<p><i>“Experimental control of the low-frequency fluctuations by current modulation in a semiconductor laser with optical feedback”</i></p> <p>I.R. Andrei¹, C.M. Ticos¹, M. Bulinski², M. L. Pascu¹</p> <p>¹Laser Department, National Institute for Laser, Plasma and Radiation Physics, Bucharest-Magurele, Romania</p> <p>²Faculty of Physics, University of Bucharest, Romania</p>
	15.30	<p><i>“Thermal and microstructural analysis of some hybrid metal-organic complex materials and thin films deposition by MAPLE”</i></p> <p>C. Constantinescu</p> <p>Laser Department, National Institute for Laser, Plasma and Radiation Physics, Bucharest-Magurele, Romania</p>

	15.45	<p><i>“Molecular modifications of chlorpromazine prepared as solution in micro-droplets form by exposure to laser radiation”</i></p> <p>V. Nastasa¹, A. Militaru¹, L. Amaral², M.L. Pascu¹</p> <p>¹Laser Department, National Institute for Laser, Plasma and Radiation Physics, Bucharest-Magurele, Romania</p> <p>² Unit of Mycobacteriology and 2UPMM, Instituto de Higiene e Medicina Tropical, Universidade Nova de Lisboa, Lisbon, Portugal</p>
	16.00	Coffee Break
INVITED LECTURE	16.30	<p><i>“The nanoparticles synthesis by laser pyrolysis”</i></p> <p>Catalin Luculescu</p> <p>Laser Department, National Institute for Laser, Plasma and Radiation Physics, Bucharest-Magurele, Romania</p>
	17.00	<p><i>“3D Micro-target Engineering for Laser-Matter Interaction Studies”</i></p> <p>F. Jipa, M. Zamfirescu, D. Ursescu, R. Dabu</p> <p>Laser Department, National Institute for Laser, Plasma and Radiation Physics, Bucharest-Magurele, Romania</p>
	17.15	<p><i>“Transient analysis of a V system with incoherent pumping and spontaneously generated coherence”</i></p> <p>O. Budriga</p> <p>Laser Department, National Institute for Laser, Plasma and Radiation Physics, Bucharest-Magurele, Romania</p>
	17.30	<p><i>“Reconfigurable soliton waveguides recorded with blue laser diodes for light guiding at telecom wavelengths”</i></p> <p>S.T. Popescu¹, A. Petris¹, V.I. Vlad¹, E. Fazio²</p> <p>¹Laser Department, National Institute for Laser, Plasma and Radiation Physics, Bucharest-Magurele, Romania</p> <p>²University “La Sapienza” of Rome, Italy</p>
	17.45	<p><i>“Formation of 3D gratings by interferometric-mask method in LiNbO3:Fe crystals”</i></p> <p>A. Badalyan, R. Hovsepyan, V. Mekhitarian, P. Mantashyan, R. Drampyan</p> <p>Institute for Physical Research, National Academy of Sciences of Armenia, 0203, Ashtarak-2, Armenia</p>
	18.00	<p><i>“Computer controlled laser”</i></p> <p>C. Chitu^{1,2}, R. Constantin Inpuscatu¹, A. Vintila¹</p> <p>¹Energetic High School, Grivitei Street, No. 1, 105600, Campina, Romania</p> <p>²University of Bucharest, Faculty of Physics, Atomistilor Street, Magurele, Romania</p>
	18.15	Free time
	19.00	Dinner
	20.30	BONE FIRE(folk music and boiled wine) KARAOKE

Wednesday June 1 st , 2011		
	08.00	Breakfast
INVITED LECTURE	09.00	<p><i>"Modification of molecular structures in liquid phase by interaction with laser beams"</i></p> <p>Prof. Dr. Mihai Lucian Pascu Laser Department, National Institute for Laser, Plasma and Radiation Physics, Bucharest-Magurele, Romania</p>
	09.45	<p><i>"Imaging C. Elegans embryogenesis by Third Harmonic Generation microscopy"</i></p> <p>G. J. Tserevelakis, G. Filippidis, E. M. Megalou, A. J. Krmpot, M. Vlachos, C. Fotakis, N. Tavernarakis ¹Foundation for Research and Technology - Hellas, Institute of Electronic Structure and Laser, N. Plastira 100, P.O. Box 1385, 71110 Heraklion, Greece ²Physics Department, University of Crete, P.O. Box 2208, 71409 Heraklion, Greece</p>
	10.00	<p><i>"Dynamic and static measurements of oxygenation and blood volume by Diffuse Optical Tomography (DOT)"</i></p> <p>M. Patachia^{1,2}, D.C.A. Dutu¹, S. Banita¹, R. Cernat¹, D.C. Dumitras¹ ¹Laser Department, National Institute for Laser, Plasma and Radiation Physics, Bucharest-Magurele, Romania ²Faculty of Physics, University of Bucharest, Romania</p>
	10.15	<p><i>"The effect of substrate roughness and chemistry on the cellular response"</i></p> <p>Ch. Simitzi, M. Barberoglou, A. Ranella, C. Fotakis, I. Athanassakis, E. Stratakis ¹Foundation for Research and Technology - Hellas, Institute of Electronic Structure and Laser, N. Plastira 100, P.O. Box 1385, 71110 Heraklion, Greece ²Physics Department, University of Crete, P.O. Box 2208, 71409 Heraklion, Greece</p>
	10.30	<p><i>"Laser ablation in the ENT surgery"</i></p> <p>M. Petrus¹, D.C. Dumitras¹, C. Sarafoleanu², C. Manea², C. Iosif², E.M. Carstea³, D.C.A. Dutu¹ ¹Laser Department, National Institute for Laser, Plasma and Radiation Physics, Bucharest-Magurele, Romania ²St. Maria Hospital, Bucharest, Romania ³National Institute of R&D Optoelectronics INOE 2000</p>
	10.45	<p><i>"Analysis of ethylene and ammonia as biomarkers for</i></p>

		<p><i>patients with renal failure</i></p> <p>C. Popa^{1,2}, A.M. Bratu¹, D.C.A. Dutu¹, C. Matei, S. Banita¹, and D.C. Dumitras¹</p> <p>¹Laser Department, National Institute for Laser, Plasma and Radiation Physics, Bucharest-Magurele, Romania</p> <p>²Faculty of Physics, University of Bucharest, Romania</p>
	11.00	Coffee break
INVITED LECTURE	11.30	<p><i>“From scientific research to industrial production – a few examples in surface engineering”</i></p> <p>C. Ruset¹, E. Grigore¹, I. Munteanu¹, N. Budica¹, I. Cernica¹, H. Maier², R. Neu², G. Matthews³, D. Heinen⁴, S. Bausch⁴, V. Zoita^{1,5}</p> <p>¹Laser Department, National Institute for Laser, Plasma and Radiation Physics, Bucharest-Magurele, Romania</p> <p>²Max-Planck Institut für Plasmaphysik, Euratom Association, 85748 Garching, Germany</p> <p>³Culham Centre for Fusion Energy, Euratom Association, Abingdon, UK</p> <p>⁴Fraunhofer Institute for Production Technology, 52074 Aachen, Germany</p>
	12.15	<p><i>“Enhanced carrier trapping efficiency in ZnO/Si micro-cones”</i></p> <p>E. Magoulakis^{1,2}, E. L. Papadopoulou¹, E. Stratakis¹, C. Fotakis^{1,2}, P. A. Loukakos¹</p> <p>¹Foundation for Research and Technology - Hellas, Institute of Electronic Structure and Laser, N. Plastira 100, P.O. Box 1385, 71110 Heraklion, Greece</p> <p>²Physics department, University of Crete, P.O. Box 2208, 71409 Heraklion, Greece</p>
	12.30	<p><i>“Functional Protein Microarrays: toward a system view of the plant cell”</i></p> <p>G. Popescu¹, S. Popescu²</p> <p>¹Laser Department, National Institute for Laser, Plasma and Radiation Physics, Bucharest-Magurele, Romania</p> <p>²Boyce Thompson Institute for Plant Research, One Tower Road, Ithaca 14853, NY, USA</p>
	12.45	<p><i>“Studies of the spectral properties of Phenothiazines”</i></p> <p>A. Smarandache¹, A. Militaru¹, V. Nastasa¹, J. Kristiansen² and M.L. Pascu¹</p> <p>¹ Laser Department, National Institute for Laser, Plasma and Radiation Physics, Bucharest-Magurele, Romania</p> <p>²Department of Clinical Microbiology, Sønderborg Sygehus, County of Sønderjylland, 6400-DK, Denmark</p>
	13.00	Lunch

	14.30	<p><i>“Beyond structural imaging – cornea examination using combined air-puff tonometry and OCT system with swept source laser”</i></p> <p>K. Karnowski¹, D.A. Caneiro¹, B. Kaluzny², M. Szkulmowski¹, A. Kowalczyk¹, M. Wojtkowski¹</p> <p>¹Institute of Physics, Nicolaus Copernicus University, ul. Grudziadzka 5, PL-87 100 Torun, Poland</p> <p>²Dept of Ophthalmology, Collegium Medicum UMK, Bydgoszcz, Poland</p>
	14.45	<p><i>“Broadband blue light in OCT”</i></p> <p>S. Kolenderska¹, M. Wojtkowski¹</p> <p>¹Department of Physics, Nicolaus Copernicus University, Torun, 87-100, Torun, Poland</p>
	15.00	<p><i>“Removal of Interfering Gases in LPAS Breath Biomarker Concentration Measurements”</i></p> <p>A.M. Bratu, C. Popa, C. Matei, S. Banita, D.C. Dumitras</p> <p>Laser Department, National Institute for Laser, Plasma and Radiation Physics, Bucharest-Magurele, Romania</p>
	15.15	<p><i>“Principles and methods of imaging in biomedicine”</i></p> <p>C. Matei</p> <p>Laser Department, National Institute for Laser, Plasma and Radiation Physics, Bucharest-Magurele, Romania</p>
	15.30	<p><i>“Ethylene concentration measurement at fruits using LPAS”</i></p> <p>S. Banita^{1,2}, D.C.A. Dutu¹, C. Matei¹, A.M. Bratu¹, M. Petrus¹, C. Achim¹, M. Patachia¹, D.C. Dumitras¹</p> <p>¹Laser Department, National Institute for Laser, Plasma and Radiation Physics, Bucharest-Magurele, Romania</p> <p>²Faculty of Applied Sciences, University Politehnica Bucharest, Romania</p>
	15.45	<p><i>“Research concerning the interaction between pulsed laser radiation and urological stones”</i></p> <p>R.F. Stancu, D. Dvornikov, B. Comanescu, M. Serbanescu</p> <p>Optoelectronica-2001 SA, 077125 Magurele, Ilfov, Romania</p>
	16.00	Coffee Break
	16.30	POSTER SESSION
	18.00	Free time
	19.00	Dinner
	20.30	FOLK MUSIC RECITAL

Thursday June 2 nd , 2011		
	08.00	Breakfast
	09.00	<p><i>“Method for measuring the effective pulse duration of nanosecond laser pulses”</i> L. Neagu¹, L. Rusen¹, A. Zorilă¹, A. Stratan¹, G. Nemeş^{1,2} ¹Laser Department, National Institute for Laser, Plasma and Radiation Physics, Bucharest-Magurele, Romania ²ASTiGMATTM, Santa Clara, CA 95050, USA</p>
	09.15	<p><i>“Experimental study of femtosecond laser-induced periodic surface structures on metals”</i> C. Radu¹, A. Dinescu², M. Zamfirescu^{1,2} ¹Laser Department, National Institute for Laser, Plasma and Radiation Physics, Bucharest-Magurele, Romania ²National Institute for Research and Development in Microtechnology, Str. Erou Iancu Nicolae 126A, 077190 Bucharest, Romania</p>
	9.30	<p><i>“Effective area measurement of real laser beams”</i> L. Rusen¹, A. Zorila¹, L. Neagu¹, A. Stratan¹, G. Nemes^{1,2} ¹Laser Department, National Institute for Laser, Plasma and Radiation Physics, Bucharest-Magurele, Romania ²ASTiGMATTM, Santa Clara, CA 95050, USA</p>
	9.45	<p><i>“Development of a high power transverse diode pumped Nd:YAG rod module”</i> B. Oreshkov, A. Gaydardzhiev, I. Buchvarov, A. Trifonov Department of Physics, Sofia University, 5 James Bourchier Blvd., BG-1164 Sofia, Bulgaria</p>
	10.00	<p><i>“$\chi^{(2)}$-Lens Mode-Locking of Diode-Pumped Nd-doped Vanadate Lasers”</i> V. Aleksandrov, H. Iliev and I. Buchvarov Department of Physics, University of Sofia, 5 James Bourchier Boulevard, BG-1164 Sofia, Bulgaria</p>
INVITED LECTURE	10.15	<p><i>“Professional Associations : benefits and responsibilities”</i> Dr. Clementina Timus Laser Department, National Institute for Laser, Plasma and Radiation Physics, Bucharest-Magurele, Romania</p>
	11.00	Coffee break
INVITED LECTURE	11.30	<p><i>“THz wave photonics and applications to biology and chemistry”</i> Prof. Dr. Traian Dascalu National Institute for Laser, Plasma and Radiation Physics, Bucharest-Magurele, Romania</p>
	12.15	<i>“Study of laser ignition and flame kernel development</i>

		<p><i>in methane-air mixture</i></p> <p>G. Salamu¹, O. Sandu¹, M. Dejanu², F. Voicu¹, C. Ticos³, D. Popa², S. Parlac², N. Pavel¹, T. Dascalu¹</p> <p>¹Laboratory of Solid-State Quantum Electronics, National Institute for Laser, Plasma and Radiation Physics, Bucharest-Magurele, Romania</p> <p>²Faculty of Mechanics and Technology, University of Pitesti, Targu din Vale Street, 110040, Pitesti, Romania</p> <p>³Low Temperature Plasma Laboratory, National Institute for Lasers, Plasma and Radiation Physics, Magurele, P.O. Box MG-36, 077125, Bucharest, Romania</p>
	12.30	<p><i>“Sub-nanosecond, tunable between 3 μm and 3.5 μm OPO based on PPSLT, pumped by 0.5 kHz Nd:YAG laser”</i></p> <p>D. Chuchumishev¹, I. Buchvarov¹, A. Gaydardzhiev¹, A. Trifonov¹, O. Sandu², G. Salamu²</p> <p>¹Department of Physics, Sofia University, 5 James Bourchier Blvd., BG-1164, Sofia, Bulgaria</p> <p>²National Institute for Laser, Plasma and Radiation Physics, Bucharest-Magurele, Romania</p>
	12.45	<p><i>“Finite-Difference Time-Domain Method (FDTD) used to Simulate Micro-ring Resonator for Student Applications”</i></p> <p>A. Fazacas¹, P. Sterian,²</p> <p>¹M.Sc. at University Politehnica, Bucharest, 060811, Bucharest, Romania</p> <p>²Prof. at Department Physics II, University Politehnica, Bucharest, 060811, Bucharest, Romania</p>
	13.00	Lunch
	14.00	Trip
	19.00	Dinner
	20.30	LIVE DISCO RECITAL

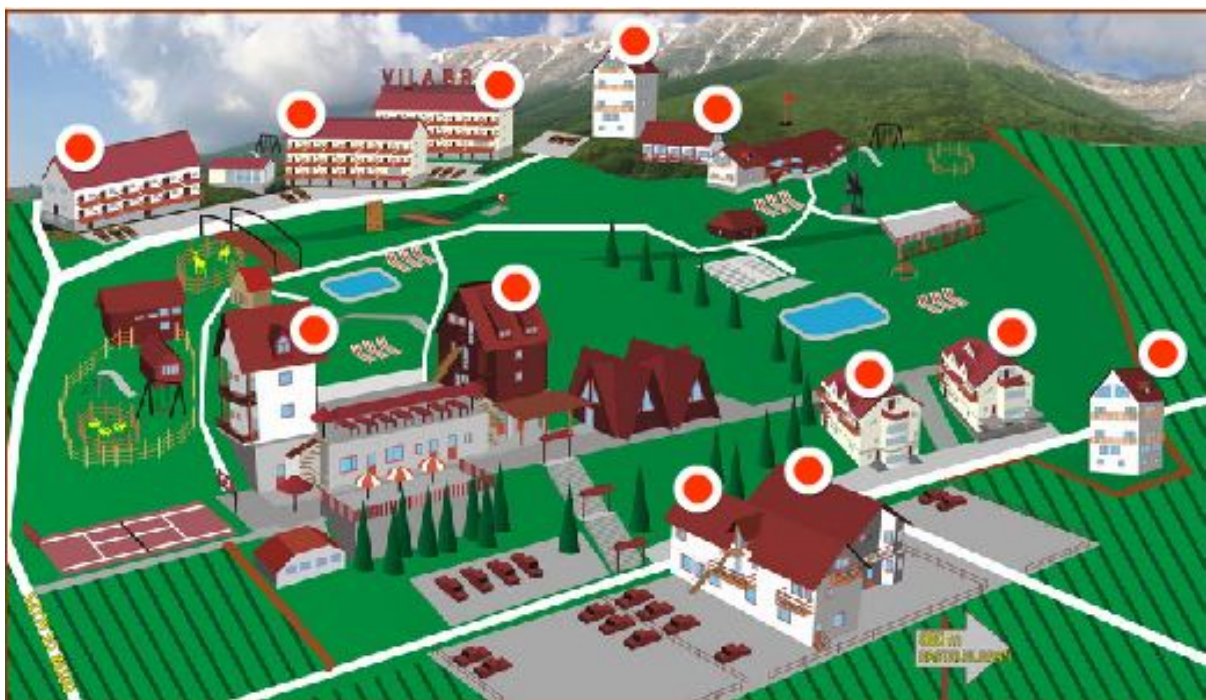
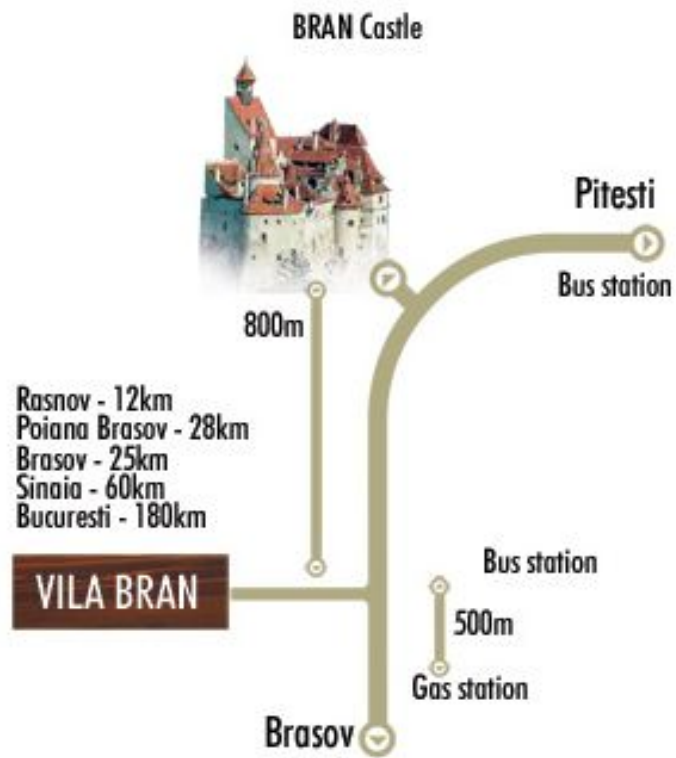
Friday June 3 rd , 2011		
	08.00	Breakfast
INVITED LECTURE	09.00	<p><i>“Structuring a scientific paper”</i> Prof. Dr. Jean-luc Doumond</p> <p>Principiae, Kapellelaan 103 1950 Kraainem, Belgium</p>
	11.00	Coffee break
INVITED LECTURE	11.30	<p><i>“Structuring a scientific paper”</i> Prof. Dr. Jean-luc Doumond</p> <p>Principiae, Kapellelaan 103 1950 Kraainem, Belgium</p>
	13.00	Lunch

INVITED LECTURE	14.30	<i>“Progress at the Multi-PW ELI-NP laser facility in Romania”</i> Dr. Daniel Ursescu Laser Department National Institute for Lasers, Plasma and Radiation Physics, Magurele, P.O. Box MG-36, 077125, Bucharest, Romania
	15.00	<i>“Online damage detection using scattered radiation of the test beam”</i> A. Zorilă, S. Sandel, L. Rusen, L. Neagu, C. Fenic, A. Stratan Laser Department, National Institute for Laser, Plasma and Radiation Physics, Bucharest-Magurele, Romania
	15.15	<i>“Toward control of spatio-temporal couplings in ultra-short laser pulses”</i> R. Ungureanu ^{1,2} , D. Ursescu ¹ ¹ Laser Department, National Institute for Laser, Plasma and Radiation Physics, Bucharest-Magurele, Romania ² Faculty of Physics, University of Bucharest, Romania
	15.30	<i>Multiple pulses experiments at 15 TW TEWALAS laser facility</i> O. Manta ^{1,2} , R. Ungureanu ^{1,2} , R. Banici ^{1,2} , L. Neagu ¹ , D. Ursescu ¹ ¹ Laser Department, National Institute for Laser, Plasma and Radiation Physics, Bucharest-Magurele, Romania ² Faculty of Physics, University of Bucharest, Romania
	16.30	Group Activities
	19.00	Dinner
	20.00	ROMANIAN TRADITIONAL DANCES - RETRO LIVE MUSIC RECITAL

Saturday June 4 th , 2011		
	08.00	Breakfast
	09.00	Poster and Oral Presentation Awards
	11.00	Conference Closing

Location

Registration, lectures, coffee breaks, poster session will be held at Club Vila Bran, 9th Alunis Street, Bran, Brasov, Romania.



Oral presentations

Laser 50: From the First Laser to ELI – Unfolding History

Dan C. Dumitras

Department of Lasers, National Institute for Laser, Plasma and Radiation Physics,
Bucharest, Romania (e-mail: dan.dumitras@inflpr.ro)

Last year we celebrated 50 years of laser history. If fifty years ago people thought that the laser is “a solution looking for a problem”, today lasers have gone on to be one of the outstanding success stories in physics.

The development of lasers was possible owing to the general progress in physics and particularly in optics and quantum electronics, with the contributions of Fabry-Pérot (1899), Einstein (1916), Ladenburg (1928), Fabrikant (1939), Lamb (1947), Kastler (1950), Purcell (1951), Weber (1953), and many others. But, the first device based on the principles developed by Einstein was built in December 1953 by Townes – the ammonia MASER. Other maser types were described theoretically by Basov and Prokhorov (1954) and Bloembergen (1956), and subsequently operated in different laboratories (1957 - 1960). Scientists were looking for a maser at optical frequencies since 1957, and the race to build a LASER was won by Maiman on May 16th, 1960.

Since then, many laser pioneers have contributed to the discovery of new lasers and laser operating regimes. These steps will be presented chronologically, emphasizing the role of many brilliant scientists (1960 - 2011). Detailed information will be given on first commercial lasers and on Nobel Prizes for laser related discoveries.

The second part of the talk will focus on Romanian contributions in the field (1960 - 1975). Romania is believed to be the fourth country in the world that succeeded to operate a laser (October 20th, 1962). Many details will be presented regarding the scientific and technologic contributions of Romanian scientists in the first two decades of laser history (published papers, communications at conferences, books, PhD Thesis, patents). An important role for our community have played the international conferences organized by our institute (1982 - 2011), that offered the possibility to present our results at international level and to meet researchers from many other countries.

2010 was a yearlong celebration of the 50th anniversary of the laser. Many conferences had special sessions dedicated to this event. The author have participated in several of them (CLEO/QELS, San Jose, May; Laser in the City of Light, Paris, June; LPHYS, Foz do Iguacu, July; ALT, Egmont aan Zee, September) and the presentation will be accompanied by numerous pictures from those celebrations.

In 2009 Romania was chosen as a site of the ambitious European project Extreme Light Infrastructure (ELI) as a result of our efforts and contributions to ELI – Preparatory Phase (FP 7 Program, 2007-2010). The mission of ELI – NP (Nuclear Physics) pillar, the laser architecture, the experiments envisaged, and the structure of the future infrastructure will be mentioned.

The last question approached is: do masers and lasers exist in nature? The answer is affirmative.

Matrix treatment of optical systems and laser beams: first-order design of laser optics

George Nemeş

ASTiGMAT™, Santa Clara, CA 95050, USA, <http://astigmat-us.com>; gnemes@astigmat-us.com

Keywords: ray transfer matrix, symplecticity, beam matrix, beam transformation, beam characterization, beam propagation ratio, beam intrinsic astigmatism, beam-limited spot size, lens-limited spot size, lens spherical aberration, diffraction-limited lens.

The lecture is intended to give the essentials of treating the optical systems and the laser beams transformed by (propagating through) them to first order. Its aim is to be tutorial and also inspiring.

Historically, two main approaches are used in optical design. The first one is centuries old and was developed within the context of imaging optics (geodetic instruments, binoculars, microscopes, projection systems, astronomic telescopes, and the like), and using broadband (low temporal coherence) and low spatial coherence light sources (white light). It is based on geometrical optics, wave optics, and also on the aberration theory to push the imaging capabilities of optical systems to their limits. The second approach appeared after the emergence of lasers (1960) and deals with optical systems for beam conditioning (focusing, collimating, beam matching to a target, beam transforming, measuring the beam spatial properties) and not necessarily imaging optics. This latter approach uses mostly quasi-monochromatic light with good spatial coherence properties (laser light). It also developed the beam concept as a physical system in itself, independent of, and using both the geometrical optics and the wave optics approach, and something more. Laser beam optics has, in general, different goals than imaging optics, even though these goals can be demanding. However, many times, a first-order approach suffices to describe the optical systems and the spatial properties of the beams transformed by them. Finer treatments include the aberrations of optical systems (from imaging optics), especially the spherical aberration. Unfortunately, the two subfields of optics (imaging optics and laser beam optics) are not taught on equal footing, and it is not uncommon that concepts from one subfield are not well understood, or are wrongly applied to the other subfield. A classical example is the wrong understanding of the "image" within the optics of gaussian beams: one wrongly speaks about the waist of a beam after a certain optic representing the "image" of the waist of the beam before that optic.

The lecture aims to give a clear understanding of the optical systems, of the spatial properties of laser beams and their change made by the optical systems, and some design considerations for laser optics. It has three parts.

The first part develops the matrix theory to describe idealized (linear, thin, centered, aberration-free) optical systems [1]. Real, 2x2 matrices with unit determinant describe optical systems made by spherical lenses/mirrors, or by cylindrical lenses/mirrors with their axes orthogonally positioned, and free spaces. Real, symplectic 4x4 matrices allows one to describe also non-orthogonally positioned cylindrical lenses/mirrors. The analysis and the synthesis of such systems is described.

The second part develops the 2x2 and 4x4 matrix theory to describe laser beams [1,2]. The idealized gaussian beam (IGB) is the simplest one, used as a reference beam, and from it, the real laser beam can be described using the same approach (named the correlation matrix approach, or the second-order moments approach). Each beam has a 2x2 or a 4x4 beam matrix associated to it, describing all spatial beam properties. The beam transformation by (propagation through) symplectic optical systems preserves two intrinsic beam invariants, named, in the simplest case "beam propagation ratios", M^2 , (for stigmatic beams) M_x^2 , M_y^2 (for aligned simple astigmatic beams), and "effective beam propagation ratio" M_{eff}^4 and "intrinsic astigmatism", a , for general astigmatic beams. Elements of beam transformation and beam measurements are discussed.

The third part discusses, as an example, the issue of focusing laser beams to a smallest spot [3]. It shows that there are two independent limiting factors to get the smallest spot size, the beam itself through its M^2 parameter (beam-limited spot size), and the spherical aberration of the singlet focusing lens (lens-limited spot size). Methods to assess which one is the predominant limiting factor, and the revision of the "diffraction-limited lens" are discussed.

References:

- [1] G. Nemes, *Optics Fundamentals*, Graduate Course, Santa Clara University, CA, USA (2006-2008), Polytechnic University of Bucharest (2010), and Laser Department, NILPRP, Bucharest (2010).
- [2] G. Nemes, *Laser Beam Characterization*, ASTiGMAT™ Technical Text TT_032105, Santa Clara, CA, USA, 2005.
- [3] G. Nemes, "Merit factors to assess the causes limiting the smallest size of a focused spot: beam-limited, lens-limited, or both?", ASTiGMAT™

Modern Laser Applications in Industry: innovation and efficiency

Vasile Sava, Mircea Udrea

Apel Laser SRL

Lasers become more and more a common industrial tool. The applications of lasers in industry cover very different fields: material macro-processing, microprocessing in the electronic industry, fabrication of photovoltaics cells or MEMS, etc.

A critical problem is to determine if the laser is the most suitable tool for a specific application from an economical point of view or it is only a luxury tool. There are many applications which are not feasible otherwise but using lasers. In these cases the problem is only the opportunity

of the task. Also, there are other applications where the water jet or plasma cutting, for example, are very competitive.

We'll present our experience in the field of laser applications in industry and we explain in each case what was the proper choice. We mention high power 9 kW laser for metal cutting and welding till short UV laser pulses.

A presentation of different industrial lasers from the old CO₂ laser till the most powerful fiber lasers is performed.

Optical emission by micro- and nano-droplets

Mihai Boni, Viorel Nastasa, Ionut Relu Andrei, George Viorel Popescu, Mihai Lucian Pascu

Laser Department, National Institute for Laser, Plasma and Radiation Physics, Bucharest-Magurele, Romania

Keywords: microdroplets, Nd:YAG laser, laser dyes, optical emission, lasing.

In this paper we present lasing effect in pendant droplets having different volumes. The droplets were seeded with an organic dye (Rhodamine 6G – R6G) in ultrapure water at different concentrations and irradiated by pulsed laser beam emitted at 532 nm by a SHG Nd:YAG laser, (pulse time width 6ns, laser pulses repetition rate 10 pps, energy per pulse 330 kW/pulse). [1]

The droplets were generated using a computer controlled system Hamilton Microlab 500. The liquid volumes pumped were typically 12.5 μ l. This produced droplets with diameter of 3mm.

To observe the lasing emission we measured the laser induced fluorescence emitted by the droplets when excited at 532 nm (Fig.1). The fluorescence signal is collected by an optical fiber (1mm core), and analyzed with HR4000 Ocean Optics spectrometer (0.65mm resolution, 200-1100nm).

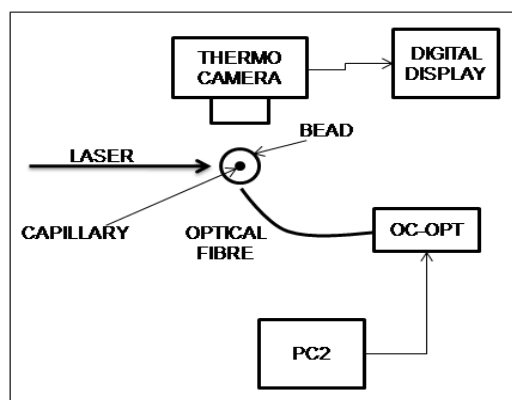


Figure 1. Experimental set-up

We observed that the effect depends on several parameters, such as: the concentration of the Rh 6G in water; the droplet's volume; the interaction angle of the pumping laser beam with the droplet's surface.

By varying the concentration of the R6G in water we obtained the typical fluorescence broad band and a narrow peak assigned to the lasing effect. The best results obtained on the measured samples were at the R6G 10^{-3} M concentration in ultra pure water. In Fig.2 is shown the typical spectrum of the LIF signal emitted by the droplet when pumped at 532 nm with a pulsed beam having the energy 0.330 mJ.

The data acquisition was such that for each spectrum an average of the LIF signal integrated on 1 minute.

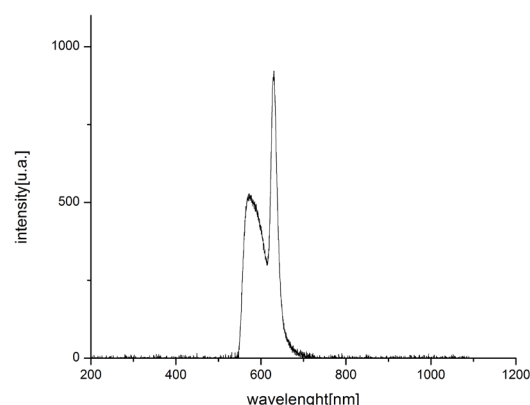


Figure 2. The emission spectrum of a droplet ($R=1.5$ mm) containing R6G at 10^{-3} M in ultrapure water.

In order to study how the volume changes by evaporation of the droplets during irradiation, we measured the temperature variations of the pendant droplets following their resonant interaction with laser radiation emitted at 532nm.[2] The droplet temperature was measured with the thermo-camera ThermoCAM® E45. Depending of the droplet dye concentration and irradiation time, the increase of the temperature was maximum 3° C.

Acknowledgements

The authors from NILPRP acknowledge the financing of the research by Rom. ANCS project 41-018/2007 and Program LAPLAS 3, PN 09 39/2009.

References

1. *J. Opt. Am. B*/Vol. 16, No.8/August 1999, Chemical lasing in pendant droplets; lasing-spectra, emission-pattern and cavity-lifetime measurements, Seongsik Chang, Nathan B. Rex, and Richard K. Chang
2. *M. Sc. Thesis*, Hatim Azzouz, Liquid Droplet Dye Laser.

Stability properties of medicines solutions: spectral evidence and wire-like formations

Andra Militaru¹, Adriana Smarandache¹, Ligia Frunza², Jean-Marie Pagès³ and Mihail-Lucian Pascu¹

¹National Institute for Laser, Plasma and Radiation Physics, 077125, Magurele, Romania

²National Institute of Material Physics, 077125, Magurele, Romania

³UMR-MD1, Faculté de Pharmacie, Université Méditerranée, IFR88, Marseille, France

Keywords: phenothiazines, quinazoline derivatives, medicines stability, laser irradiation, spectroscopy.

The knowledge of the stability properties of medicines are particularly needed in view of their use as solutions in different solvents; from the user's point of view it is important to know the temperature and time constraints which must be considered during the storage of the medicine solutions and their use on bacteria, cell cultures and other targets.

For the stability studies two types of medicines were considered: phenothiazines and quinazoline derivatives.

The stability of phenothiazines was studied from two points of view: time stability and interaction with laser beams.

Results on Chlorpromazine, which is a compound in the phenothiazines class, are first reported in this paper. Solutions were prepared in ultrapure de-ionized water at three concentrations: 20 mg/ml (approximately $5 \times 10^{-2} \text{M}$), 10^{-3}M and 10^{-4}M .

Time stability of the solutions was studied by comparing the absorption spectra recorded daily; the solutions remained stable, in the limits of measurements errors, for the whole period of the study. The solutions were kept in dark, at 4°C , between measurements. Further, phenothiazines solutions in ultrapure water were irradiated to study the interaction with laser beams.

The laser beam was emitted by second, third and fourth harmonic generation at, respectively, 532 nm, 355 nm, 266 nm starting from Nd:YAG laser beam emitted at $1.064 \mu\text{m}$. The pulse repetition rate was 10 pps and the average beam energy was varied between 0.2 and 30 mJ. A second laser was used, as well, namely a pulsed nitrogen laser (PNL) that emits at 337.1nm, 1 ns pulse full time width, at a repetition rate of 10 pps and an average beam energy of 0.5mJ. The exposure time of the samples to each of the two laser beams varied between 2 minutes and 4 hours.

Modifications of phenothiazines after irradiation were recorded measuring UV-Vis absorption spectra.

The stability of the quinazoline derivatives solutions was studied considering the factors: time, temperature, solvent and the interactions with laser beams.

BG1188, a quinazoline derivative designed and prepared at UMR-MD1 (Marseille, France), was studied; solutions were prepared in ultrapure de-

ionized water, dimethyl sulfoxide (DMSO) and distilled water.

Absorption spectra recorded along 4 months evidenced that BG1188 solutions in ultrapure water remained stable, in the limits of measuring errors.

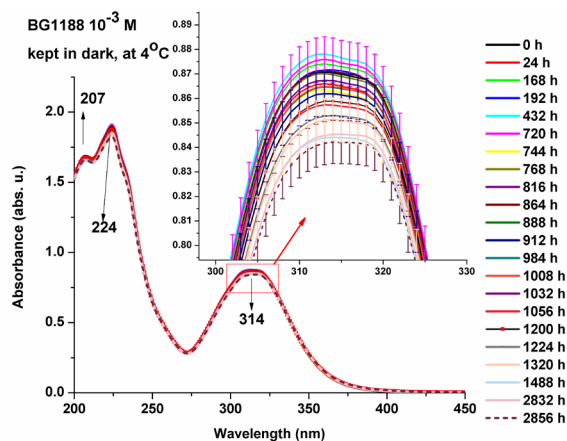


Figure 1. Absorption spectra revealing time evolution of BG1188 at 10^{-3}M in ultrapure water solution.

On the other hand, BG1188 solutions in DMSO may be considered unstable because the absorption spectra are changed in terms of peak shapes and intensities, indicating that the samples exhibit modifications immediately after preparation.

The differences of the stability of the BG1188 solutions in ultrapure water at 4°C and 22°C storage temperatures were not significant.

The experimental conditions for studying the quinazoline derivatives interaction with laser beams were the same as in the case of phenothiazines.

An interesting process which takes place after BG1188 solution preparation in all solvents is the appearance of wire-like precipitates containing BG1188 molecules in solutions kept longer time intervals. It seems that the processes leading to the aggregates formation start immediately after the preparation of the solutions. These wire-like aggregates were studied using FTIR spectroscopy and images of the studied aggregates were obtained using the Spotlight 400 FTIR imaging system.

Acknowledgements:

The authors from NILPRP acknowledge the financing of the research by Rom. ANCS project 41-018/2007 and Program LAPLAS 3, PN 09 39/2009.

Photophysical studies on amino acids and proteins oxidation

Staicu, Angela¹, Enescu, Mironel², Pascu, Alexandru¹, Foley Sarah², Boni, Mihai¹, Pascu, Mihail Lucian¹

¹Laser Department, National Institute for Lasers, Plasma and Radiation Physics,
Atomistilor 409, 077125 Magurele, Bucharest, Romania

²Laboratoire de Chimie Physique et Rayonnement Alain Chabaudet UMR EA, Université de Franche-Comté,
16 Route de Gray, 25030, Besancon, France

Keywords: amino acids, proteins, singlet oxygen, photo-oxidation

Thiol groups (SH) are known to be the most reactive sites of proteins. The oxidation of thiols leading to formation of di-sulphide bridges S-S, is a key in regulating cellular oxidation-reduction processes and it is at the same time at the origin of the stabilization of tertiary structures of many proteins.

Thiols oxidation involves exploring the generation of oxidative species, especially singlet oxygen, and the identification of the final compounds needs the analysis of these compounds. In this respect, studies on the kinetics of oxygen generation and its interaction with biological molecules containing thiol constituents and the products analysis by Raman spectroscopy were performed.

As biological molecules of interest were chosen the protein constituent amino acids (cysteine, tryptophan, tyrosine) which play a role in the thiols photo-oxidation, some proteins (as serum albumins) which may give information about the conformational effect of oxidation, and enzymes (like the lysozyme). As photosensitizers, methylene blue (MB) and phthalocyanine compounds were used.

In an experimental study regarding the thiols photo-oxidation by oxygen singlet, the constant of the oxygen singlet quenching produced by the cysteine was determined. The photo-oxidation of cysteine to cistine by UV irradiation in the presence of (the photosensitizer) Zn-phthalocyanine, was emphasized using Raman spectroscopy.

The intrinsic generation of oxygen singlet by the biological molecules as the aminoacids (tryptophan, tyrosine) and the proteins (human seric albumin, bovine seric albumin) was measured via the phosphorescence emission of oxygen at 1 270nm.

Studies of the photo-oxidation produced by the singlet oxygen generated by the laser excited methylene blue on the biological compounds: BSA, lysozyme, and aminoacids (tryptophan, tyrosine), were performed. The oxygen singlet quenching constants by these compounds in heavy water solutions at different pD were determined. These parameters are important in establishing the protein conformational structure and the exposure level of the aminoacids present in proteins to the harmful UV radiation.

The measurement of singlet oxygen phosphorescence decay allows the calculation of the

singlet state oxygen lifetime (Figure 1, in case of the MB - BSA pair in solution with pD = 7.4), while the Stern-Volmer representation -the inverse of the singlet oxygen lifetime versus the quencher concentration (BSA) - allows the calculation of the quenching constant ($4.8 \times 10^8 \text{s}^{-1}$). The values of the singlet oxygen quenching constant decrease with decreasing the solution pD, indicating less photo-oxidation of the aminoacid residues in case of the unfolded protein.

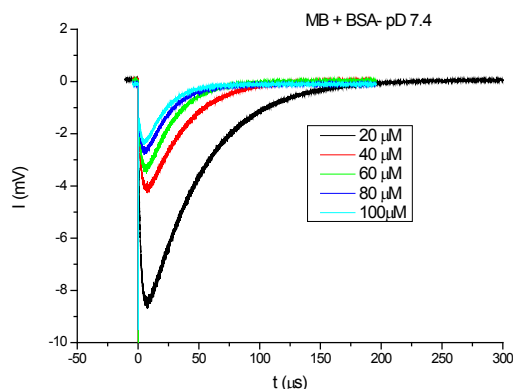


Figure 1. The phosphorescence decay curves for methylene blue and BSA at different concentrations

Acknowledgement: This work was supported by ANCS through the Brancusi French-Romanian bilateral program (ctr. no. 207/2009) and by CNMP (ctr. no. 61-023/2007)

References:

David, C., Foley, S., Mavon, C., Enescu, M., "Reductive unfolding of serum albumins uncovered by Raman Spectroscopy", *Biopolymers* (2008), 89, 623-634.

Pascu, R. A., Trifu, M., Dumitrescu, M., Mahamoud, A. Staicu, A., Dicu, M., Smarandache, A., Carstocea, B., Pascu, M. L., In vivo studies of the effects of alkyl substituted Benzo[b]pyridinium compounds exposed to optical radiation, *AIP Conf. Proc.* (2009) 1142, 8-14.

IR Stimulated Raman-Spectroscopy for Advanced Gear-Oil Analysis

Dorigo, Daniel G.¹, Wiesent, Benjamin R.¹, Şimşek, Özlem¹, Pérez Grassi, Ana C.¹, and Koch, Alexander W.¹

¹Institute for Measurement Systems and Sensor Technology, Technische Universität München, Theresienstr. 90 / N5, D-80333, Munich

Keywords: Oil Analysis, Raman, IR, Spectroscopy.

Raman-Spectroscopy is known as a well-established non-destructive technique for substance analysis on molecular level in chemistry. By Raman-effect, the scattered light of a laser beam focussed on the sample under test shows a frequency shift with respect to the excitation light source. This is caused by the interaction of the laser beam with the molecules of the analyzed sample. The frequency shift can be either positive or negative, depending on the energy level of the molecules after excitation (Long 2002).

Important oil parameters can be deduced from different kinds of spectra, like Mid-IR and Near-IR ones, using multivariate data analysis (Kessler 2006). These parameters provide valuable information about the quality and the properties of the oil under test and its additive depletion state. One of the most important parameters is the Total Acid Number (TAN), a measure of the acidity of the analyzed sample (Pirro, Wessol, and Wills 2001). The TAN can be considered as a proxy variable for oil "age".

As far as we know, the application on oil Raman-Spectra of the methods mentioned above has not been published by now. In this work we present a new approach for gear-oil analysis, based on Raman-Spectroscopy and subsequent multivariate data analysis. Gear-oil analysis was performed on Raman-Spectra gained by excitation of the sample with an 800 mW laser at 1064 nm (Bruker RAM II FT-Raman module). The scattered Raman signal was collected by a Fourier Transform Infrared (FTIR) Spectrometer.

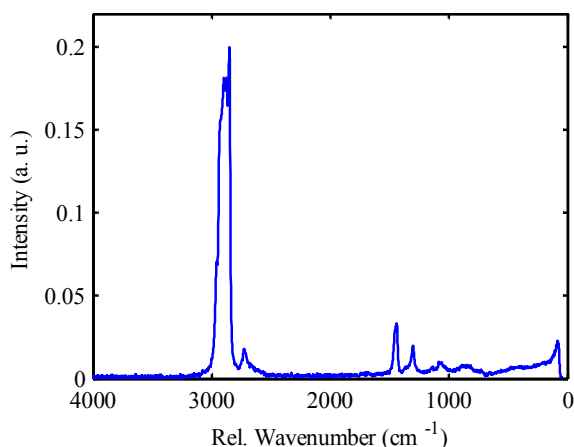


Figure 1. Raman-Spectrum of a common commercially available synthetic gear-oil for wind turbines.

Figure 1 shows the Raman-Spectrum of a typical synthetic gear-oil for wind turbines. The spectral region between 500 cm^{-1} and 1800 cm^{-1} is the so-called "fingerprint" region. The analysis of this region allows a clear identification of the sample under test. Figure 2 shows the IR-Spectrum of the same sample as in Figure 1.

The results of the multivariate data analysis applied to the Raman-Spectra are compared to the ones obtained by analyzing the IR-Spectra (Wiesent et al. 2011) of the same samples. Correlations with different parameters, like TAN and element concentrations, are performed and discussed.

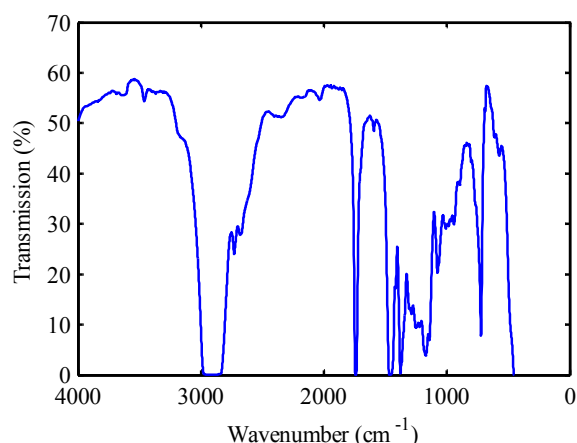


Figure 2. IR-Spectrum of the same gear-oil sample as analyzed in Figure 1.

Kessler, W. 2006. *Multivariate Datenanalyse in der Bio-und Prozessanalytik*. Weinheim: Wiley-VCH.

Long, D.A. 2002. *The Raman effect: a unified treatment of the theory of Raman scattering by molecules*. John Wiley & Sons Inc.

Pirro, D. M., A. A. Wessol, and J. G. Wills. 2001. *Lubrication Fundamentals*. Second Edi. CRC.

Wiesent, Benjamin R., Daniel G. Dorigo, Michael Schardt, and Alexander W. Koch. 2011. "Gear oil condition monitoring for offshore wind turbines using band limited low resolution spectra." *Proceedings of Oildoc*.

Experimental control of the low-frequency fluctuations by current modulation in a semiconductor laser with optical feedback

Andrei, Ionut-Relu¹, Ticos, Catalin-Mihai¹, Bulinski, Mircea² and Pascu, Mihail-Lucian^{1,2}

¹ National Institute for Laser, Plasma and Radiation Physics, Department of Lasers, str. Atomistilor 409, 077125, Magurele, Romania

² University of Bucharest, Faculty of Physics, str. Atomistilor 405, 077125, Magurele, Romania

Keywords: laser diode, optical feedback, LFF (low-frequency fluctuation), current modulation, chaos control

Semiconductor lasers with optical feedback are a category of nonlinear systems that exhibit a variety of chaotic dynamics. Their interesting behavior is mainly related to the simultaneous existence of two different temporal scales: a relatively slow regime of large power fluctuations also called low-frequency fluctuations (LFFs) in the range of a few MHz up to 100 MHz, when the laser emission drops to almost zero, and high-frequency fluctuations of about 1 GHz as the output power is restored back to its initial level. The LFF represent an envelope for high-frequency fluctuations. The chaotic oscillations arise when the laser is subjected to optical feedback obtained from a reflector placed in the optical path of the laser beam (Fig.1).

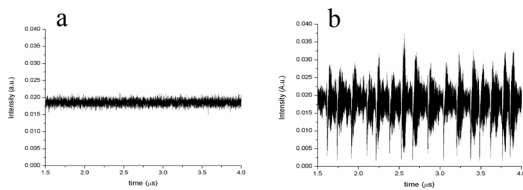


Fig. 1. LD emission dynamics: a) without optical feedback; and b) with optical feedback, LFF regime (chaotic oscillations).

A topic of great interest is the entrainment of the chaotic oscillations in laser diodes (LDs), which can be achieved by modulating the driving current of the diode at low frequency. Modulation of the injection current at high frequency resulted in LFFs synchronized with the driving signal. In this work, the LFFs of a LD with optical feedback are experimentally studied when the injection current is modulated at frequencies close to the mean frequency of power dropouts. The synchronization state between the laser and the external modulator is studied by finding the statistics of power dropouts in the laser emission. The study uses Shannon's entropy on evaluating the distribution of time intervals between consecutive reductions in the laser intensity. In addition, the synchronization between the laser and the modulator is investigated by introducing two new variables, the phase of the laser LFF and the phase of the driving signal. The ratio of these two phases is estimated during the evolution in time of the chaotic laser. The behavior of the synchronized chaotic diode laser with an external modulator is qualitatively similar to deterministic coherence

resonance; it is observed when one of the system's parameters such as the injection current is slightly modified or when the state of pure coherence resonance, when noise is added, leads to more regular spikes in the laser emission. In this paper, no noise is added into the system.

The injection current of an external-cavity semiconductor laser working in a regime of low-frequency fluctuations (LFFs) is modulated at several MHz. The rate of power dropouts in the laser emission is correlated with the amplitude and frequency of the modulating signal. The occurrence of dropouts becomes more regular when the laser is driven at 7 MHz, which is close to the dominant frequency of dropouts in the solitary laser. Driving the laser at 10MHz also induces dropouts with a periodicity of 0.1μs, resulting in LFFs with two dominant frequencies.

The experimental setup used is schematically shown in Figure 2.

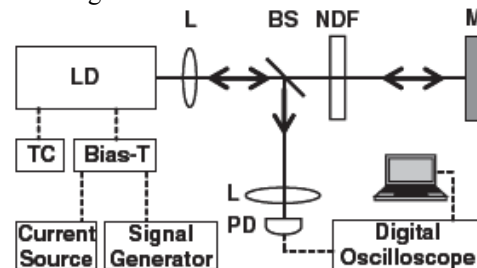


Fig. 2. Setup of the LD driven by a periodic signal generator. PD, photodiode; BS, beam-splitter; NDF, neutral density filter; M, mirror; L- collimating optical system; and TC, temperature controller, respectively.

Acknowledgments. This work was supported by the National Centre for the Management of Programs (CNMP) under contract no. 72-219 within the PNCDI2 program and by the National Authority for Scientific Research (ANCS) under contract Nucleu-LAPLAS 2010.

References: *Mørk J, Tromborg B and Mark J, Chaos in semiconductor lasers with optical feedback: theory and experiment *IEEE J. Quantum Electron*, 28, 93 (1992).

*Lang R and Kobayashi K, External optical feedback effects on semiconductor injection laser properties *IEEE J. Quantum Electron*,. 16, 347 (1980).

*C.M. Ticos, I.R. Andrei, M. L. Pascu, M. Bulinski, Experimental control of power dropouts by current modulation in a semiconductor laser with optical feedback, *Phys. Scr.* 83 (2011), 055402.

Thermal and microstructural analysis of some hybrid metal-organic complex materials and thin films deposition by MAPLE

Catalin Constantinescu

INFPLR - National Institute for Laser, Plasma and Radiation Physics, Department of lasers,
409 Atomistilor st., Magurele RO-077125, Bucharest, Romania

Keywords: thin films, MAPLE, hybrid metal-organics.

Hybrid metal-organic complex materials which exhibit crystalline nature, nonlinear optical properties and chemoselective behavior generate interest as new materials for various applications. Such hybrid metal-organic compounds with azobenzene (AB) rings are novel materials with high industrial and economic potential as thin films for non-linear optical coatings, optical storage (molecular photo-memory and photoswitches), membranes, chemical sensors and detectors.

microscopy and spectroscopic ellipsometry were performed in order to investigate thin film properties. Micrometric pixels of the compounds have been transferred on glass plates by laser-induced forward transfer for chemoselective sensor development purposes.

Books: R.W. Eason, Pulsed Laser Deposition of Thin Films, John Wiley & Sons, New York, 2007;

Journals:

C. Constantinescu, E. Morintale, V. Ion, A. Moldovan, C. Luculescu, M. Dinescu, P. Rotaru, "Thermal, morphological and optical investigation of Cu(DAB)₂ thin films grown by pulsed laser technique for sensor development", Thin Solid Films (in press);

C. Constantinescu, E. Morintale, A. Emandi, M. Dinescu, P. Rotaru, "Thermal and microstructural analysis of Cu(II) 2,2'-dihydroxy azobenzene and thin films deposition by MAPLE technique", Journal of Thermal Analysis and Calorimetry 104 (2011) 707;

C. Constantinescu, A. Emandi, C. Vasiliu, C. Negriila, C. Logofatu, C. Cotarlan, M. Lazarescu, "Thin films of Cu(II)-o,o'-dihydroxy azobenzene nanoparticle-embedded polyacrylic acid (PAA) for nonlinear optical applications developed by MAPLE", Applied Surface Science 255 (2009) 5480.

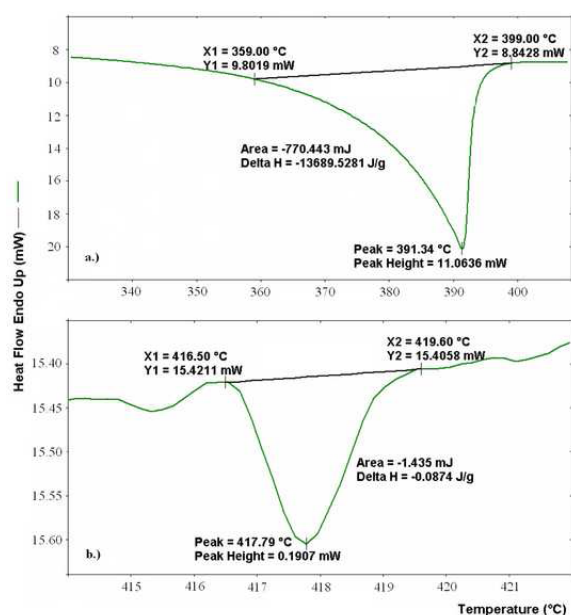


Figure 1. Detail of thermal behavior for Cu(DAB)₂ complex oxidative decomposition in bulk (a.), and as thin film (b.).

This paper presents some results on Cu(II) and Er(III) 2,2'-dihydroxyazobenzene (DAB) thin films deposited on silicon and quartz substrates by matrix assisted pulsed laser evaporation using a Nd:YAG laser, at 266 and 355 nm laser wavelength. Thermal analysis, atomic force microscopy, scanning electron

Molecular modifications of chlorpromazine prepared as solution in micro-droplets form by exposure to laser radiation

Viorel Nastasa, Andra Militaru, Len Amaral, Mihai Lucian Pascu

¹ National Institute for Laser, Plasma and Radiation Physics, Laser Department, P.O. Box MG-36, Str. Atomistilor nr. 409, Magurele, Ilfov, Bucharest 077125, Romania.

² Unit of Mycobacteriology and UPMM, Instituto de Higiene e Medicina Tropical, Universidade Nova de Lisboa, Lisbon, Portugal

The vast majority of drugs employed in modern medicine have their origins in the chemical manipulation of phenothiazines. Chemical manipulation of a compound for the creation of new derivatives is limited by the existing science of organic chemistry, is time consuming and the percent yield of an active product is quite small. Exposure of a phenothiazine to UV –VIS yields a product that is more biologically active than the un-exposed parent. However, because the product is highly unstable, the demonstration of increased activity is usually possible only when exposure of the phenothiazine to UV (incoherent) takes place in the presence of the biological target: example - bacteria. Moreover, because the source of incoherent UV provides a wide spectrum of wavelength, little is known of the response of a given phenothiazine to a much narrower spectrum.

Lasers have been used in recent years for localized effects on tissues when the tissue and the phenothiazine are simultaneously irradiated. The difference between exposures of a phenothiazine to a UV laser beam versus that to incoherent UV is that a laser emits radiation of a specific wavelength with a higher energy level at that wavelength. Because of the specificity of wavelength and beam energy provided by a laser, one would suppose that exposure of a phenothiazine to laser radiation would produce rearrangements of the molecule whose bioactivity could be studied without concurrent exposure of the biological target to the laser, that is, provided that the rearranged compound is sufficiently stable for study. Moreover, if exposure of the phenothiazine to the laser beam is conducted in the presence of a reactive compound, there is the distinct possibility that entirely new compounds can be quickly created within hours if not minutes that may be difficult, if not impossible to create via conventional chemical manipulation. [1]

The reported study examines the optical properties of three neuroleptic phenothiazines with antimicrobial activities prior to and subsequent to exposure to different laser beams singly or in sequence and evaluates the activity of the laser exposed products against a reference *Staphylococcus aureus* strain.

Acknowledgements

. The research was funded by the PALIRT, 41-018/2007 project of the Romanian CNMP and the ANCS Nucleu Project PN 09 39 01/2009 – 2011

References:

- [1] "Direct modification of bioactive phenothiazines by exposure to laser radiation"
M.L. Pascu et. all
Recent Patents on Anti-Infective Drug Discovery,
2011, 6

The nanoparticles synthesis by laser pyrolysis

Catalin Luculescu

Department of Lasers, National Institute for Laser, Plasma and Radiation Physics, Atomistilor 409, 077125, Magurele, Romania

Keywords: laser pyrolysis, nanoparticles, gas-phase synthesis, nanomaterials, metal oxides.

In the last decades the progress achieved on the synthesis of inorganic nanostructures has been accompanied by exploitation of these systems in various fields. Nanoparticles can be generated via a number of synthetic routes based on gas, liquid or solid phase approaches. Among gas-phase synthesis methods, laser pyrolysis has been distinguished as an economically viable route for various nanoparticles. This method is based on homogeneous nucleation in the gas phase, followed by condensation and coagulation. It allows highly localized heating and rapid cooling, since only the gas (or a portion of the gas) is heated, and its heat capacity is small. Heating is generally done using an infrared (CO₂) laser, whose energy is either absorbed by one of the precursors or by an inert photosensitizer (Morjan *et al.*, 2010).

In this work the capabilities of laser pyrolysis method will be presented together with several examples complex materials currently being synthesized, and the available levels of control will be outlined. One of the main advantages of using this method is that it generates ultrafine powders in a continuous way with narrow particle-size distribution and without any sort of contaminants.

The usual cross-flow-configuration flow zone setup for laser pyrolysis is sketched in figure 1.

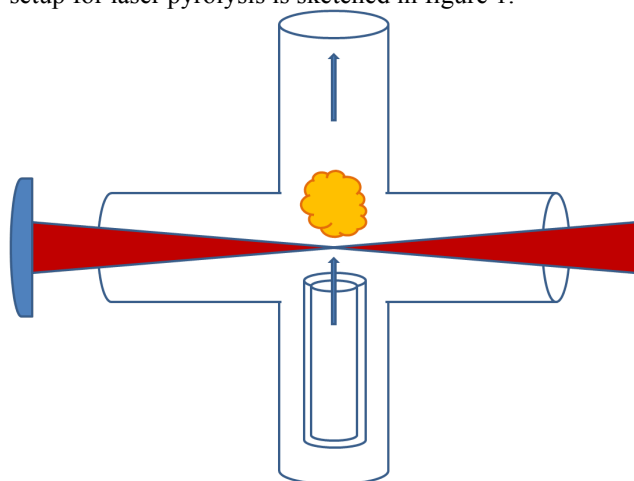


Figure 1. The cross-flow-configuration experimental setup for laser pyrolysis

Among all the functional materials to be synthesized on the nanoscale, metal oxides are particularly attractive candidates, from a scientific as well as from a technological point of view (Alexandrescu *et al.*, 2011).

The iron-based nanoparticle obtained by laser pyrolysis are presented in figure 2.

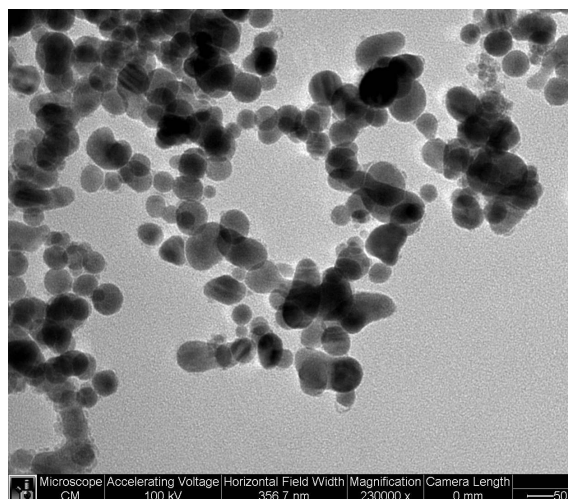


Figure 2. Transmission electron micrograph of the iron-based nanoparticles

The results will demonstrate the laser pyrolysis versatility and opportunities for the fabrication of new nanomaterials and composites.

I. Morjan, R. Alexandrescu, F. Dumitrache, R. Barjega, C. Fleaca, I. Soare, C. Luculescu, G. Filoti, V. Kuncser, L. Vekas, N. Popa, G. Prodan, V. Ciupina, Iron Oxide-Based Nanoparticles with Different Mean Sizes Obtained by the Laser Pyrolysis: Structural and Magnetic Properties, *Journal of Nanoscience and Nanotechnology* 10, 2010, 1223-1234

R. Alexandrescu, I. Morjan, F. Dumitrache, R. Birjega, C. Fleaca, I. Soare, L. Gavrilă, C. Luculescu, G. Prodan, V. Kuncser, G. Filoti, Recent developments in the formation and structure of tin-iron oxides by laser pyrolysis, *Applied Surface Science* 257, 2011, 5460-5464

3D Micro-target Engineering for Laser-Matter Interaction Studies

Jipa Florin Cosmin, Zamfirescu Marian, Ursescu Daniel and Dabu Razvan

Department of Lasers, National Institute for Laser, Plasma and Radiation Physics, Magurele, 077125, Romania.

Keywords: two-photon polymerization, photosensitive materials, femtosecond laser, laser target.

Two Photon Polymerization (TPP) is a 3D microfabrication technique that use the nonlinear absorption of IR femtosecond laser pulses in photoresists. (S.Maruo, 1997; T.Tanaka, 2002). Because these materials have a negligible absorption in near infrared (NIR), and are highly absorptive in the UV spectral domain, the two-photon absorption (TPA) of NIR femtosecond laser pulses occurs deeply inside the volume of the material.

Based on the TPA effect, complex 3D microstructures can be produced using the rapid prototyping algorithms. A solid design can be created in photopolymers layer by layer, and then any 3D structure can be produced with resolution below 100 nm (S.Steenhusen, 2010). Such structures are commonly used for applications like photonics, microfluidics or micro-electro-mechanical systems (MEMS).

In this work we propose a new application of 3D structured polymers, used as micro-target for high power laser experiments. The development of target designs can increase plasma structuring and optimization of radiation emission. Different micro-target designs in Ormocore material are presented.

The micro-targets are optimized for experiments with TW class lasers.

References:

Shoji Maruo, Osamu Nakamura, and Satoshi Kawata, Three-dimensional microfabrication with two-photon-absorbed photopolymerization, *Optics Letters*, 1997, pp. 132–134.

Tomokazu Tanaka, Hong-Bo Sun, and Satoshi Kawata, Rapid sub-diffraction-limit laser micro/nanoprocessing in a threshold material system, *Appl. Phys. Lett.*, 2002, pp. 312-314.

Wojciech Haske, Vincent W. Chen, Joel M. Hales, Wenting Dong, Stephen Barlow, Seth R. Marder, and Joseph W. Perry, 65 nm feature sizes using visible wavelength 3-D multiphoton lithography, *Optics Express*, 2007, pp. 3426–3436.

Transient analysis of a V system with incoherent pumping and spontaneously generated coherence

Budriga, Olimpia

Laser Department, National Institute for Laser, Plasma and Radiation Physics, P.O. Box MG-36, 077125, Bucharest-Măgurele, Romania

Keywords: transient analysis, spontaneously generated coherence, incoherent pumping, relative phase.

In our days there is a considerable interest in the study of the quantum interference effects arising from spontaneous emission of an atom with two closely lying levels (Zhou and Swain, 1999). Effects of spontaneously generated coherence (SGC) on the three-level V-type system was studied related to the lasing without population inversion (LWI) (Menon and Agarwal, 2000). Practically LWI can be used for achieving laser actions in the spectral regions where lasing with population inversion is impractical with the conventional pumping schemes, such as in the XUV and X domains.

An atomic Vee type system (Xu, Wu and Gao, 2003) without an incoherent pumping, in the transient analysis including SGC can exhibit gain without population inversion under the conditions of a resonant coupling field and a resonant probe field. The gain is very sensitive at the relative phase of the two fields, and can be enhanced due to interference from spontaneous emission. There is an experiment who reported the spontaneous emission cancellation via spontaneously generated coherence in sodium dimers (Xia *et al*, 1996).

Our system of interest is a closed V-type system with ground state $|3\rangle$ and excited states $|1\rangle$ and $|2\rangle$. The transition from state $|2\rangle$ to state $|3\rangle$ is driven by a strong-coupling field with ω_2 frequency, the complex Rabi frequency $2G'=2G\cdot\exp(i\varphi_c)$ and a detuning Δ_2 . A probe laser with the ω_1 frequency, complex Rabi frequency $2g'=2g\cdot\exp(i\varphi_p)$, detuning Δ_1 and an unidirectional incoherent pumping laser with rate 2Λ are applied between the states $|1\rangle$ and $|3\rangle$. $2\gamma_1(2\gamma_2)$ is the spontaneous decay rate from excited level $|1\rangle$ ($|2\rangle$) to level $|3\rangle$. We consider a strong coupling laser and a weak probe laser, i.e. $G \gg g, \gamma_1, \gamma_2$.

The dynamic of this system is described with the density-matrix elements in the atom state base, in a rotating-wave frame. If we choose linear polarized electric fields and denote with θ the angle between the dipolar momentums of the two transition the SGC is described by the $\eta=2\eta_0(\gamma_1\gamma_2)^{1/2}\cos\theta$ parameter, which represent the quantum effect resulting from the cross-coupling between spontaneous emission $|1\rangle \rightarrow |3\rangle$ and $|2\rangle \rightarrow |3\rangle$. The absorption coefficient of the probe field and the gain is proportional with the imaginary part of the density-matrix element between levels $|3\rangle$ and $|1\rangle$, $\text{Im}(\rho_{31})$. There is gain if $\text{Im}(\rho_{31}) > 0$.

We solved numerically the differential equations system of the density-matrix elements in the atom state base. In Fig. 1. we plotted the time evolution of the $\text{Im}(\rho_{31})$ for different values of Λ . On observe that there is gain at the most of the time. Parameters used in Figure 1. are: $\gamma_2=3\gamma_1$, $\Delta_1=0$, $\Delta_2=\gamma_1$, $G=50\gamma_1\sin\theta$, $g=0.1\gamma_1\sin\theta$, $\varphi=\pi$, $\theta=45^\circ$, where φ is the relative phase of the probe and coupling fields. Initial conditions are: $\rho_{11}(0)=\rho_{22}(0)=0$, $\rho_{33}(0)=1$ and $\rho_{ij}(0)=0$ ($i, j = 1, 2, 3$). Time evolution of the level populations show us that at any time, population of state $|1\rangle$ (ρ_{11}) is smaller than the populations of state $|2\rangle$ (ρ_{22}) and state $|3\rangle$ (ρ_{33}), for $\Lambda \leq 0.5$. This is the case of LWI. For $\Lambda > 0.5$ we observed that will have LWI until a time.

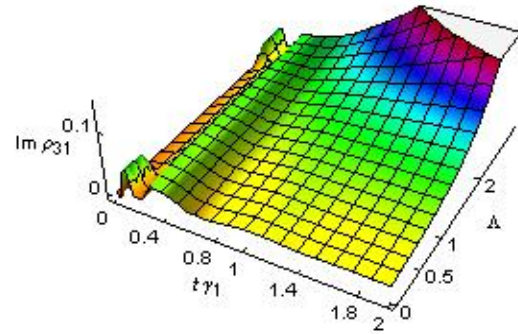


Figure 1. Time evolution of $\text{Im}(\rho_{31})$ versus Λ (2Λ is the incoherent pumping laser rate).

References

- P. Zhu, S. Swain, Phase-Dependent Spectra in a Driven Two-Level Atom, *Phys. Rev. Lett.* 82, 1999, 2500.
- S. Menon, G. S. Agarwal, Gain components in the Autler-Townes doublet from quantum interferences in decay channels, *Phys. Rev. A* 61, 1999, 013807.
- W. H. Xu, J. H. Wu, J. Y. Gao, Transient response in a three-level V system with spontaneously generated coherence, *Optics Comm.* 215, 2003, 345.
- H. R. Xia, C. Y. Ye, S. Y. Zhu, Experimental Observation of Spontaneous Emission Cancellation, *Phys. Rev. Lett.* 77, 1996, 1032.

Reconfigurable soliton waveguides recorded with blue laser diodes for light guiding at telecom wavelengths

S. T. Popescu¹, A. Petris¹, V. I. Vlad¹, E. Fazio²

¹National Institute for Laser, Plasma and Radiation Physics, Bucharest-Magurele, Romania

²University "La Sapienza" of Rome, Italy

Keywords: lithium niobate, soliton waveguides, femtosecond pulse guiding.

2D bright spatial solitons were experimentally proved several years ago in lithium niobate (LN) [1]. By using spatial solitons, so called soliton waveguides (SWGs) can be recorded in the volume of the material. We show that soliton waveguides can be written fast using a blue-violet laser diode, at $\lambda=405\text{nm}$. Using this wavelength, the writing process is optimized. The optimization is in terms of reduced writing time and input power. Previous SWGs were recorded in green, at $\lambda=532\text{nm}$. We compare the writing process in green to that in blue-violet, for the same LN crystal and same SWG parameters. The writing time at $\lambda=405\text{nm}$ decreases with two orders of magnitude for an input beam intensity with four orders of magnitude lower.

A setup similar to that used in [1, 2] is used to write SWGs. A writing beam is focused on the input face of a LN crystal, while a uniform external electrical field is applied in the direction of the crystal c-axis. The writing beam gives rise to a positive change of the refractive index in the illuminated region. The refractive index change follows the spatial beam profile and generates a bright spatial soliton. Thus, a graded-index waveguide is induced.

The SWGs are reconfigurable [3] before their permanent fixing in the volume of the LN crystal. This property adds flexibility in the writing process, allowing new cycles of recording and erasing.

Several parameters can be used to characterize the writing process: the writing (signal beam) wavelength, the writing beam size, the signal-to-background intensity ratio, the external electrical field and the signal polarization. The writing time can be described by the formula $t_w[s]=C/I$, where I is the signal intensity (in W/cm^2) and C is a constant dependent on the input condition. At $\lambda=405\text{nm}$, for an applied field of $45\text{kV}/\text{cm}$ and e-polarization of the signal beam, $C\approx 508\text{ s}\cdot\text{cm}^2/\text{W}$. The writing time decreases from 150s to 100s with the increase of external electrical field from $40\text{kV}/\text{cm}$ to $50\text{kV}/\text{cm}$, for signal intensity of $5\text{ W}/\text{cm}^2$.

To test the infrared (IR) guiding properties of SWGs written in blue-violet, we used two femtosecond pulsed lasers, with $\lambda=1030\text{nm}$ and $\lambda=1550\text{nm}$ and pulse durations of $\sim 200\text{fs}$. The guiding of the IR beam is visualized by imaging the beam profiles at the input and output faces of the crystal (Fig.1a and Fig.1c). One can observe a good

single mode guiding of femtosecond laser pulses at telecom wavelength $\lambda=1550\text{nm}$. The guiding properties, without permanent fixing, remained practically unchanged for more than nine months from the moment of SWGs recording.

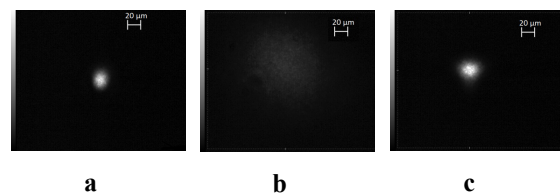


Fig. 1 Spatial beam profile at the input face of the LN crystal (a), output face of the LN crystal in free propagation (b) and in propagation through a SWG (c), for $\lambda=1550\text{nm}$.

An advantage for propagating telecom pulses is low material dispersion ($D_m\sim -0.7\text{ fs}/\text{cm}/\text{nm}$) at $\lambda=1550\text{nm}$. There is also a very low material absorption [2, 3] at this wavelength. This makes SWGs robust to very high optical intensities in IR. The peak intensity of the propagating pulses is nine orders of magnitude higher than the writing beam intensity.

Fast writing of SWGs is an important advantage when writing large SWG arrays.

[1] E. Fazio, F. Renzi, R. Rinaldi, M. Bertolotti, M. Chauvet, W. Ramadan, A. Petris, V. I. Vlad, "Screening-photovoltaic bright solitons in lithium niobate and associated single-mode waveguides", *Appl. Phys. Lett.* 85, 2193 (2004)

[2] A. Petris, A. Bosco, V.I. Vlad, E. Fazio, M. Bertolotti, "Laser induced soliton waveguides in lithium niobate crystals for guiding femtosecond light pulses", *J. Optoelectron. Adv. M.* 7, 2133 (2005)

[3] S.T. Popescu, A. Petris, V.I. Vlad, E. Fazio, "Arrays of soliton waveguides in lithium niobate for parallel coupling", *J. Optoelectron. Adv. M.* 12, 19 (2010)

Formation of 3D gratings by interferometric-mask method in $\text{LiNbO}_3:\text{Fe}$ crystals

Anahit Badalyan, Ruben Hovsepyan, Vahram Mekhitarian, Paytsar Mantashyan and Rafael Drampyan

Institute for Physical Research, National Academy of Sciences of Armenia, 0203, Ashtarak-2, Armenia

Keywords: holographic gratings, diffraction, photorefractive materials, micro- and nano-structures

We report the formation of 3D artificial quasi-periodic structures in photorefractive Fe-doped lithium niobate (LN) crystals by combined interferometric-mask method which we developed and reported in [Drampyan *et al.* 2010]. The formed 3D grating has the period of the order of 30 micrometers in azimuthal direction and 266 nm in axial direction. The method is based on the illumination of the crystal through the 2D masks, having micrometric scale speckles disposition with different axial symmetries, by Gaussian beam in combination with back reflecting mirror. The counter-propagating beam geometry builds up Gaussian standing wave, which determines the third half-wave period of the grating in the axial direction. Thus, the created 3D intensity pattern is a set of numerous mask-generated 2D quasi-periodic structures located in each anti-node of standing wave. The mask used in experiment has 2-fold axial symmetry and consists of transparent holes periodically disposed along the equidistantly positioned concentric circles, surrounding the central spot (Fig.1a). The distance between holes is about 30 micrometers and the total number of spots is equaled ~ 35000 . For comparison, the recording of 2D grating using only mask technique, without standing wave, was also performed. The gratings were recorded by cw single mode 100 mW green 532nm laser beam traversed through the mask and illuminating LN:Fe crystal during 60 min. The back reflecting mirror was placed 1 cm far from the crystal when creating the 3D grating. The non-uniform intensity distribution of the beam can be imparted into the irradiating photorefractive crystal via electro-optic effect thus creating 2D and 3D refractive index gratings.

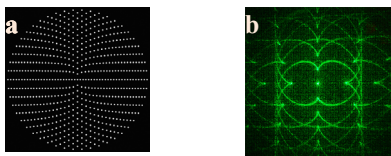


Figure 1. (a) Fragment of enlarged pattern of 2-fold symmetry mask. (b) Interference pattern from 2-fold symmetry mask obtained by green laser beam.

The gratings were tested by diffraction of red laser 633 nm Gaussian beam on the grating. The results are shown in Fig.2a-b. The obtained diffraction

patterns from the mask replica inside the crystal should be compared with Fig.1b, illustrating the diffraction from original mask. The diffraction pattern from 2D grating (Fig.2a) showed more diffraction orders in the direction of optical C-axis of the crystal compared with diffraction from 3D gratings (Fig.2b). Both gratings were recorded in 0.5 mm thick LN:Fe to minimize the diffraction effects from the holes of mask and avoid the interference effect of diffracted beams inside the crystal. Analogous experimental results performed in 2mm thick LN:Fe crystal (Drampyan *et al.* 2010) showed more isotropic intensity distribution in diffraction pattern from 3D gratings.

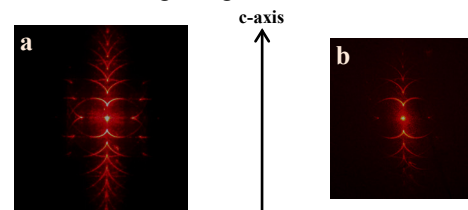


Figure 2. Diffraction patterns from 2D (a) and 3D (b) 2-fold symmetry mask replica

The direct observation of 2D and 3D gratings recorded in LN:Fe 0.5mm thick crystal by phase microscope was also performed. The results are shown in Fig.3a-b. 3D grating shows higher contrast.

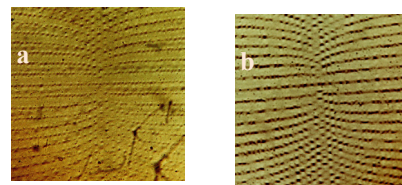


Figure 3. Fragments of phase microscope images of 2D (a) and 3D (b) 2-fold symmetry mask replicas.

2D and 3D quasi-periodic artificial structures are promising materials for many applications including guiding and trapping systems, information storage etc.

1. A. Badalyan, R. Hovsepyan, V. Mekhitarian, P. Mantashyan, R. Drampyan, “Combined interferometric- mask method for creation of micro- and sub-micrometric scale 3D structures in photorefractive materials”, Proc. of SPIE, 7998, 32, 2011.

Computer controlled laser

Catalin Chitu^{1,2}, Razvan Constantin Inpuscatu¹ and Alexandra Vintila¹

¹Energetic High School, Grivitei Street, No. 1, 105600, Campina, Romania

²University of Bucharest, Faculty of Physics, Atomistilor Street, Magurele, Romania

Keywords: laser, remote control, computer application, electronics device.

Differential treatment of students is a necessity in terms of diversification of skills, learning styles, educational profiles and their future professions.

Students learn to enjoy those parts of the curriculum that is close to areas where they are passionate. Therefore, the teacher is able to launch this challenge to students. Attracting students to science has multiple results, such as attending school curricula in good condition, getting school performance in this area, increasing the number of future specialists in natural sciences.

After using Visual Basic programming environment for implementation of microcomputers and appropriate graphical interfaces required in the laboratory experiments, this time our focus has shifted and the unidirectional circuit elements such as semiconductors. Our article combines elements of programming language with elements of physical discipline and has an interdisciplinary character.

The project theme is creating a computer controlled laser. The user can switch on or off the laser just by pressing a button on his computer. The application that makes all this possible was created in Visual Basic 2008 Express Edition.

Figure 1 represents the electronic circuit that, after connecting to the computer, take command of starting or stopping laser device.

Visual Basic is a programming language developed by Microsoft, derived from the Basic language. It is popular due to its graphic user interface which is relatively simple compared to other programming languages.

The use of this language is a general one. It can be used for creating simple application, educational ones but also for complex ones (games). Theoretically anybody (more or less experienced) can create an application using this language because it's a simple one.

In order to make this project we created a home-built laser, using a laser pointer and an integrated circuit board (Figure 1). The board is connected to the computer via a serial port. It is switched on and off via the created application which turns on or off the power in the serial port.^[1]

Therefore, through this project, we intend to show that it is possible to build a simple circuit having a laser integrated and control it from the computer.



Figure 1. The integrated circuit board and the laser

Acknowledgements:

This work was supported through the project launched by the Ministry of Education, Research, Youth and Sport and by the University of Bucharest through the POSDRU/6/1.5/S/24 project.

References:

Lidia Panaiotu, Iunian Chelu, Maria Petrescu Prahova, Elena Adriana Teodoru, Experimental work in physics for high school, Didactic and Pedagogic Publishing House, Bucharest, 1972, p. 291-297

Constantin Cucos, Pedagogy, Polirom Publishing House, Iasi, 2006, p.223-226

George Vladuca & Co., Problems of Physics for class XI-XII, Didactic and Pedagogic Publishing House, 1983, p.104-112, 114-118

Catalin Chitu, Razvan Constantin Inpuscatu, Marilena Viziru, Visual Basic Applications to Physics Teaching, Proceedings of the 5th International Conference on Virtual Learning, Section Software Solutions, p. 403-409, 2010

http://ro.wikipedia.org/wiki/Visual_Basic, date accessed: March 23rd, 2011

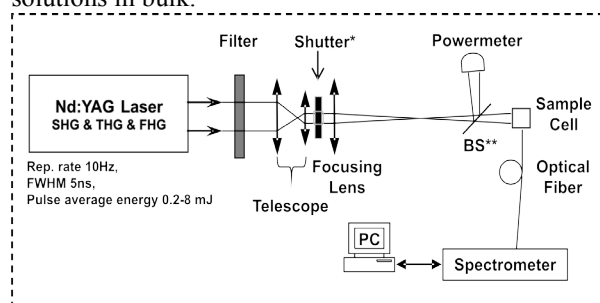
Modification of molecular structures in liquid phase by interaction with laser beams

Mihai Lucian Pascu

National Institute for Laser, Plasma and Radiation Physics, Bucharest

E-mail: mihai.pascu@inflpr.ro

Solutions prepared in many classes of solvents, among which the most utilised is water (either distilled or ultrapure) exhibit different time stability degrees if kept in dark at different temperatures. This is important if they are not used immediately after preparation, a particular case of high interest being the application/use of the solutions to “treat” multidrug resistance developed by bacteria. The stability degree of a solution is, in many cases, also function of its exposure (either accidental or made on purpose) to optical uncoherent or laser beams. In this talk, a synthesis is made about the results obtained by us on the modifications induced in molecular structures of several substances, as a consequence of exposure of their solutions to laser radiation of suitable characteristics. The studied compounds belonged to three classes of substances: phenothiazines, cytostatics and antibiotics; two lasers were used: a nitrogen pulsed laser emitting at 337nm in pulsed regime (0.7nm FTW pulses) at pulse repetition rates of several Hz, and a Nd:YAG laser coupled with an OPO emitting 10ns pulses tuneable in the UV and visible. In the figure is shown a variant of the experimental set-up used to expose 2.5 mL of solutions in bulk.



* Shutter speed: < 1ms; ** BS reflection 8%.

The sample cell in the figure may be replaced by microdroplets of solutions, generated by computer controlled systems at volumes between 2.5 μ L and 15 μ L.

For all the types of studied substances the absorption spectra were conducted prior to and post-exposure, fluorescence spectra similarly determined and the products of laser exposure evaluated; in the chlorpromazine (CPZ) case the evaluation was further made for activity against a *Staphylococcus aureus* ATCC strain via a disk susceptibility assay. The main result was that the exposure to lasers alters the absorption spectra of the phenothiazines; alters their fluorescence spectra; produces a highly active chlorpromazine compound against the test organism. The main conclusion is that exposure of the medicines solutions to laser radiation alters the structure of the compounds that result in possible altered activity against bacteria, as demonstrated for CPZ. This is among the first reports that show that laser radiation can alter the physico-chemical characteristics of molecules, particularly of medicines molecules, to the extent that altered bioactivity results.

Acknowledgements: The data reported in this talk were obtained by the Laser Spectroscopy Group of the Laser Department at INFLPR, within the ANCS project 42-018 PALIRT and Nucleu project LAPLAS 3/2009/PN0939.

Imaging *C. Elegans* embryogenesis by Third Harmonic Generation microscopy

G.J. Tserevelakis, G. Filippidis, E.M. Megalou, A.J. Krmpot, M. Vlachos, C. Fotakis, N. Tavernarakis

¹Foundation for Research and Technology - Hellas, Institute of Electronic Structure and Laser, N. Plastira 100,

P.O. Box 1385, 71110 Heraklion, Greece

²Physics Department, University of Crete, P.O. Box 2208, 71409 Heraklion, Greece

In this study, we demonstrate the potential of employing third harmonic generation (THG) imaging microscopy measurements for the study of *Caenorhabditis elegans* (*C. elegans*) embryogenesis. A 1028-nm femtosecond laser was used for the excitation of unstained *C. elegans* samples. Different *C. elegans* developmental stages (from early to 3-fold) were characterized. Furthermore, time lapse measurements were performed for cell tracking studies in early stage embryos. Live biological specimens were irradiated for prolonged periods of time (up to 7 h), testifying to the non-destructive nature of this nonlinear imaging technique. Thus, THG image contrast modality has proved to be a powerful diagnostic tool in providing useful and unique information into the complex biological process of embryogenesis.

Dynamic and static measurements of oxygenation and blood volume by Diffuse Optical Tomography (DOT)

M. Patachia^{1,2}, D. C. A. Dutu¹, S. Banita¹, R. Cernat¹, D. C. Dumitras¹

¹*Department of Lasers, National Institute for Laser, Plasma and Radiation Physics, 409 Atomistilor St., PO Box MG-36, 077125 Bucharest, Romania*

²*Faculty of Physics, University of Bucharest, Romania*

e-mail: mihai.patachia@inflpr.ro

The multispectral DOT enables the non-invasive reconstruction of the internal tissue structure and the evaluation of the tissue pathology. Total hemoglobin concentration (THC) and tissue blood oxygenation (StO₂) are used for evaluation of the tissue pathology.

Using optical measurements at multiple source-detector positions on the tissue surface, one can reconstruct the internal distribution of the absorption coefficient (μ_a) and the reduced scattering coefficient (μ'_s) in two or three dimensions based on the transport model.

We have built an inexpensive continuous-wave DOT system containing two spatially combined laser diode sources (at 785 nm and 830 nm), one silicon photo diode (SiPD), a transimpedance amplifier and two lock-in amplifiers, which can acquire 128 independent measurements in less than 50 seconds through two time-division-multiplexed optic scheme with eight illumination fibers and eight detector fibers in the measuring head (optode) [1].

The spectral selectivity of a multispectral DOT system enables also the evaluation of some new physiological parameters related to hemoglobin concentration and blood oxygenation (THC and StO₂ distributions) which can better characterize the angiogenesis in the tumor zone, improving the resolution and the contrast of the tomographic image.

A dynamic liquid phantom simulating the optical properties of the tissue was used in order to test the efficiency of the system. The basis of the phantom was formed by a scattering solution of Intralipid (Lipofundin) and water with an overall reduced scattering coefficient of 0.8 mm⁻¹ (785 nm). The solution was placed in a cylindrical beaker. A magnetic stirring rod maintains the homogeneity during the experiment. Red blood cells obtained from healthy human blood were added to scattering solution to achieve a volume fraction of 1.5% and total hemoglobin concentration of 26 μ M. This is a typical value for normal physiological conditions with an assumption of 4.0% blood volume and 40% hematocrit. The hemoglobin saturation was measured to be 85%.

In order to induce deoxygenation on the liquid phantom, 4 g of dry bakers yeast was added to the solution. The temperature of the phantom was maintained at 37°C to keep the yeast active. This

condition was maintained over a time of about 20–30 min. Deoxygenation was observed until hemoglobin saturation reached a steady state at 25%. After deoxygenation of yeast-intralipid solution reached steady state, oxygenation was simulated again by delivering extra oxygen to the phantom from an oxygen tank. Oxygen supply was maintained until a steady state level of oxygenation was obtained. Steady state hemoglobin saturation was 89%.

The chromophore distribution analysis through continuous-wave Near Infrared Spectroscopy (cwNIRS) can enhance the resolution and accuracy in various deep-tissue applications of the cw DOT, including breast cancer imaging [2]. The THC increase in tumour is expected due to angiogenesis accompanying tumour growth.

The obtained results [3] confirm the design parameters of the liquid phantom and the ability of the system to evaluate the hemoglobin and oxyhemoglobin concentration.

The good agreement of the static and dynamic measurements demonstrates the homogeneity of the liquid phantom. The resulted data presented less than 5% variations in the measurements, which are due to the oxygen bubbles flowing in solution during the oxygenation process and to the yeast mud resulting from the insertion of the yeast bag in the liquid phantom.

1. D.C.A. Dutu, D.C. Dumitras, C. Matei, A. M. Magureanu, M. Patachia, S. Miclos, D. Savastru, X. Liang, H. Jiang, and N. Iftimia, "Design and parametric evaluation of a continuous-wave diffuse optical tomography system", ICPEPA '09 Sapporo, Japan (2009).

2. S. Srinivasan, B. W. Pogue, S. D. Jiang, H. Dehghani, C. Kogel, S. Soho, J. J. Gibson, T. D. Tosteson, S. P. Poplack, and K. D. Paulsen, "Interpreting haemoglobin and water concentration, oxygen saturation, and scattering measured in vivo by near-infrared breast tomography", Proc. Natl. Acad. Sci. U. S. A. 100, 12349–12354 (2003).

3. M. Patachia, D.C.A. Dutu, D.C. Dumitras, "Blood oxygenation monitoring by diffuse optical tomography", Quantum Electronics 40 (12) 1062 – 1066 (2010).

The effect of substrate roughness and chemistry on the cellular response

Ch. Simitzi, M. Barberoglou, A. Ranella, C. Fotakis, I. Athanassakis, E. Stratakis

The aim of this study is to investigate the cellular response on silicon and polymeric surfaces exhibiting different roughness and hydrophilicities. The silicon surfaces were fabricated via fs laser structuring, and were comprised forests of conical spikes exhibiting controlled dual-scale roughness at both the micro- and the nano-scale. As the laser energy increases the substrate roughness is gradually increased giving rise to a gradient decrease of the surface wettability. Following fabrication, the laser treated silicon areas were used as master for the microreplication of the structures on different polymeric materials (such as ORMOCER and PLGA) via PDMS stamping.

Accordingly, the replicated polymeric surfaces displayed different roughness and wettability. Cell culture experiments were performed with the fibroblast NIH/3T3 and PC12 neuron cell lines in order to investigate the cellular response, regarding cell viability, adhesion,

morphology on the different topography and chemistry of the surfaces. It is observed that both types of cells preferentially adhered in the rough compared to the flat surfaces used as controls. In particular, the NIH/3T3 showed optimal cell adhesion for small roughness ratios, independently of the surface wettability and chemistry. PC12 adhered well in all surfaces, but they formed into clusters on the surfaces with higher roughness degrees. On going studies aim at the investigation of the cellular response and differentiation behavior of PC12 after NGF treatment of these culture surfaces. Furthermore, in vitro experiments with primary neuronal cultures are under way to study the effect of dual-scale roughness and the role of surface energy on the ability of primary neurons to make functional neural networks.

Laser ablation in the ENT surgery

M. Petrus¹, D. C. Dumitras¹, C. Sarafoleanu², C. Manea², C. Iosif², E.M. Carstea³, D. C. A. Dutu¹

¹Department of Lasers, National Institute for Laser, Plasma and Radiation Physics,
409 Atomistilor St., PO Box MG-36, 077125 Bucharest, Romania

²St. Maria Hospital, Bucharest, Romania

³National Institute of R&D Optoelectronics INOE 2000
409 Atomistilor St., PO Box MG-5, 077125 Bucharest, Romania

e-mail: mioara.petrus@inflpr.ro

Keywords: laser ablation, CO₂ laser, diode laser, radio frequency, Optical Coherence Tomography, ENT (ear-nose-throat).

The laser technique offers excellent view of the operating site and of the surrounding structures with greater margin of safety. Laser ablation surgery diminishes the collateral symptoms and the recovery time. Ablation of the tissue through vaporization is a photothermal effect that uses low energy photons. For a better control of the interaction processes a special attention was given to the propagation of the laser radiation in the heterogeneous structures of the biological tissue. The intense radiation with the wavelengths 10.6 μm and 980 nm emitted by CO₂ laser and diode laser (LD), are currently used in ENT (ear-nose-throat) surgery for tissue ablation by vaporization of the pathological tissues and enable large ablation volumes of the tissues with carbonization of the edges limited at 50 – 350 μm .

The functional dependence between the laser parameters and the interaction effects (absorption, thermal heating, ablation, scatter, acoustic damage, coagulation etc.) in the irradiated tissue was put in evidence using measurements based on histopathological examination, Spectral Radar Optical Coherence Tomography (SROCT). Using two different wide spread laser surgical system (a CO₂ laser, emitting at 10.6 μm , and a laser diode (LD) array emitting at 980 nm) and a radio frequency (RF) generator with a similar 25 W output power, we have investigated and compared the action of these systems by analyzing the modifications produced at the cellular level in the interaction process. The interaction time or the laser pulse length was adjusted between 100 msec and 1.5 sec. As biological materials we have used: *in vitro* human tonsils extracted by classic tonsillectomy and polypectomy and several samples of pork liver and pork muscle to extend the experimental data basis; *in vivo* nasal mucosa of different patients with allergic rhinitis.

1. T. Şapçı, B. Sahin, A. Karavus, U.G. Akbulut Laryngoscope **113**, 514 (2003).
2. M. Maurizi, G. Almadori, G. Plaudetti Otolaryngology Head Neck Surg. **132**, 857 (2005).
3. Behrooz A. Torkian, Shuguang Guo, Alexander W. Jahng, Lih-Huei L. Liaw, Zhongping Chen, Brian J.F. Wong, Noninvasive Measurement of Ablation Crater Size and Thermal Injury After CO₂ Laser in the Vocal Cord With Optical Coherence Tomography, Otolaryngol Head Neck Surg **134**:86-91 (2006).
4. M.A. Shakhova, G. Yu. Golubiatnikov, V.A. Kamensky, and L.B. Snopova “Comparative analysis of laser and radio frequency impact on biotissues” International Symposium TPB’09, Nizhny Novgorod, Russia (2009).
5. D.C. Dumitras, D.C.A. Dutu, M.Petrus, C. Sarafoleanu, C. Manea, C. Iosif, Optical Coherence Tomography monitoring of laser ablation processes in ENT tissues, International Conference Advanced Lasers Technologies (ALT 2010), Egmond aan Zee, Holland (2010)

Analysis of ethylene and ammonia as biomarkers for patients with renal failure

Cristina Popa^{1,2}, Ana M. Bratu¹, Doru C. A. Dutu¹, Consuela Matei, Stefan Banita¹,
and Dan C. Dumitras¹

¹Department of Lasers, National Institute for Laser, Plasma, and Radiation Physics,
409 Atomistilor St., PO Box MG-36, 077125 Bucharest, Romania

²Faculty of Physics, University of Bucharest, Romania

Keywords: laser photoacoustic spectroscopy, biomarkers, haemodialysis, breath test

Human breath includes hundreds of volatile organic compounds in low concentrations even though fewer than fifty of these are found in the majority of normal human's breath. Some of these volatile organic compounds have been identified as biomarkers to some specific pathologies, including lipid peroxidation, heart failure, asthma, cystic fibrosis, diabetic ketoacidosis, alcohol intoxication, renal failure, and others [1]. However, due to the low concentrations and presence of a large number of chemical species in exhaled air, breath analysis requires high sensitive and selective instrumentation to detect and identify the atypical concentrations of specific biomarkers [2, 3].

Ethylene from the human breath is a marker of oxidant stress (in patients on haemodialysis, in acute myocardial infarction, in inflammatory diseases and ultraviolet radiation damage of human skin) and can be directly attributed to biochemical events surrounding lipid peroxidation [4].

What causes too much ammonia in human body?

Ammonia and ammonium ions (as small molecules), can penetrate the blood-lung barrier, and appear in exhaled breath. In the case of kidney dysfunction, urea is unable to be excreted, causing an excessive build up of ammonia in the blood. People with kidney failure have a marked odor of ammonia ("fishy") on their breath, which can be an indicator of this disease [5, 6].

In the present study, measurements were made to detect ethylene and ammonia from the exhaled breath of patients with renal disease and also for healthy volunteers. Breath test is noninvasive, easily repeated, and does not have the discomfort or embarrassment associated with blood and urine tests.

The application of laser photoacoustic spectroscopy for fast and precise measurements of breath biomarkers has opened up new promises for monitoring and diagnostics in recent years, especially because breath test is a non-invasive method, safe, rapid and acceptable to patients.

1. P. R. Galassetti, B. Novak, D. Nemet, C. Rose-Gottron, D. M. Cooper, S. Meinardi, R. Newcomb, F. Zaldivar, D. R. Blake, "Breath Ethanol and Acetone as Indicators of Serum Glucose Levels: An Initial Report", *Diabetes Technology & Therapeutics* **7**, 2005, pp: 115 – 123.
2. W. Miekisch, J. K. Schubert, G. F. E. Noeldge-Scomburg, "Diagnostic potential of breath analysis-focus on volatile organic compounds", *Clinica Chimica Acta* **347**, 2004, pp: 25-39.
3. F. Ferreira da Silva, M. Nobre, A. Fernandes, R. Antunes, D. Almeida, G. Garcia, N. J. Mason, P. Limão-Vieira, "Spectroscopic studies of ketones as a marker for patients with diabetes", *Journal of Physics: Conference Series* **101**, 2008, pp: 1-7.
4. G. J. Handelman, "Current Studies on Oxidant Stress in Dialysis", *Blood Purification* **21**, 2003, pp: 46-50.
5. L.R. Narasimhan, W. Goodman, .C. Kumar N. Patel, "Correlation of breath ammonia with blood urea nitrogen and creatinine during hemodialysis", *Proceedings of the National Academy of Sciences* **98**, 2001, pp: 4617-4621.
6. M. R. McCurdy, Y. Bakhirkin, G. Wysocki, R. Lewicki, F. K. Tittel, "Recent advances of laser-spectroscopy-based techniques for applications in breath analysis", *Journal of Breath Research* **1**, 2007, 014001.

From scientific research to industrial production – a few examples in surface engineering

C. Ruset¹, E. Grigore¹, I. Munteanu¹, N. Budica¹, I. Cernica¹, H. Maier², R. Neu², G. Matthews³,
D. Heinen⁴, S. Bausch⁴, V. Zoita^{1,5}

¹ National Institute for Laser, Plasma and Radiation Physics, 077125 Magurele-Bucharest, Romania

² Max-Planck Institut für Plasmaphysik, Euratom Association, 85748 Garching, Germany

³ Culham Centre for Fusion Energy, Euratom Association, Abingdon, UK

⁴ Fraunhofer Institute for Production Technology, 52074 Aachen, Germany

⁵ EFDA Close Support Unit, Culham, Abingdon, UK

Keywords: tungsten coating, nuclear fusion, laser alloying, plasma nitriding, anti-sticking layers

Depending on its main goal, the scientific research could be classified as fundamental when the objective is to produce new knowledge or applied research when the aim is to use the existing knowledge in various fields of human activity. A research project can include both fundamental and applied activities, but the final objective must be clearly defined.

Big, complex projects have usually the following three phases: (i) research, (ii) development and (iii) application (production). The specific activities for each phase are usually carried out by different teams, with different coordinators, but under the same general management. This seems to be a key factor for a success project. Close monitoring of all activities is extremely important. A few examples of projects running from research to production are given below in the field of surface engineering. This field covers the research and technical activity concerning design, manufacture, investigation and utilization of surface layers. It comprises techniques involving surface modification of the components with the aim to improve the performances in terms of mechanical, chemical, thermal, electrical, magnetic, optical, biocompatible or decorative characteristics.

The first example concerns nuclear fusion. The first wall of ITER (International Thermonuclear Experimental Reactor) will consist of beryllium at the main chamber and tungsten at divertor. Since this configuration was never tested in a tokamak on a relevant scale, a decision was taken to replace the carbon first wall of JET (Joint European Torus) with a new wall similar with that designed for ITER. JET located at the Culham Center for Fusion Energy, UK is the biggest operational tokamak in the world. In the framework of this project called "ITER-like Wall -ILW" about 2,000 CFC (Carbon Fiber Composite) tiles of different shapes and dimensions had to be coated with W layers of 10-25 μm . During JET operation the W coatings can reach 1,600 $^{\circ}\text{C}$ or even more and they should survive these conditions without delamination. In the research phase of the ILW project it was demonstrated that Combined Magnetron Sputtering

and Ion Implantation (CMSII), a deposition method developed at the National Institute for Laser, Plasma and Radiation Physics (INFLPR) produced the best W coatings in terms of thermo-mechanical properties in comparison with other PVD or CVD techniques. In the development phase of the project an industrial coating unit with a chamber ($\Phi 800 \times 750$ mm) equipped with 24 magnetrons was designed, build and commissioned. The next step was qualification of the CMSII technology for all types of CFC tiles and production of W coatings on about 2,000 tiles. A quality control program was implemented in accordance with ISO 9001:2001 standard and additional JET requirements. Ten percent of the coated tiles were tested in the high heat flux test facility GLADIS at the Max-Planck Institute of Plasma Physics, Garching, Germany.

A second example is in the field of tooling. A combined technology between laser alloying and plasma nitriding was developed in the framework of two European projects (Research for SMEs) and applied for forging dies. Two research institutes (Fraunhofer Institute for Production Technology IPT, Aachen, Germany and INFLPR, Romania), five forging companies from Germany, Italy, Portugal and Slovakia and two companies specialized in laser processing from Portugal and Italy were involved in the project. By applying this combined treatment the lifetime of the forging dies increased up to 200% in comparison with that obtained by the current treatments.

Another example of a project developed from laboratory to industrial scale in INFLPR is in the rubber industry. In the tyre manufacturing process the non-vulcanized rubber come in contact with the metal forming tools. The adhesion phenomenon between the rubber and the metal surface affects negatively the tyre quality. Starting from a request of the Michelin Company a technology producing a non-sticking layer on the metal surface of the forming/cutting tools was developed. The anti-sticking properties of this layer are about 3 times better than that of Teflon. This technology was approved by Marks laboratory, USA and it is currently applied in INFLPR on commercial basis.

Enhanced carrier trapping efficiency in ZnO/Si micro-cones

E. Magoulakis^{1,2}, E. L. Papadopoulou¹, E. Stratakis¹, C. Fotakis^{1,2}, and P. A. Loukakos¹

¹Foundation for Research and Technology - Hellas, Institute of Electronic Structure and Laser, N. Plastira 100, P.O. Box 1385, 71110 Heraklion, Greece

²Physics department, University of Crete, P.O.Box 2208, 71409 Heraklion, Greece

Keywords: ultrafast, pump-probe, micro-structures, micro-cones.

When matter reduces to the nanoscale, its properties are altered. Knowledge of the effect on the microscopic processes is vital for applications (such as optimization of optoelectronics). With the development of femtosecond lasers, we can utilize various techniques, such as pump-probe spectroscopy to study these processes.

In this work, a comparative study of the ultrafast dynamics in ZnO thin films deposited on flat Si substrates (Fig. 1a) and on Si micro-cones (Fig. 1b-d) following ultrashort laser excitation has been carried out by measuring the time-resolved reflectivity^{1 (1)}.

By monitoring the transient band gap renormalization induced by nonlinearly excited carriers it is found that fast electron scattering and trapping occurs more efficiently in the microcones as compared to the flat films (Fig.2).

From Fig 1, we find three structural differences that can be responsible for this acceleration: a) the micrometre sized conical shape, b) nanometre-sized protrusions along the cone surface and c) possibly film thickness variation from the top of the cones to their base. Additional measurements on films with different thicknesses (Fig. 3) and different cone sizes (Fig. 4) show that the measured signal is independent of both.

Therefore, the enhanced trapping efficiency is attributed to the defects and imperfections that are introduced by the increased surface roughness due to the conical shape.

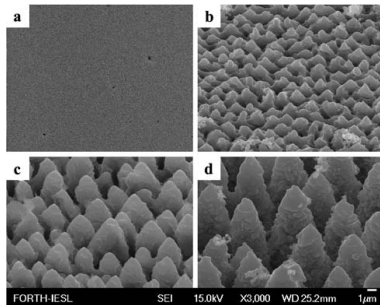


Figure 1. FE-SEM images of ZnO deposited on flat Si (a) and micro-conical Si with 1.6:1.5 (b), 4.7:3.6 (c) and 9.9:6.0 (d) aspect ratio (cone height/base diameter)

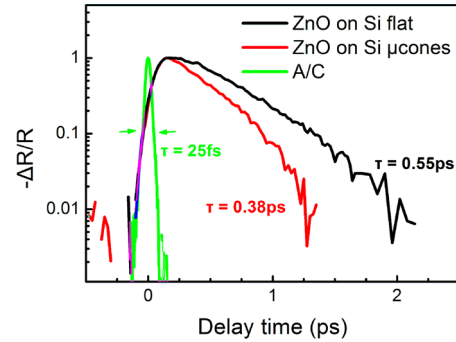


Figure 2. Ultrafast time-resolved reflectivity of ZnO films deposited on flat (black) and micro-conical (red) Si. Pulse autocorrelation (green) is also displayed for reference.

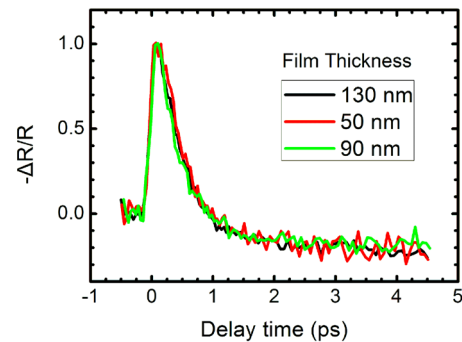


Figure 3. Ultrafast time-resolved reflectivity of ZnO films with various thicknesses on flat Si.

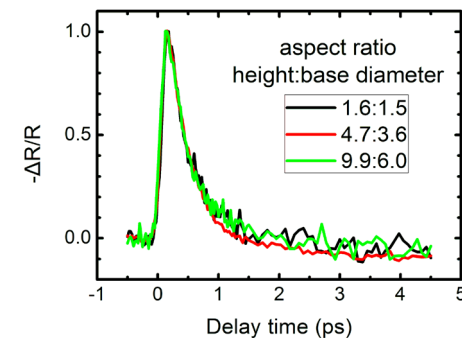


Figure 4. Ultrafast time-resolved reflectivity of ZnO on micro-conical Si with various cone aspect ratios (cone height:base diameter).

¹ E. Magoulakis et al, *Appl. Phys. A* **98**, 701 (2010).

Functional Protein Microarrays: toward a system view of the plant cell

Popescu¹, George, Popescu², Sorina

¹NILPRP, Str. Atomistilor, Nr. 409, Magurele 077125, Bucharest, Romania

²Boyce Thompson Institute for Plant Research, One Tower Road, Ithaca 14853, NY, USA

Keywords: protein microarrays, MAPK networks, systems biology.

Protein microarrays (PMA) are one of the newest tools for studying plant cell interactions. They are being used to investigate various cellular processes such as signaling, transcription, cellular trafficking, plant pathogen interaction and development. Due to the high number of observations one can make on protein functions, they hold the potential for uncovering complex cell biology mechanisms.

We outline here key features of protein microarray technology and its main applications in functional protein characterization, identification of cellular pathways, and the study of dynamics of cellular processes. We highlight recent results on plant kinome identification, functional characterization of CaM proteins and identification of new immune system components in plants.

Pioneering work in protein microarray technology was conducted by Zhu et al. (Zhu, et al., 2000) and MacBeath (MacBeath & Schreiber, 2000). Novel ideas such as self-assembly protein microarrays (Ramachandran, et al., 2004) promise a rapid development of whole-organism protein microarrays, with applications in proteome analysis and interactome identification. While great progress has been made in whole-proteome analysis of prokaryotic organisms and yeast, complex eukaryote proteomes pose a significant challenge even when using high-throughput methods.

Among the main applications of protein microarrays are functional protein characterization and kinome analysis. In yeast, a comprehensive analysis of protein phosphorylation events was conducted by Ptacek et al. (Ptacek, et al., 2005). High-density protein microarrays were developed by Popescu et al. (2007) and applied for the characterization of the Arabidopsis CaM interactome. A comprehensive MAPK signaling network was uncovered using high-density protein microarrays and kinase assays in (S. C. Popescu, et al., 2009). As many as 5000 proteins (S. C. Popescu, et al., 2010) have been used to dissect the interactome for immune system pathways, with 10000 proteins PMA being currently used in functional assays.

Recently, protein microarrays designs are specializing for functional characterization of biological processes. Current results in identifying components of plant immune system (Lee, et al., 2010) demonstrate the key role of PMA in uncovering complex cellular mechanisms, when used in combination with genetic screening methods and in vivo bioluminescence assays.

One of the main challenges in analyzing cellular interactions using protein microarrays is the development of computational models that approximate well cellular dynamics and perturbation effects of experimental assays. Recent systems biology results demonstrate that modeling cellular dynamics can significantly improve prediction of cellular events from high-throughput data.

Protein microarrays allow not only a significant speed up in traditional research areas such as immunity and development, but offer a systems view of cell processes which can lead to a much in depth understanding of complexity of cellular mechanisms.

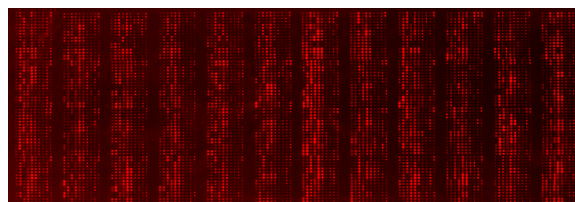


Figure 1. The high-throughput 2133 unique *Arabidopsis Thaliana* protein microarray.

References:

- Lee, H. Y., et al. (2011). BTI1 and BTI2 reticulon-like proteins regulate activity and intracellular trafficking of the FLS2 immune receptor . *submission*.
- MacBeath, G., & Schreiber, S. L. (2000). Printing proteins as microarrays for high-throughput function determination. *Science*, 289(5485), 1760-1763.
- Popescu, S. C. et al. (2009). MAPK target networks in Arabidopsis thaliana revealed using functional protein microarrays. *Genes & Development*, 23(1), 80-92.
- Popescu, G. V., Popescu, S. C., Ma, S., Bachan, S., Kato, N., Snyder, M., et al. (2010). Comparative analysis of FLS2 and EFR signaling networks in *Arabidopsis Thaliana*. *submission*.
- Popescu, S. C. , et al. (2007). Differential binding of calmodulin-related proteins to their targets revealed through high-density Arabidopsis protein microarrays. *PNAS*, 104(11), 4730-4735.
- Ptacek, J. et al. (2005). Global analysis of protein phosphorylation in yeast. *438(7068)*, 679-684.
- Ramachandran, N., Hainsworth, E., Bhullar, B., Eisenstein, S., Rosen, B., Lau, A. Y., et al. (2004). Self-assembling protein microarrays. *Science*, 305(5680), 86-90.
- Zhu, H. et al. (2000). Analysis of yeast protein kinases using protein chips. *Nat Genet*, 26(3), 283-289.

Studies of the spectral properties of Phenothiazines

Adriana, Smarandache¹, Andra, Militaru¹, Viorel, Nastasa¹, Jette, Kristiansen² and Mihail-Lucian, Pascu¹

¹Department of Lasers, National Institute for Lasers, Plasma and Radiation Physics, 409 Atomistilor str., 077125, Bucharest-Magurele, Romania

²Department of Clinical Microbiology, Sønderborg Sygehus, County of Sønderjylland, 6400-DK, Denmark

Keywords: phenothiazines, thioridazine, absorption, laser, surface tension.

Frequent occurrences of cumulated drugs in the environment could induce an irreversible adversity by directly threatening the function of the ecosystem, increasing the resistance of bacteria to drugs, and spreading the medicines resistance genes into the environment (The Handbook of Environmental Chemistry, 2005).

Therefore, it is very important to establish and permanently improve sensitive and selective analytical methods and procedures for identifying, detecting and determining such pollutants in the environment. One of the most sensitive methods is based on the spectroscopic properties (absorption and emission of radiation) of these substances.

In the past decade there are many studies concerning the occurrence, evolution, detection and removal of some pharmaceutical pollutants from environment. They are focused on the most frequent used drugs: antibiotics, analgesics, β -blockers, some neuro-psychiatrics. Considering the last category this report is focused on the Phenothiazines class, particularly on Thioridazine.

Thioridazine (10-[2-(1-methyl-2-piperidyl)ethyl]-2-(methylthio)phenothiazine) is a piperidine typical antipsychotic drug belonging to the phenothiazine drug group and is widely used in the treatment of schizophrenia and psychosis. Also, it is used in congestive heart failure and recent studies provide antibacterial properties, which allow to consider this substance in the context of reversal of drug resistance (L.Amaral, J.E.Kristiansen, 2006).

Thioridazine is a compound existing in two mirror image forms. Enantiomers have the same physical properties except for their interaction with polarized light, leading to rotation of the plane of polarization. This property is used for chiral compounds and the direction of the rotation is given by (+) for right-rotation and (-) for left-rotation. The sum of the degree of polarization of the enantiomers may be zero for racemic mixture -Rac- (O.Hendricks, Ph-D thesis, 2006).

This study reports time evolution absorption measurements of Thioridazine HCl (Thr) in its three forms: Rac / (-) / (+). The stability measurements were carried out in solutions in ultra-pure, de-ionized water (delivered via a sterile filter). The concentration range was 10^{-5} M – 10^{-3} M. The samples were kept in three temperature/light conditions: 4°C in dark, 22°C in dark and 22°C in daylight. The

absorption spectra were recorded between (200 – 1300) nm, using a Perkin-Elmer Lambda 950 UV-Vis-NIR spectrophotometer, with an intrinsic error limit of $\pm 0.004\%$. Optical cells of 1cm thickness were used.

The absorption spectra exhibit broad peaks in UV at 262nm and 313nm and very short peaks in NIR at 966nm, 1153nm and 1240nm. In daylight conditions, the 10^{-3} M solutions change their color as follows: after ~ 45h in light-blue, after ~ 70h in blue-green, after ~ 96h in light-yellow and after ~ 150h in light-brown. These changes are associated with the appearance in the absorption spectra of two peaks at 632nm and 882nm.

We exposed Rac / (-) / (+) 10^{-5} M solutions at 266nm Nd : YAG pulsed laser radiation for 1h, 2h and 3h. The laser beam has the repetition rate 10pps, FTW 5ns and the pulse average energy on the sample 0.263mJ. Following the irradiation, the absorption spectra were recorded using 1cm optical length cell. These spectra highlight a flattening of the curves with the increasing of the time irradiation.

The Rac / (-) / (+) 5×10^{-2} M solutions were exposed at 355nm Nd:YAG pulsed laser radiation for 1, 5, 10, 15 and 30min, as well. The laser beam had the same characteristics except for the beam energy (1.45mJ/pulse). The absorption spectra following irradiation were conducted in 1mm optical length cells. These spectra marked out the appearance of the 632nm peak, but only for the 1min. and 5min. irradiation time.

The surface tension measurements were conducted for the fresh Rac / (-) / (+) 10^{-3} M solutions in ultra-pure water and for Rac / (-) / (+) 10^{-3} M kept in 22°C daylight conditions.

In conclusion, the exposure of Thr solutions in water to coherent or un-coherent light for a short time leads to reversible modifications of Thr molecules.

References:

1. The Handbook of Environmental Chemistry Vol. 5, Part O (2005): 181–244;
2. Amaral L, Viveiros M, Kristiansen JE., Curr. Drug Targets 2006; 887–91.
3. O.Hendricks, Ph-D thesis, 2006;

Acknowledgements: This research was supported by: ANCS, project LAPLAS 3-PN 09 33 and COST Action BM0701 (ATENS).

Beyond structural imaging – cornea examination using combined air-puff tonometry and OCT system with swept source laser.

Karol Karnowski¹, David Alonso Caneiro¹, Bartłomiej Kaluzny², Maciej Szkulmowski¹, Andrzej Kowalczyk¹, Maciej Wojtkowski¹

¹Institute of Physics, Nicolaus Copernicus University, ul. Grudziadzka 5, PL-87 100 Torun, Poland

²Dept of Ophthalmology, Collegium Medicum UMK, Bydgoszcz, Poland

Keywords: Optical Coherence Tomography, tonometry, swept source, cornea, intraocular pressure.

Optical Coherence Tomography (OCT) is noninvasive and noncontact biomedical imaging method widely used for *in vivo* human eye examination. Its potential for anterior segment was already presented. Even though first OCT images of cornea were performed with 800nm time domain OCT system [1], light sources as swept lasers centred at 1300nm ensure better penetration through the sclera [2-4]. Since high repetition rates of swept sources are feasible, not only structural imaging but also functional analysis of anterior segment is possible.

Tonometry - procedure of determining the intraocular pressure (IOP) of the human eye - is especially important for diagnose and evaluation of patients with different pathologies such as glaucoma. Non-contact tonometry uses air-puff system to flatten cornea and infer IOP value from cornea response [5-6].

In this contribution a novel system combining tonometry air-puff method with high speed SSOCT system working with a 1300nm tunable laser is presented (Fig 1). The system provides 50 000 axial scans per second with high resolution.

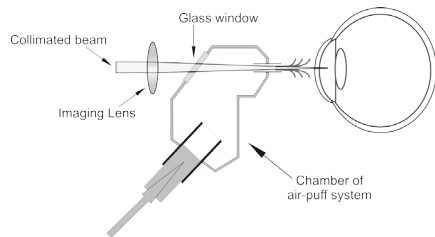


Figure 1. Basic scheme of combined air-puff SSOCT system.

Imaging head and air-puff chamber are aligned in axis to ensure the measurements are taken at the central point of the applied air stream. During cornea applanation/relaxation a M-scan is recorded. Temporal changes of cornea surfaces and the anterior surface of the human eye are observed in time period of approximately 20ms (Fig 2 top).

The dynamics of relative cornea surfaces and anterior surface of the lens can be analysed separately (Fig 2 bottom).

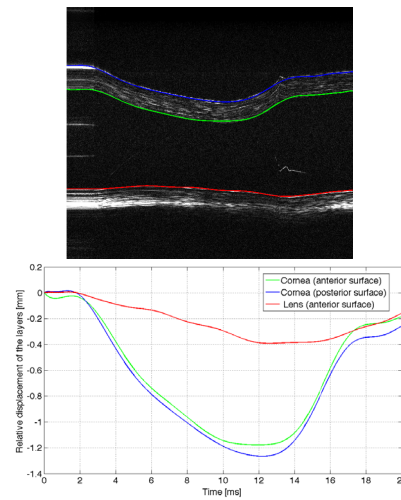


Figure 2. Top: M-scan taken during applanation/relaxation process. Detected layers are superposed to the image. Bottom: Relative displacements of cornea and lens layers during measurement.

[1] J. A. Izatt, M. R. Hee, E. A. Swanson, C. P. Lin, D. Huang, J. S. Schuman, C. A. Puliafito and J. G. Fujimoto "Micrometer-scale resolution imaging of the anterior eye *in vivo* with optical coherence tomography", *Arch Ophthalmology*; 112:1584-1589

[2] S. Radhakrishnan, A. M. Rollins, J. E. Roth, S. Yazdanfar, V. Westphal, D. S. Bardenstein, and J. A. Izatt, "Real-time optical coherence tomography of the anterior segment at 1310 nm," *Arch Ophthalmol* 119, 1179-1185 (2001)

[3] M. Miura, K. Kawana, T. Iwasaki, T. Kiuchi, T. Oshika, H. Mori, M. Yamanari, S. Makita, T. Yatagai, and Y. Yasuno, "Three-dimensional anterior segment optical coherence tomography of filtering blebs after trabeculectomy," *Journal of glaucoma* 17, 193-196 (2008)

[4] Michalina Gora, Karol Karnowski, Maciej Szkulmowski, Bartłomiej J. Kaluzny, Robert Huber, Andrzej Kowalczyk, and Maciej Wojtkowski, "Ultra high-speed swept source OCT imaging of the anterior segment of human eye at 200 kHz with adjustable imaging range," *Opt. Express* 17, 14880-14894 (2009)

[5] Goldman H, Schmidt TH. Uber Applanations-tonometrie. *Ophthalmologica*. 1957; 134: 221-242

[6] Goldman H, Schmidt TH. Uber Applanations-tonometrie. *Ophthalmologica*. 1957; 134: 221-242

Broadband blue light in OCT

Sylwia Kolenderska¹, Maciej Wojtkowski¹

¹Department of Physics, Nicolaus Copernicus University, Torun, 87-100, Torun, Poland

Keywords: SHG, OCT, blue light.

The Optical Coherence Tomography (OCT) is relatively new, effective, noninvasive method used mainly for eye imaging. It uses Michelson's interferometer to locate consecutive layers in tissue and gives images that can be extremely helpful for physicians. The natural direction of development of such interferometric techniques is to increase an amount of information being obtained and to accomplish this goal it seems obvious to use shorter wavelengths and broader spectra. The easy way to get to the wavelengths of light shorter than those presently used in OCT such as 1300 nm, 1060 nm or 810 nm is to introduce second harmonic generation (SHG), which enables us to obtain 405 nm.

SHG is a nonlinear phenomenon that makes its appearance while illuminating a crystal with light of a high energy – as a result after passing the medium the light contains wavelength that is two times shorter than the original. Some conditions must be met, though, to observe the effect for particular wavelength and the most important is the phase matching condition that can be extracted either from calculating intensity formula for SHG (1):

$$I_2 = |E(2\omega, L)|^2 \propto I_1^2 \left[\frac{\sin(2k_1 - k_2)L}{(2k_1 - k_2)L} \right]^2$$

(1)

or the formula for energy conservation in the process. The final result remains the same:

$$\Delta \vec{k} = \vec{k}_2 - 2\vec{k}_1 = \frac{2\omega}{c} [n(2\omega) - n(\omega)] = 0$$

It means that refractive index for second harmonic ($n(2\omega)$) must be equal to the refractive index of the original light so the intensity of second harmonic is biggest. In isotropic media it can not be performed due to dispersion and that is why SHG appears only in anisotropic media – it is possible to find direction in which both refractive indices are equal by simply changing the position of crystal with respect to the incoming beam.

Second harmonic light generated in our setup is estimated to have FWHM of about 80 nm, but as far as the method itself is concerned it seems that presented way of obtaining broadband blue light is not very efficient. Great amount of red light is lost because of low SHG conversion efficiency that is proportional to the square of intensity of original light illuminating the crystal (what can be deduced from (1)). Nevertheless the amount of blue light generated in this way is useful in OCT imaging, for example for imaging tissues, which is the next step of this research.

Book: V. G. Dmitriev, G. G. Gurzadyan, D. N. Nikogosyan, Handbook of Nonlinear Optical Crystals, Springer-Verlag, 1957.

Journal: I. S. Ruddock, Nonlinear optical second harmonic generation, European Journal of Physics, 1994, 15 53.

Removal of Interfering Gases in LPAS Breath Biomarker Concentration Measurements

Ana M. Bratu, Cristina Popa, Consuela Matei, Stefan Banita, and Dan C. Dumitras

Department of Lasers, National Institute for Laser, Plasma, and Radiation Physics,
409 Atomistilor St., PO Box MG-36, 077125 Bucharest, Romania

Keywords: ethylene, laser photoacoustic spectroscopy (LPAS), breath analysis, KOH scrubber

Normal human breath contains a few atmospheric molecules, e.g., H₂O, CO₂, N₂, O₂, in relatively high concentrations, several volatile compounds (VOC's), e.g., acetone, ammonia, ethane, methane, nitric oxide etc., at parts per million (ppm) or sub ppm levels and about four hundred major VOC's at the ppb or parts per trillion (ppt) levels [1]. To date, some VOC's have been established as biomarkers for specific diseases or metabolic disorders.

Ethylene from the human breath is a biomarker of oxidant stress and can be directly attributed to biochemical events surrounding lipid peroxidation [2].

LPAS experimental setup used in the present work consists of a home-built CO₂ laser, a photoacoustic (PA) cell, a vacuum/gas handling system, and a detection unit [3]. We monitored the time evolution of PA signal detected from a healthy human in different experimental conditions with the purpose of removing of interfering gases.

At present many research groups are actively involved in the development of LPAS systems for various applications in different disciplines, including nondestructive evaluation of materials, environmental analysis, agricultural, biological, and medical applications, investigation of physical and many others. Our facility, which was originally designed for ethylene analysis at the low parts per billion level, is adaptable with minor modifications to a broad range of gases and vapors having absorption spectra in the infrared (IR).

Biological samples for exhaled air contains CO₂ in much higher quantities than other compounds and interfere with the useful signal due to ethylene absorption. In order to reduce the high quantity of CO₂ from human breath, it is necessary to introduce in the system a chemical scrubber such as KOH. We have investigated the efficiency of the KOH scrubber using three recipients with different volumes (13 cm³, 90 cm³, 213 cm³), and found out what type has to be used in order to reduce the amount of the CO₂ in the measured sample, which interfere with the trace gas to be measured.

Due to the exact coincidence of the vibrational-rotational transitions with the CO₂ laser lines, the carbon dioxide is inevitably excited by CO₂ laser radiation ($\alpha(\text{CO}_2) \cong 2.1 \times 10^{-3} \text{ atm}^{-1} \text{ cm}^{-1}$), and

the related photoacoustic signal may exceed the trace signal [4]. In exhaled breath, the CO₂ concentration is usually ~ 5 %.

By measuring the PA signal from the breath of healthy human without a KOH scrubber, we obtained an equivalent ethylene absorption concentration of 1.8 ppm representing the contribution to absorption of the 10P(14) CO₂ laser line mainly by ethylene, carbon dioxide, water vapors and ammonia.

When we have used a trap with a small volume of KOH scrubber of 13 cm³, the PA signal decreased to an equivalent ethylene concentration of 300 ppb, indicating that the CO₂ concentration was reduced by a factor of 6.

A larger KOH trap proved to be more efficient in removal of CO₂ from the exhaled air. For a trap with a volume of 90 cm³, the measured equivalent ethylene concentration was 50 ppb, indicating that most of the CO₂ was removed. The same results were obtained with an even larger trap, having a volume of 213 cm³.

The conclusion of our study is the necessity of removal of the CO₂ from breath samples when low concentrations of ethylene or ammonia have to be measured. This can be accomplished by introducing a trap containing KOH with a volume of 50 – 100 cm³, depending on the rate at which the gas is transferred into the PA cell.

1. C. Wang and P. Sahay, "Breath Analysis Using Laser Spectroscopic Techniques: Breath Biomarkers, Spectral Fingerprints, and Detection Limits", *Sensors* 2009, 9, pp: 8230 – 82623.
2. G. J. Handelman, "Current Studies on Oxidant Stress in Dialysis", *Blood Purification* 21, 2003, pp: 46-50.
3. D.C. Dumitras, S. Banita, A.M. Bratu, R. Cernat, D.C.A. Dutu, C. Matei, M. Patachia, M. Petrus, C. Popa "Ultrasensitive CO₂ laser photoacoustic system", *Infrared Physics & Technology Journal*, 2010, 53, No. 5, pp. 308-314.
4. D.C. Dumitras, D.C. Dutu, C. Matei, A.M. Magureanu, M. Petrus, C. Popa, *Laser photoacoustic spectroscopy: principles*,

Principles and methods of imaging in biomedicine

Consuela Matei¹, Mihai Patachia¹, Stefan Banita¹, Doru C.A. Dutu¹ and Dan C. Dumitras¹

¹Department of Lasers, National Institute for Laser, Plasma and Radiation Physics, 409 Atomistilor str., P.O. Box MG-36, 077125 Bucharest-Magurele, Romania

Keywords: medical imaging, optical tomography, image reconstruction, breast cancer.

Biomedical optics is a rapidly growing area of research. The most common medical imaging modalities include X-ray radiography, ultrasound imaging (ultrasonography), X-ray computed tomography (CT), and magnetic resonance imaging (MRI). The optical imaging is the most recently emerged and combines excellent functional qualities with a good imaging depth and spatial resolution, considering fast data acquisition rates and a low cost per investigation (Wang & Wu, 2007). The optical imaging has only recently become clinically feasible as a result of significant improvements in optical detectors, sources, and components, coupled with important advances in the understanding of the interaction between light and tissue. Our interest is concentrated on the diffuse optical tomography (DOT) technique, as a potential diagnostic tool for detecting growth in translucent soft tissue. Its principle is to use multiple movable light sources and detectors attached to the tissue surface to collect information on light attenuation, and to reconstruct the internal 2d or 3d absorption and scattering distributions. Unusual growth inside the tissue may be discerned from the recovered optical densities because tumorous tissue has different scattering and absorption properties.

We have developed in our laboratory a continuous-wave (cw) near infrared spectroscopy (NIRS) system using the hardware structure of the cwDOT system. The system contains two spatially combined laser diode sources (at 785 nm and 830 nm operating wavelengths), a silicon photodiode (SiPhD), a transimpedance amplifier and two lock-in amplifiers, which can acquire 128 independent measurements through two time-division-multiplexed optic scheme with eight illumination fibers and eight detector fibers in the measuring head (optode). This complex structure enable us to investigate the signal dependence by the distance between light source and receiver and dynamic spectral measurements when the system uses eight special distributed light sources and eight receivers.

The system was developed for the near-infrared optical mammography, a noninvasive optical imaging technique that provides unique, quantitative physiological information and could greatly enhance current screening and diagnostic monitoring for the breast. Nearinfrared spectra are sensitive to several important physiological components in tissue such as oxyhemoglobin,

deoxyhemoglobin, water, and lipids. In the clinical management of breast disease, such functional information suggests a variety of potential medical applications: therapeutic monitoring (angiogenesis, chemotherapy), supplemental lesion characterization (benign vs. malignant), and risk assessment (origins of mammographic breast density).

For the clinical use, an effective reconstruction algorithm is crucial for imaging the otherwise inaccessible scattering and absorption distribution inside the tissue. Based on our specific configuration, we present our trials to develop the image reconstruction algorithm.

Photon transport in biological tissue can be numerically simulated by the Monte Carlo method. The trajectory of a photon is modeled as a persistent random walk, with the direction of each step depending on that of the previous step. By tracking a sufficient number of photons, the physical quantities characterizing the tissue can be estimated (Heiskala et al., 2005). Analytically, the same process of photon transport can be modeled by the radiative transfer equation (RTE). Because the RTE is difficult to solve, it is often approximated to a diffusion equation, which provides solutions that are more computationally efficient but less accurate than those provided by the Monte Carlo method (Chang et. al, 1998).

We shall present the underlying mathematics of our model for the scattering and absorption process, the results obtained applying the linear perturbation theory to the RTE, and mention the circumstances in which the inverse problem is reasonably well-posed. The factors influencing the system complexity and performance will be also discussed together with consideration for the future experimental design.

- 1) Lihong V. Wang, Hsin-I Wu, *Biomedical Optics*, Wiley-Interscience, 2007
- 2) J. Heiskala, K. Kotilahti and I. Nissilä, "An application of perturbation Monte Carlo in Optical Tomography ", *Proceedings of the 2005 IEEE Engineering in Medicine and Biology 27th Annual Conference*, Shanghai, China, September 1-4, (2005)
- 3) J. Chang, H.L. Graber, R.L. Barbour, "Dependence of image quality on image operator and noise for optical diffusion tomography", *Journal of Biomedical Optics*, Vol.3, No. 2, p. 137-144, 1998

Ethylene concentration measurement at fruits using LPAS

S. Banita^{1,2}, D. C. A. Dutu¹, C. Matei¹, A.M. Bratu¹, M. Petrus¹, C. Achim¹, M. Patachia¹, and D. C. Dumitras¹

¹Department of Lasers, National Institute for Laser, Plasma and Radiation Physics,
409 Atomistilor St., PO Box MG-36, 077125 Bucharest, Romania

² Faculty of Applied Sciences, University Politehnica Bucharest, Romania.

Keywords: ethylene, reactive oxygen species, lipid peroxidation, laser photoacoustic spectroscopy

e-mail: stefan.banita@inflpr.ro

Laser photoacoustic spectroscopy (LPAS) is a highly sensitive method for analyzing low molecular weight gases such as the natural plant hormone (phytohormone) ethylene [1].

Plants (unlike animals) lack glands that produce and secrete hormones, instead each cell is capable of producing hormones [2]. Under normal conditions plants grow and reproduce; yet, plants are often faced with a changing – sometime extreme – environment that can cause unfavorable conditions and in such an environment plants are considered to be stressed [3].

Environmental stress (abiotic) includes: salinity, toxicity (pesticides or fertilizers), irradiation, exposure to high temperature, flooding and drought, freezing and growth hormone. These metabolic disturbances in fruits (vegetables) are followed by significant and rapid changes in the rate of ethylene emission [4]. A result of stress is the formation of reactive oxygen species (ROS) and the ROS in plant tissue can initiate the lipid peroxidation that causes damage on cell membranes and is considered the most important mechanism of tissue damage [5]. Lipid peroxidation is the free radical induced oxidative degradation of polyunsaturated fatty acids (PUFA).

These studies concentrate on the accurate measurement of ethylene concentrations at fruits (vegetables) under stress conditions and comparing them with ethylene concentrations from the organic fruits (without toxicity, artificial hormones or irradiation etc.).

To evaluate the concentration of ethylene released by plants we have used a very performant laser photoacoustic system [6, 7] able to measure concentrations at sub-ppb level. We started the measurements to compare the ethylene concentrations of organic fruits compared to stressed fruits.

What we expect? We should obtain a higher level of ethylene at fruits under stress conditions whereas for organic fruits we should obtain a lower level of ethylene.

Trace gas detection techniques based on photoacoustic spectroscopy make it possible to discover and control plant physiology mechanism. Many agriculturally interesting gases can be

measured in situ and in real time with CO₂ based photoacoustic spectrometers.

1. R. Cernat, C. Matei, A.M. Bratu, C. Popa, D.C.A. Dutu, M. Patachia, M. Petrus, S. Banita and D.C. Dumitras, "Laser photoacoustic spectroscopy method for measurements of trace gas concentration from human breath", Romanian Reports in Physics 62, 2010, pp. 610-616.
2. www.essortment.com, 17.03.2011
3. E. Santosa, 2002, "Oxidative stress and pathogenic attack in plants, studied by laser based photoacoustic trace gas detection", PhD thesis, University of Nijmegen, The Netherlands.
4. F. Bijnen, 1995, "Refined CO-laser photoacoustic trace gas detection; Observation of anaerobic processes in insects, soil and fruit", PhD thesis, University of Nijmegen, The Netherlands.
5. T. Groot, 2001, "Trace gas exchange by rice, soil and pears; A study based on laser photoacoustic detection", PhD thesis, University of Nijmegen, The Netherlands.
6. D. C. Dumitras, D. C. Dutu, C. Matei, A. M. Magureanu, M. Petrus, C. Popa, "Laser photoacoustic spectroscopy: principles, instrumentation, and characterization", JOAM 9, 2007, pp. 3655-3701.
7. D.C. Dumitras, S. Banita, A. M. Bratu, R. Cernat, D. C. A. Dutu, C. Matei, M. Patachia, M. Petrus, C. Popa, "Ultrasensitive CO₂ laser photoacoustic system", Infrared Physics & Technology Journal 53, 2010, pp. 308-314.

Research concerning the interaction between pulsed laser radiation and urological stones

Radu-Florin Stancu, Dmitri Dvornikov, Brindus Comanescu, Mihai Serbanescu

¹Optoelectronica-2001 SA, 077125 Magurele, Ilfov, Romania

Keywords: laser, urology, stones, lithotripsy

Laser lithotripsy is a surgical procedure mainly used for fragmenting and removing stones from the urinary tract (kidneys, bladder).

Our research aims to study and improve the lithotripsy procedure by experiments involving in vitro interactions between Thulium fiber laser pulsed radiation and urological stones.

Nowadays, the commonly used for the urological stone fragmentation is the Ho:YAG laser. The mechanism of lithotripsy is mainly photo-thermal and implicates a process of thermal drilling and less a shockwave impact (obtained using ultrasound lithotripters). The laser pulses create a weak acoustic wave that causes the movement of stones in the urinary tract. The laser energy is transmitted to the stone through a quartz optical fiber. To obtain optimum results, the quartz fiber must be guided by a cystoscope that is in direct contact with the urological stone's surface. The most powerful effect takes place exactly at the end of the fiber. While emitting the laser pulse, there is a microscopic air bubble on the tip of the fiber which allows the delivery of the entire pulse energy in the stone, avoiding the dispersion in the fluid medium around.

In our experiments, we propose the Tm fiber laser as a viable alternative for the Ho:YAG laser.

In laser lithotripsy, fragmentation is due to two mechanisms. First - ablation of material directly due to interaction of laser radiation with matter of surface layer of stone. Second - creation of shock waves inside the stone with the expansion of plasma bubbles produced while the interaction of laser radiation with the stone's surface.

Effectiveness of the method depends on size, mechanical properties, stone localization, as well as the parameters of the laser pulses and the characteristics of laser interaction with matter. Mechanical and strength properties are largely determined by the composition and structural features of stones.

To increase the efficiency of laser ablation of a particular type of stone material, reducing the impact of laser radiation to surrounding tissue, preventing the destruction of the output end of the fiber and as a consequence, the selection of the most effective and benign modes of fragmentation of stones, is necessary to investigate a number of factors, whose influence must be considered when designing equipment for laser lithotripsy:

- The change of microstructure and mechanical

properties of stones matter under the influence of laser pulses.

- Effect of parameters of laser radiation on the effectiveness of ablation of stones.
- Efficiency of fragmentation in dependence on exposure mode settings.

It is necessary to evaluate the change of micro-mechanical parameters and the effectiveness of fragmentation according to the following factors: wavelength of laser light, pulse energy, pulse duration, repetition rate, number of pulses N in a train, features of radiation focusing conditions on the sample.

The experiments using the Tm fiber laser showed good and interesting results, fast and efficient stone fragmentation. Based on our conclusions, the Tm fiber laser technology may become an important solution for laser lithotripsy in the near future.

References:

Book: Prokar Dasgupta, John Fitzpatrick, Roger Kirby, Indebir S. Gill, "New technologies in urology", Springer Verlag London, 2010

Journals:

1. Larizgoitia, J.M.V. Pons. 'A systematic review of the clinical efficacy and effectiveness of the holmium YAG laser in urology.' *BJU International*, 1999, 84, 1- 9.
2. John Canning, 'Fiber lasers and related technologies', *Optics and Lasers in Engineering* 44 (2006) 647-676

Method for measuring the effective pulse duration of nanosecond laser pulses

Liviu Neagu¹, Laurențiu Rusen¹, Alexandru Zorilă¹, Aurel Stratan¹, George Nemeș²

¹Solid State Laser Laboratory, Laser Department, National Institute for Laser, Plasma and Radiation Physics, 077125, Măgurele, Romania, <http://sll.inflpr.ro>; liviu.neagu@inflpr.ro

²ASTiGMATTM, Santa Clara, CA 95050, USA, <http://astigmat-us.com>; gnemes@astigmat-us.com

Keywords: effective pulse duration, nanosecond laser pulses, laser-induced damage threshold, ISO measurements, fast photodiode.

A method to measure the effective pulse duration of a real, 10 Hz repetitively pulsed, nanosecond laser beam, according to the definition used in the current ISO 11254 and in the draft ISO 21254 standards, is reported. The effective pulse duration of a laser pulse is an important parameter of the procedure S-on-1, used to characterize the laser-induced damage threshold (LIDT) of optical materials and components. It is different than the more conventional definition of the pulse duration using the full-width at half-maximum (FWHM) criterion. The effective pulse duration, in comparison to other pulse-width definitions, is better suited to characterize the LIDT of optical materials [1]. This advantage is based on the averaging procedure used in the definition of the effective pulse duration, making it relatively insensitive to the pulse-to-pulse fluctuations of the pulse shapes from repetitive lasers. The effective pulse duration, t_{eff} , is defined as

t_{eff} = integrated area under the pulse shape versus time (in units of photodiode signal x time units) / peak pulse value (in units of photodiode signal)

The technique uses a fast photodiode with a bandwidth greater than 1.5 GHz for measuring the temporal intensity profiles of nanosecond laser pulses with 10 Hz repetition frequency. The photodiode signal is recorded by a wide bandwidth

digital sampling oscilloscope. The two parameters involved in the calculation of the effective pulse duration are the sampling time and the maximum amplitude of the signal collected by the photodiode. These parameters are extracted from the signal curve recorded by the oscilloscope after computation.

Preliminary results of measurements at 1064 nm, 532 nm, and 355 nm pulses from the Quantel type Brilliant B 10 SLM flash-pumped Nd:YAG laser are reported.

The technique of measuring the effective pulse duration will be implemented to an automated test-station under development within the framework of the Project ISOTEST – "Facility for laser beam diagnosis and ISO characterization/certification of behavior of optical components/materials subjected to high power laser beams".

References:

[1] ISO/FDIS 21254 - 1, "Lasers and laser-related equipment - Test methods for laser-radiation-induced damage threshold - Part 1: Definitions and general principles".

Acknowledgments: This work is done within the framework of the Project No. 172/2010 - ISOTEST- sponsored by the National Authority for Scientific Research (ANCS-POSCCE), Romania.

Experimental study of femtosecond laser-induced periodic surface structures on metals

Catalina Radu¹, Adrian Dinescu², Marian Zamfirescu^{1,2}

¹ National Institute for Laser, Plasma and Radiation Physics, Atomistilor 409, 077125 Magurele, Romania

² National Institute for Research and Development in Microtechnology, Str. Erou Iancu Nicolae 126A, 077190 Bucharest, Romania

Keywords: surface laser nanostructuring, LIPSS, femtosecond laser ablation.

Ripples or laser-induced periodic surface structures (LIPSS) have been observed near the ablation threshold of materials since the beginning of laser processing of materials [1]. Further experimental studies reported different types of LIPSS: low-spatial frequency LIPSS (LSFL) [2] and high-spatial frequency LIPSS (HSFL) with the spatial period in some cases $\lambda/6$ [3]. This surface ripple formation during the laser irradiation has been reported on many types of materials [1-4].

In this work, we performed an experimental study of LIPSS formation in air. Metallic samples (Cr, Ti, Pt, Ni) were processed by linearly polarised Ti:Sapphire laser beam (Clark CPA-2101) with $\lambda = 775$ nm, rep. rate – 2 kHz, pulse duration – 200 fs. A laser scan head with 100 mm focal length lens was used to process the samples.

To determine the influence of the laser processing parameters on the surface morphology, parallel series of lines were produced on each sample. These were produced by varying the scan speed from 0.5 mm/s to 10 mm/s.

The surface morphology is determined from SEM images (Fig. 1).

of incident electrical laser field is indicated with double arrows.

In our experiments low-spatial frequency LIPSS (LSFL) perpendicular to the laser polarization and high-spatial-frequency LIPSS (HSFL) parallel to the laser polarization direction were obtained.

From Table 1, we see the periodicity of the ripple structures on different surfaces after the laser irradiation in regular laboratory environment.

Table 1. The periodicity of LIPSS on different surfaces.

Materials	Periodicity Λ (nm)	
Ni	HSFL: 160-190 nm	
	HSFL: 300-330 nm	⊥
	LSFL: 600-660 nm	⊥
Ti	HSFL: 90-120 nm	
	LSFL: 460-530 nm	⊥
Pt	HSFL: 190-220 nm	
	LSFL: 650-680 nm	⊥
Cr	HSFL : 120-140 nm	⊥
	LSFL: 630-690 nm	⊥

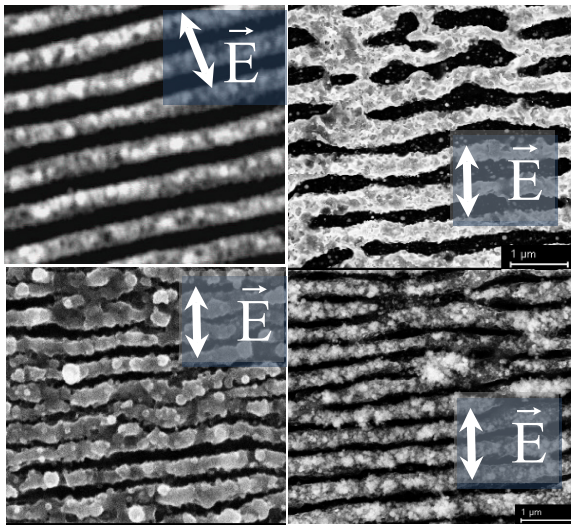


Figure 1. SEM images of ripples obtained on Ni, Pt, Cr, Ti for different irradiation conditions. Direction

Acknowledgment

M. Zamfirescu acknowledges the support of the Sectoral Operational Programme Human Resources Development (SOP HRD), financed from European Social Fund and by Romanian Government under the contract number POSDRU/89/1.5/S/63700.

[1] M. Birnbaum, Semiconductor surface damage produced by ruby lasers, *J. Appl. Phys.* **36**, 3688 (1965).

[2] D. Dufft, A. Rosenfeld, S.K. Das, R. Grunwald, and J. Bonse, Femtosecond laser-induced periodic surface structures revisited: A comparative study on ZnO, *J. Appl. Phys.* **105**, 034908 (2009).

[3] J. Bonse, H. Sturm, D. Schmidt, W. Kautek, Chemical, morphological and accumulation phenomena in ultrashort-pulse laser ablation of TiN in air, *Appl. Phys. A* **71**, 657–665 (2000).

Effective area measurement of real laser beams

Laurentiu Rusen¹, Alexandru Zorila¹, Liviu Neagu¹, Aurel Stratan¹, George Nemes²

¹Solid State Laser Laboratory, Laser Department, National Institute for Laser, Plasma and Radiation Physics, 077125, Magurele, Romania

²ASTIGMAT-Optical Systems and Laser Beams - San Jose, California, USA

Keywords: effective area, ISO measurement, CCD beam profiler.

This paper reports an investigation for a measurement technique for effective area of a real laser beam, according to ISO 21254. Effective area is a key parameter in S-on-1 procedure for laser induced damage threshold of optical surfaces in accordance with International Standards [1].

This technique uses spatial intensity profiles measurement of the laser radiation along the direction of propagation using a CCD beam profiler. Two types of laser have been used: a homemade diode-pumped, passively Q-switched Picosecond Laser System as well as a Thorlabs He-Ne laser. The method used to estimate the effective area is based on the Converging Second Moment measurement procedure [2]. The effective area is determined by measurement of the pixels energy distribution over a selected software aperture.

The effective area measurement technique will be implemented to an automated test-station under development in the frame of Project ISOTEST-Facility for laser beam diagnosis and ISO characterization / certification of behavior of optical components / materials subjected to high power laser beams. The preliminary experimental results are presented.

References:

- [1] ISO 21254 Laser and laser related equipment – Test methods for laser radiation-induced damage threshold,
- [2] SRG Hall and SD Knox, Traceable measurements for beam propagation ratio M^2 , Journal of Physics: Conference Series 85 (2007).

Acknowledgments: This work is made in the frame of the Project ISOTEST - supported by the ANCS-POSCCE.

Development of a high power transverse diode pumped Nd:YAG rod module

Bozhidar Oreshkov, Alexander Gaydardzhiev, Ivan Buchvarov and Anton Trifonov

Department of Physics, Sofia University, 5 James Bourchier Blvd., BG-1164 Sofia, Bulgaria

Keywords: diode-pumped, rod geometry, high power, large clear aperture

Reliable and robust diode-pumped solid-state oscillators and amplifiers with high output power, high efficiency and good beam quality are required in numerous industry applications and research areas (W. Koechner, 2007). Integral part of these systems is the diode-pumped laser module (chamber), whose characteristics determine to large extent the output parameters of the entire laser setup. For high output-power operation usually side-pumping is used and thus various pump configurations have been studied. Main focus of attention has been the development of an efficient transverse pump reflective optical systems, for which different options exist, i.e. compound parabolic (cylindrical) concentrator optical transport systems, silver- or gold-coated reflectors or diffusive reflectors ensuring uniform distribution of the pump intensity over the crystal rod. Although the diffusive ceramic reflectors are commonly used in pump chambers (H. Moon *at al.*, 1999), the ceramic reflectivity is comparably low ~96%, and the fabrication process is somewhat demanding.

In the present work we demonstrate two designs of high-power transversely diode-pumped Nd:YAG modules with improved reflector cavities based on the relatively new thermoplastic material Fluorilon-99W, which possesses high diffusive reflectivity (above 99 % at 808 nm), it is easy to fabricate and is thermally stable up to 300 °C. Each module employs dia.6-mm x 80-mm Nd:YAG rods mounted in a water-flow tube in the center of diffusive optical reflector. In the case of three-fold geometry (Fig.1a) three slits (70 mm length, 1.5 mm width) were cut into the reflector allowing direct illumination of the laser crystal by three linear diode arrays (6x40W). In the five-fold geometry (Fig.1b), five pump diode arrays were optically coupled with the laser rod through waveguide glass plates (65x1.2x4 mm) mounted in the reflector. When designing the modules, we took special care in minimizing the slit (plate) widths, aiming to decrease the pump losses.

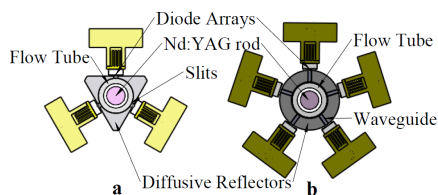


Figure 1. Schematics of the constructed modules.

We investigated the characteristics of the three-fold geometry module employing short (215

mm) flat-flat resonator with T=10 % output coupler. Lasing at 1064 nm started at 151 W of CW pump power (808 nm), the measured slope efficiency was 44%. We were able to reach a CW maximum output of 250 W, when pumping with 720 W. The measurements of the strength of the thermally induced lens, by a collimated He-Ne laser beam, show focal length from 0.8 Dpt to 2.5 Dpt for pump power 180 W and 500 W, respectively. At all levels of the output power, the observed beam spot was round with no apparent hot spots, signifying for homogeneous distribution of the pump intensity over the cross-section of the rod.

An imaging beam profiler was used to measure the fluorescence intensity integrated along the rod axis for the case of five-fold geometry module. The observed distribution is homogenous over the central 3 mm of the aperture. However, the high concentration (0.8% at) of the Nd³⁺ in crystal causes absorption of significant amount of the pump power in the first 2.5 mm of the crystal depth, close to the diode arrays. Currently we aim to ensure homogenous pump distribution over the entire aperture of the rod by optimizing the geometry of reflector cavity and selecting crystal with optimal Nd³⁺ concentration and diameter.

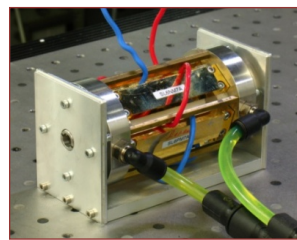


Figure 2. Prototype of fivefold geometry module.

The presented work shows an intermediate stage (Fig.2) in the development process aimed towards the construction of a high-energy (~100mJ) and high-average power (~100W) master-oscillator power-amplifier system. We plan to equip this system with a down-conversion stage for mid-IR generation in order to explore its potential for advanced medical applications.

We acknowledge financial support under grants DRG 02-4/2010 and D02-134/2009 of the Bulgarian national science fund.

W. Koechner: *Solid-State Laser Engineering* (Springer Series in optical sciences, 2007);

H. J. Moon *at al.*, Efficient Diffusive Reflector-Type Diode Side-Pumped Nd:YAG Rod Laser with an Optical Slope Efficiency of 55%, *Appl. Opt.*, (1999), **38**, 1772;

$\chi^{(2)}$ -Lens Mode-Locking of Diode-Pumped Nd-doped Vanadate Lasers

Veselin Aleksandrov, Hristo Iliev and Ivan Buchvarov

Department of Physics, University of Sofia, 5 James Bourchier Boulevard, BG-1164 Sofia, Bulgaria

Keywords: Mode-locked lasers, second-order nonlinearity, diode-pumped lasers, Nd-doped materials.

Multi-Watt operation of picosecond diode-pumped Nd oscillators has been demonstrated using two passive mode-locking methods, one based on semiconductor saturable absorber mirrors (SESAMs) and the other on intracavity frequency doubling. Although SESAMs are well established devices for use in lasers emitting around 1 μm , their residual absorption, leading to heating, is the major intrinsic drawback that limits their power scaling capabilities. On the other side, intracavity frequency doubling is a promising mode-locking approach for up-scaling the power of such picosecond solid-state lasers (Hristo Iliev, Danail Chuchumishev at all, 2010; Hristo Iliev, Ivan Buchvarov at all, 2010) because the damage threshold of the nonlinear crystals usually is an order of magnitude higher than of the SESAMs and the low residual absorption at the fundamental wave enables operation at high average power. Furthermore, this approach is generally free of spectral limitation and easily extendable to virtually any laser spectral region (Hristo Iliev, Ivan Buchvarov, Veselin Alexandrov at all, 2011).

The intracavity type-I SHG provides two different types of passive mode-locking mechanisms: The first one is amplitude shaping based on the intensity dependent reflectivity of the frequency-doubling nonlinear mirror (FDNLM) and the second one is phase shaping based on $\chi^{(2)}$ -nonlinear phase shift of the fundamental wave, i.e. $\chi^{(2)}$ -lens mode-locking (fig.1). Although this is a natural combination of two effects taking place in the same mode-locking device, $\chi^{(2)}$ -lens mode-locking assisted by FDNLM has a potential which has not been exploited effectively by far. Moreover the $\chi^{(2)}$ -lens mode-locking in contrast of Kerr-lens mode-locking is easily applicable technique to narrow bandwidth laser materials as neodymium-doped crystals.

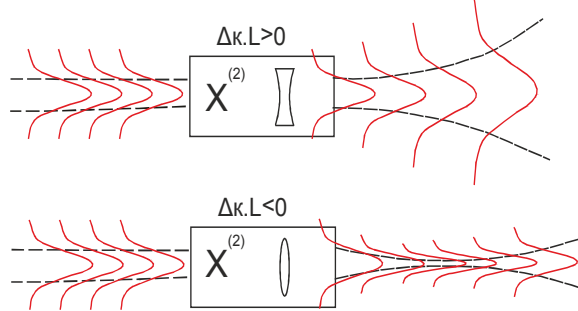


Figure 1. A schematic illustration of the $\chi^{(2)}$ -lens formation

In this work we present our experimental results on passive mode-locking of different Nd: TVO_4 ($\text{T}=\text{Y, Gd, Lu}$) laser crystals operating on the ${}^4F_{3/2} \rightarrow {}^4I_{11/2}$ and ${}^4F_{3/2} \rightarrow {}^4I_{13/2}$ transitions around 1 μm and 1.3 μm respectively.

An alternative, passive mode-locking technique based on second-order nonlinearity inside the laser cavity which utilizes $\chi^{(2)}$ -lens formation in SHG crystal assisted by the nonlinear reflection of the FDNLM is used in all experiments. FDNLM initiates the passive mode-locking process and ensures self-sustained operation while the defocusing $\chi^{(2)}$ -lens effect leads to shortening of the pulses (2.9 ps in the case of 1- μm laser system and 3.6 ps at ${}^4F_{3/2} \rightarrow {}^4I_{13/2}$ transition around 1.3 μm). Although each of the two mode-locking mechanisms in principle can be used alone for passive mode-locking of the laser, the hybrid scheme proves beneficial for the robust performance of the lasers in this study. $\chi^{(2)}$ -lens mode-locking technique provides much shorter pulse duration of the generated laser pulses which is close to the amplification bandwidths. The other advantage of the proposed method is that obtained output powers are close to the maximum value for TEM_{00} CW operation of the lasers which range from 0.5 to 5 W in both cases of 1- μm and 1.3- μm lasers. We acknowledge financial support from grant DRG 02-4/2010 and DNTS 02-24/2010 of the Bulgarian national science fund.

References

- [1] Hristo Iliev, Danail Chuchumishev, Ivan Buchvarov, and Valentin Petrov, "Passive mode-locking of a diode-pumped Nd:YVO₄ laser by intracavity SHG in PPKTP", OPTICS EXPRESS/ Vol.18, No.6, 15 March 2010, 5754-5762.
- [2] Hristo Iliev, Ivan Buchvarov, Sunao Kurimura, and Valentin Petrov, "High-power picosecond Nd:GdVO₄ laser mode locked by SHG in periodically poled stoichiometric lithium tantalate", OPTICS LETTERS/ Vol.35, No.7, April 1 2010, 1016-1018.
- [3] Hristo Iliev, Ivan Buchvarov, Veselin Alexandrov, Sunao Kurimura, and Valentin Petrov, "Steady state mode-locking of the Nd:YVO₄ laser operating on the 1.3 μm transition using intracavity SHG in BIBO or PPMgSLT", 2011, (Proceedings of SPIE 7912, 79120T

Professional Associations : benefits and responsibilities

Clementina Timus

National Institute for Laser, Plasma and Radiation Physics

Magurele, P.O. Box MG-36

077 125 Romania

E-mail: clementina.timus@inflpr.ro

The paper is discussing the importance to belong to the professional associations national and international, as well, not only as a proud but as a life school to ever improve the professional level and keep an up-dated status.

The experience to be in contact with such associations for many years allows making comments and sharing it to who is concerned.

The 10 years as advisor of SPIE Student Chapter is a proof that this talk is pertinent. The previous membership as regular SPIE member and the several responsibilities in the national organization imposed to keep contacts and acquire some skill in managing the partnership.

Some features of this experience will be discussed and mainly the activities developed during the 10 years since the SPIE Student Chapter was recognized by the SPIE board in April 2001.

The experience as SPIE Scholarship evaluator represent the subject of comments and discussions , as well as recommendations for students to take profit of this opportunity that SPIE and OSA offer to young scientists to improve the professional level.

In an ever moving economical and political systems the education should be developed in an innovative, open mind and flexible style in which the formation of a mind means a better organization, than the amount of information. The experience resulted from extra activities with young people are discussed and proposed as some good practices.

The Eastern and Central Europe countries were confronted in the last two decades with the brain drain phenomenon and many of the most brilliant minds are enrolled in the big research centers all over the world. It is known that the Romanian math school is very appreciated in States and the winners of the International Olympiad contests in mathematics, informatics and physics are invited to graduate from the most famous universities. Statistics are presented regarding recent evaluations.

Comparing education and research in a recently EU joined country – Romania with other developed countries it is possible to understand the gap the high difference and explain the drawbacks of an unstable system and tremendous consequences. A new education law had been recently launched [1] to limit the non ethical aspects happened: lack of professional authority, high level degrees too easily

obtained, too many private universities non competitive with the state universities.

The many reforms, the too large university autonomy – administrative independence opened the way of hard deregulations in the university hierarchy: too many professors and easier promotion, the barrier for the prestigious university graduated young people to access in the university hierarchy, the lack of motivation to return back and serve in the home country, frustration and disappointment of young scientists.

In research and development more than in other domains the globalization is a reality as evaluating the statistics [2] regarding the bibliometric indicators the conclusion is that the share of world scientific publications declined in the developed countries over the last 20 years. It is to note an increased share of publications in collaboration of scientists from developing countries with those from developed countries.

According the data provided by the UIS – UNESCO Institute of Statistics in 2009 referring to the human resources in R&D it is to note that the highest representation is in Asia when in the other principal regions a decrease is to note in America and Europe from 2002 to 2007 [3].

The evaluation of GERD in 2007 shows that the highest figure 4.7% is allocated in Israel 2.7% in North America, 1.6% Europe and Asia. It is easy to understand that in emerging countries the situation could be critical.

References:

1. <http://www.nature.com/news/2011/110112/full/469142a.html>
2. UIS Bulletin on Science and Technology Statistics Issue No.2, September 2005 <http://www.uis.unesco.org/template/pdf/S&T/BulletinNo2EN.pdf>
3. UIS Fact Sheet, October 2009, No.2 A Global Perspective on Research and Development <http://www.uis.unesco.org/template/pdf/S&T/BulletinNo2EN.pdf>

THz wave photonics and applications to biology and chemistry

Dascalu Traian

National Institute for Laser, Plasma and Radiation Physics, 409 Atomistilor Street,
Magurele, Jud. Ilfov, 077125, Romania

There are many new technologies which have been developed in this field since the first pulsed THz time domain spectroscopic system was invented. Benefiting from those novel technologies, THz unique properties were deeply analyzed and promising applications in biology and chemistry emerged.

In this lecture we will review the state of the art THz generation and detection methods, discuss THz wave interaction with matter and finally introduces THz applications in chemistry and biology.

In Protein structure and flexibility knowledge is crucial for understanding protein function at the molecular level.

Low frequency collective movements of proteins associated with biologically relevant conformational transitions are situated in the THz spectral region. Therefore, Time-domain spectroscopy (TDS) became a promising technology for protein structure and conformational changes investigation. We present here the experimentally derived THz spectrum of BSA against the simulated THz spectrum based on our 3D model of BSA. The observed THz absorption of BSA is explained based on the results of normal modes analysis. Experimental results of THz-TDS skin tissues with basal cell carcinoma are presented too. Finally, the use of THz spectroscopy in detecting new properties of chemical substances is introduced.

Study of laser ignition and flame kernel development in methane-air mixture

Salamu, Gabriela¹, Sandu, Oana¹, Dejanu, Marcel², Voicu, Flavius¹, Ticos, Catalin³, Popa, Dinel², Parlac, Sebastian²,

Pavel, Nicolai¹, Dascalu, Traian¹

¹Laboratory of Solid-State Quantum Electronics, National Institute for Lasers, Plasma and Radiation Physics, Magurele, PO Box MG-36, 077125, Bucharest, Romania

²Faculty of Mechanics and Technology, University of Pitesti, Targu din Vale Street, 110040, Pitesti, Romania

³Low Temperature Plasma Laboratory, National Institute for Lasers, Plasma and Radiation Physics, Magurele, PO Box MG-36, 077125, Bucharest, Romania

Keywords: Internal combustion, methane-air mixture, spark-plug, flame kernel, Shadowgraphy method.

During the last decades great effort was done for reducing the pollutant emissions caused by vehicles with internal combustion engines, because it has a large impact on the environment. The noxes reduction is mainly influenced by the ignition process.

Replacing the conventional electric spark plug with a laser-induced igniter (Koeffler *et al.*, 2007; Tsunekane *et al.*, 2010) can provide several advantages, such as ignition of leaner fuel/ air mixtures comparative with spark plug ignition. This operation brings environmental benefits because the NO_x emissions are reduced. In this presentation we report a comparative study of laser spark plug and laser induced ignition in methane-air mixtures.

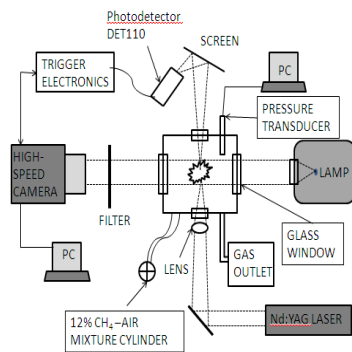


Figure 1. A sketch of the experimental set-up is shown.

The experimental set-up is shown in Figure 1. The ignition process of CH₄/ air mixture was studied experimentally in a constant- volume vessel at filling pressures between 0.1 and 0.5 MPa. The air was introduced in the combustion bomb after mixing it with 12% methane concentration. Shadowgraphy flow visualization technique (Settles, 2001) was used to investigate the flame front speed. A small dimensions Xenon lamp was used as source of illumination. A pulsed Nd:YAG laser delivering pulse energies from 12.85 to 22.85-mJ at the fundamental wavelength 1064 nm was used. The flame front development was recorded by a Photron FASTCAM 1024 PCI digital video camera and analyzed by computer.

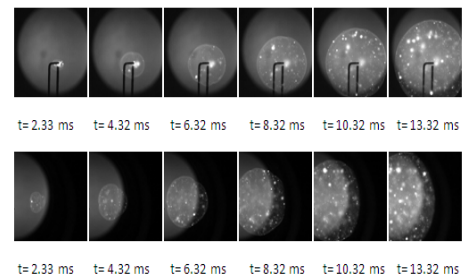


Figure 2 : Flame photographs for spark plug (upper row) and laser ignition (lower row).

Experimental conditions: CH₄/ air initial mixture; pressure: 0.1 MPa; laser energy: 22.85 mJ, light source: flash lamp; image dimensions 512 x 512 pixels.

Figure 2 shows flame photographs of the two types of ignition for the methane mixture at 0.1 MPa filling pressure of the combustion chamber. It can be seen that the cross-section area of the flame kernel generated by the laser is larger than the one generated by the spark plug for the same time range.

Further investigations aim realization and analysis of ignition process realized with a microlaser system, and comparison of the results obtained with the classical electrical-spark device.

This work was supported through the project 72150/01.10.2008 that is financed by the Romanian Ministry of Education, Research, Youth and Sports.

- H. Kofler, J. Tauer, G. Tartar, K. Iskra, J. Klausner, G. Herdin, E. Wintner, "An innovative solid-state laser for engine ignition," *Laser Phys. Lett.* **4**, 322-327 (2007).

- M. Tsunekane, T. Inohara, A. Ando, N. Kido, K. Kanehara, T. Taira, "High Peak Power, Passively Q-switched Microlaser for Ignition of Engines," *IEEE J. Quantum Electron.* **46** (2), 277-284 (2010).

- G.S. Settles, "Schlieren and shadowgraph techniques: Visualizing phenomena in transparent media," Berlin:Springer-Verlag, 2001.

Sub-nanosecond, tunable between 3 μm and 3.5 μm OPO based on PPSLT, pumped by 0.5 kHz Nd:YAG laser

Danail Chuchumishev¹, Ivan Buchvarov¹, Alexander Gaydardzhiev¹, Anton Trifonov¹, Oana Sandu², Gabriela Salamu²

¹Department of Physics, Sofia University, 5 James Bourchier Blvd., BG-1164, Sofia, Bulgaria

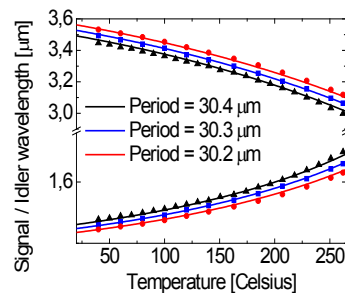
²National Institute for Laser Plasma and Radiation Physics, Atomistilor 409, CP MG 36 Bucuresti, Maguere, Romania

Sub-nanosecond coherent sources in the IR spectral region (2-4 microns) combining high average power and high pulse energy with broad tunability are of fundamental interest for both scientific and industrial applications, e.g. remote sensing, molecular spectroscopy and wide-ranging medical applications targeting water absorption band around 3 μm (Jean and Bende 2003). One of the effective ways to cover this spectral region is by utilizing optical parametric oscillators (OPO) based on periodically poled quasi phase-matched (QPM) nonlinear materials. Using QPM crystals, in an OPO pumped by 1 micron laser, is especially promising due to their exceptionally large nonlinearity, absence of spatial walk-off and ease of fabrication. One relatively new nonlinear material for a QPM based OPO in the mid-IR is periodically poled stoichiometric lithium tantalate (PPSLT). Its low coercive field (<2 kV/mm), high photorefractive damage threshold and transparency up to 5 μm make it suitable for design of high pulse-energy OPOs at high repetition rates. Here, we present a compact sub-nanosecond, short cavity, singly resonant OPO based on PPSLT, pumped by a single frequency 0.5 kHz, 1 ns Nd:YAG laser. The OPO is tuned across the 3-3.5 μm spectral range by changing the temperature of the PPSLT crystal.

We employ an 11 mm long, 10 mm wide and 2 mm (along z axis) thick PPSLT crystal with three different poled zones with domain inversion periods (30.2, 30.3 and 30.4 μm respectively). The crystal is antireflection coated for the pump, the signal and idler waves. The OPO cavity length is 23 mm with plane parallel mirrors. The rear mirror of the OPO is a silver coated mirror and the output coupler is a dielectric mirror that has high reflection for the signal and high transmission for the idler wave. The pump source is a diode pumped Nd:YAG microchip laser oscillator amplified in a two stage rod amplifier emitting up to 10 mJ at 0.5 kHz, 1 ns pulse duration with high beam quality ($M^2 < 1.4$). The maximum pump energy applied in the present work is limited to 3.9 mJ, due to the low damage threshold of the rear mirror. The pump beam is collimated to a beam diameter of 1 mm in the position of the PPSLT crystal. The idler wave is measured, after the idler-pump-separation mirror and the residual pump and signal radiations are blocked with a set of band-pass filters.

By changing the temperature of the PPSLT crystal from room temperature up to 265°C we were

able to achieve continuous tuning from 3 to 3.5 μm , employing the three domain inversion periods, Fig.1. The experimental results are in good agreement with the theoretically calculated curves, with the Sellmeyer equations derived by (Dolev, Ganany-Padowicz et al. 2009).



(solid curves).

Fig. 1. OPO temperature tuning versus domain inversion period, measured data (dots) and calculated tuning curves

The maximum output idler energy is 290 μJ at 3422 nm (idler conversion efficiency of $\sim 13\%$), whilst the overall quantum conversion efficiency is $\sim 42\%$. The idler output power remains almost constant ($\pm 15\%$) in the whole tuning range. The OPO threshold is around 500 μJ (~ 76 MW/cm²). After deconvolution with the response function of the measurement setup, the pulse duration (FWHM) of the frequency doubled idler is found to be 505 ps, corresponding to 714 ps idler duration, shorter as expected than the undepleted pump pulse duration (1 ns).

In conclusion, we have developed a sub-nanosecond mid-IR laser source, tunable between 3 μm and 3.5 μm , with 0.5 kHz repetition rate, pulse energies up to 290 μJ and ~ 700 ps idler pulse duration. To our knowledge this is the first source with such simultaneously high average power and high pulse energy. Further power scaling is possible and in progress.

We acknowledge financial support under grants DRG 02-4/2009 and D02-134/2009 of the Bulgarian national science fund.

Dolev, I., A. Ganany-Padowicz, et al. (2009). "Linear and nonlinear optical properties of MgO:LiTaO(3)." *Applied Physics B-Lasers and Optics* **96**(2-3): 423-432.

Jean, B. and T. Bende (2003). "Mid-IR laser applications in medicine." *Solid-State Mid-Infrared Laser Sources* **89**: 511-544.

Finite-Difference Time-Domain Method (FDTD) used to Simulate Micro-ring Resonator for Student Applications

Andreea Fazacaș¹, Paul Sterian,²

¹M.Sc. at University Politehnica, Bucharest, 060811, Bucharest, Romania

²Prof. at Department Physics II, University Politehnica, Bucharest, 060811, Bucharest, Romania

Keywords: micro-ring resonators, microstructure devices, integrated optics, FDTD.

Abstract

In this paper we used the Finite Difference Time-Domain Method (FDTD) to solve Maxwell equations in micro-ring resonator filter for different conditions. The simulations based on this mathematical model are very suitable to describe the losses in different types of micro-ring resonators filters.

Micro-ring resonators are the potential building block integrated circuits and they may be used as electro-optic switches or modulators, in Photonic VLSI circuits or as passive filters, for sensing and for optical telecommunications.

In 3D the system is characterized by six coupled equations, which are derived from Maxwell equations:

$$\frac{\partial \vec{H}_{x,y,z}}{\partial t} = -\frac{1}{\mu} \left[\frac{\partial E_{y,z,x}}{\partial z} - \frac{\partial E_{z,x,y}}{\partial y} - (\vec{M}_{source_{x,y,z}} + \sigma^* \vec{H}_{x,y,z}) \right]$$

$$\frac{\partial \vec{E}_{x,y,z}}{\partial t} = \frac{1}{\varepsilon} \left[\frac{\partial H_{z,x,y}}{\partial y} - \frac{\partial H_{y,z,x}}{\partial z} - (\vec{J}_{source_{x,y,z}} + \sigma \vec{E}_{x,y,z}) \right]$$

This system of six coupled partial differential equations form the basis of the FDTD numerical algorithm for electromagnetic wave interactions with general three-dimensional objects. In our simulation we consider that σ^* and σ are equal to zero.

The simulations were made for single ring and for two rings coupled to a single waveguide at different wavelengths, different refraction index and different widths in order to reduce the losses. We also calculate the mode overlap integral in order to describe the quality of the coupling for different wavelengths.

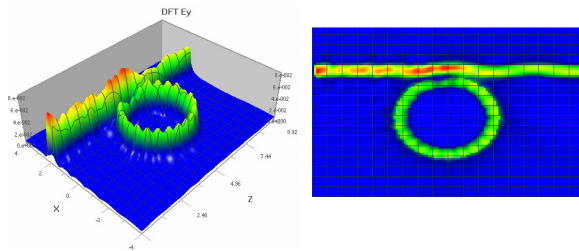


Figure 1. The evolution of Ey component versus distance in 3D and the projection (X, Z axes) in 2D for 1.4 μm.

For simulation from Figure 1 and 2 we consider a single ring coupled to a single waveguide with the following parameters: the width of the waveguide is equal to 0.5 μm, the depth 1.25 μm and the length 10 μm; the refractive index of the micro-ring and of the waveguide in the core is 2; the refractive index of the cladding is 1; the radius of the micro-ring is 1.7 μm. The separation between micro-ring and waveguide is 0.255 μm.

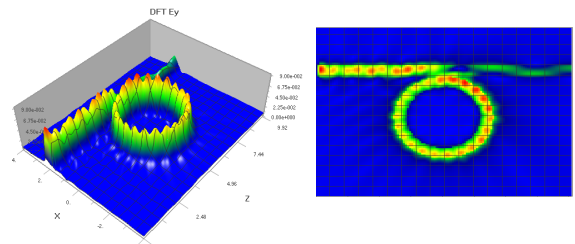


Figure 2. The evolution of Ey component versus distance in 3D and the projection (X, Z axes) in 2D for 1.42 μm

If we increase the wavelength to 1.42 μm we can see that the amplitude inside the ring is brighter than that from the input due to the constructive interference of light in the loops of the ring. For 1.42 μm this micro-ring can be used as a band-stop filter at resonance because the signal drops down.

In conclusion the FDTD Method can be useful for both designers and students performing numerical simulations as computer experiments.

References

- [1] Dennis M. Sullivan, Electromagnetic simulations using FDTD Method, New York, IEE Press, 2000
- [2] Christian Koos et al., FDTD-Modelling of Dispersive Nonlinear Ring Resonators: Accuracy Studies and Experiments, IEE Journal of Quantum Electronics, vol 42, no. 12, December 2006
- [3] S.C. Hagness et al., FDTD Microcavity Simulations: Design and Experimental Realization of waveguide-Coupled Single-Mode Ring and whispering-gallery-mode Disk Resonators, Journal of Lightwave technology, vol 15, no. 11, November 2007

Structuring your scientific paper

Prof. Dr. Jean-luc Doumond

Principiae, Kapellelaan 103 1950 Kraainem, Belgium

Papers are one of the few deliverables of the work of researchers. Well-designed, they efficiently allow each reader to learn only what he or she needs to. Poorly designed, by contrast, they confuse readers, fail to prompt decisions, or remain unread. Based on Dr Doumond's book *Trees, maps, and theorems* about “effective communication for rational minds,” the session shows how to structure scientific papers, theses, and technical reports effectively at all levels to get the readers' attention, facilitate navigation, and, in this way, get the message across optimally.

An engineer from the Louvain School of Engineering and PhD in applied physics from Stanford University, Jean-luc Doumont now devotes his time and energy to training engineers, scientists, business people, and other rational minds in effective communication, pedagogy, statistical thinking, and related themes. Articulate, entertaining, and thought-provoking, Dr Doumont is a popular invited speaker worldwide, in particular at international scientific conferences, research laboratories, and top-ranked universities. For additional information, visit www.principiae.be.

Progress at the Multi-PW ELI-NP laser facility in Romania

Daniel Ursescu¹

¹Lasers Department, National Institute for Lasers, Plasma and Radiation Physics, Atomistilor 409, 077125, Magurele, Romania

Keywords: ultra-short laser pulses, Extreme Light Infrastructure

Extreme Light Infrastructure (ELI) is one of the major research facilities to be built in Europe within next few years. It aspires to conduct fundamental and applied research at the highest intensity and the shortest duration level, through ultra intense laser beams and further radiation beams that they will generate.

The three infrastructure pillars, situated in Czech Republic, in Hungary and in Romania, will address three complementary areas of investigation: laser-produced radiation sources, attosecond pulses generation and laser-based nuclear physics, respectively. A fourth pillar is planned to be built later and to deliver intensities in the range of hundred of PW.

A short description of the multi-PW laser facility at the ELI-Nuclear Physics (ELI-NP) infrastructure will be presented. The technological issues related to the development of the laser will be presented. In the second part of my presentation I will elaborate on one major bottle-neck in the realization of the ELI-NP laser system, coherent beam combining (CBC).

CBC was chosen in several laser systems, including ELI, as a solution to increase the final attainable intensity. It is a difficult technique while it has to combine coherently in space and in time several beams amplified in different laser chains. That means in particular that the beams should be in phase in every point of the amplified beam so the spatial beam profiling techniques have to be mastered with high accuracy for all the combined beams.

Here I present alternative coherent beam combination approaches than the use of identical ultra-short pulses. The idea is to spectrally combine laser pulses with complementary spectra.

Collinear and non-collinear approaches have been modelled. Experimental demonstration of the re-phasing for two spectrally complementary ultra-short pulses will be presented.

The research leading to these results has received funding from the EC's Seventh Framework Programme (LASERLAB-EUROPE, grant agreement n° 228334) and from Extreme Light Infrastructure – Preparatory Phase project.

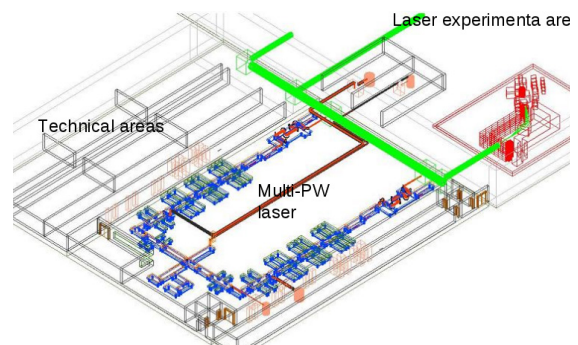


Figure 1. Lay-out of the multi-PW dual arm ELI-NP lasersystem

References:

[1] J.-P. Chambaret; O. Chekhlov; G. Cheriaux; J. Collier; R. Dabu; P. Dombi; A. M. Dunne; K. Ertel; P. Georges; J. Hebling; J. Hein; C. Hernandez-Gomez; C. Hooker; S. Karsch; G. Korn; F. Krausz; C. Le Blanc; Zs. Major; F. Mathieu; T. Metzger; G. Mourou; P. Nickles; K. Osvay; B. Rus; W. Sandner; G. Szabó; D. Ursescu; K. Varjú, Extreme light infrastructure: laser architecture and major challenges, SPIE Proceedings Vol. 7721, Solid State Lasers and Amplifiers IV, and High-Power Lasers, Thomas Graf; Jacob I. Mackenzie; Helena Jelinková; Gerhard G. Paulus; Vincent Bagnoud; Catherine Le Blanc, Editors, 77211D

[2] ELI-NP site: www.eli-np.ro

[3] R. Banici, D. Ursescu, Spectral combination of ultrashort laser pulses, EPL **94**, April 2011, p. 44002

Online damage detection using scattered radiation of the test beam

Alexandru Zorilă, Simion Săndel, Laurențiu Rusen, Liviu Neagu, Constantin Fenic, Aurel Stratan

Solid State Laser Laboratory, Laser Department, National Institute for Laser, Plasma and Radiation Physics, 077125, Măgurele, Romania, <http://ssll.inflpr.ro>, alexandru.zorila@inflpr.ro

Keywords: laser-induced damage threshold, damage detection, scattered radiation, ISO measurements.

We describe the development of a real time, online method to detect the pulsed laser-induced damages on various optical surfaces. The method is part of larger setups for S-on-1 laser-induced damage threshold (LIDT) test stations under development, for nanosecond and sub-picosecond pulses. The method is among the ones recommended by the existing ISO 11254 -1,2,3 standards and by the new, draft ISO 21254 -1,2,3,4 standards under development [1]-[4].

The method is based on the appearance and the photodetection of a pulsed scattered radiation once a permanent damage is induced by the pulsed laser beam on the sample under test. Rather than to use an independent laser beam to detect the damaged site by scattering, the scattered radiation consists of light from the damaging beam itself. The pulse from the photodetector signals that the damage was created. This pulse is used for two purposes: to stop the arrival of the subsequent laser pulses to the damaged site; and to stop the circuit counting the total number of pulses, S , arrived at the site before the damage was created. Therefore, we would be able to know the total number of pulses S inducing a permanent damage on a single site, according to the S-on-1 procedure [1]-[4]. Preliminary experimental results are presented.

This scattering detection technique is intended to be implemented in two automated test-stations under development within the framework

of the Project ISOTEST – "Facility for laser beam diagnosis and ISO characterization/certification of behavior of optical components / materials subjected to high power laser beams".

References:

- [1] ISO/FDIS 21254 - 1, "Lasers and laser-related equipment - Test methods for laser-radiation-induced damage threshold - Part 1: Definitions and general principles".
- [2] ISO/FDIS 21254 - 2, "Lasers and laser-related equipment - Test methods for laser-radiation-induced damage threshold - Part 2: Threshold determination".
- [3] ISO/FDIS 21254 - 3, "Lasers and laser-related equipment - Test methods for laser-radiation-induced damage threshold - Part 3: Assurance of laser power (energy) handling capabilities".
- [4] ISO/DTR 21254 - 4, "Lasers and laser-related equipment - Test methods for laser-radiation-induced damage threshold - Part 4: Inspection, detection and measurement".

Acknowledgments: This work is done within the framework of the Project No. 172/2010 - ISOTEST- sponsored by the National Authority for Scientific Research (ANCS-POSCCE), Romania.

Toward control of spatio-temporal couplings in ultra-short laser pulses

Razvan Ungureanu^{1,2} and Daniel Ursescu¹

¹National Institute for Laser, Plasma and Radiation Physics

409 Atomistilor St., PO Box MG-36, 077125 Bucharest, Romania

²Faculty of Physics, University of Bucharest, Romania

Keywords: ABCD optic matrix, ultra-short pulses, spatio-temporal coupling.

Following the demonstration of the chirped pulse amplification (CPA) method, tremendous progress was registered in the field of ultra-short and ultra-intense laser pulses.

However, the propagation in CPA systems used to obtain ultra-short pulses alters the beam properties by introducing of distortions in the spatio-temporal structure of the laser pulses.

Our goal is to demonstrate that several of the distortions introduced by the optical systems could be removed. This helps to maintain beam profile at system output.

In a first stage we present a simple manipulation of basic 2*2 ABCD matrix, revealing a simple situation that with three corresponding matrix of thin lenses and two of free spaces it is possible to simulate a negative distance matrix.

This result helps us to demonstrate further that any arbitrary 2*2 ABCD optical matrix can be reproduced with only five corresponding matrix of thin lens and four corresponding to free space. This means that one can compensate for spatial type distortions in the pulse.

Further, we analyse spatio-temporal couplings in ultra-short laser pulses, using the Martinez-Kostenbauder formalism [1]. The "ultimate goal" would be to find ways to transform any passive optical system in any other passive optical system, using additional compensation optical systems.

The Martinez-Kostenbauder matrix formalism includes, besides the spatial coordinates position and angle, two more coordinates, namely the time (t) and the frequency (v), providing a basis of representation for the first order spatio-temporal couplings. The general matrix system describes all possible first order distortions (fig.1).

We analyse the possibility to eliminate four kind of spatio-temporal couplings: spatial chirp (E), angular dispersion(F), pulse front tilt (G) and the so called time versus angle (H). We start from the

general matrix and we combine it with 4*4 matrices generated from thin lenses and free spaces. We succeed to eliminate each of these terms, at a time.

We also show that E and F of the general 4*4 matrix are coupled and can not be simultaneously reduced to zero using ideal thin lenses and spaces matrices. The same applies for G and H terms.

To conclude, we identify a way to control four distortion coefficients specific to ultra-short laser pulses. The study is relevant for the design of CPA amplification chains such as ELI.

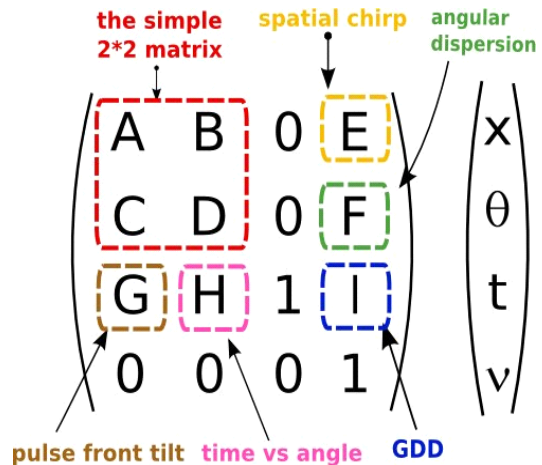


Figure 1. General matrix in Martinez-Kostenbauder formalism and spatio-temporal coordinates

References:

- [1] Selcuk Akturk, Xun Gu, Pablo Gabolde, and Rick Trebino, "The general theory of first-order spatio-temporal distortions of Gaussian pulses and beams," *Opt. Express* **13**, 8642-8661 (2005)

Multiple pulses experiments at 15 TW TEWALAS laser facility

Ovidiu, Manta^{1,2}, Razvan, Ungureanu^{1,2}, Romeo, Banici^{1,2}, Liviu, Neagu¹, and Daniel, Ursescu¹

¹The National Institute for Laser, Plasma & Radiation Physics

²University of Bucharest, Atomistilor 405, 077125, Magurele, Bucharest, Romania

Keywords: ultrashort pulses, multiple pulses generation, stretcher, compressors.

Since 2009, INFLPR uses TEWALAS laser facility. It consist in a laser with oscillator, booster, optical stretcher, a regenerative amplifier, two multi-pass amplifiers, optical compressor and interaction chamber. TEWALAS generates ultrashort pulses with less than 30 fs pulse duration, up to 390 mJ pulse energy, at 10Hz repetition rate [1].

The first TEWALAS experiments in vacuum are dedicated to studies of absorption of laser pulses in laser-produced plasmas, plasma mirrors studies for temporal contrast enhancement and soft x-ray lasers demonstration. For all these experiments, a combination of synchronized multiple pulses is needed. We generated multiple short pulses, with sub-picosecond duration, with controllable intensities ratio and delay in the tens of picoseconds time domain [2].

To create multiple short pulses, we use a beam splitter or pieces of glass to extract one pulse. We can generate short and long pulses depending on the experiment.

For the envisaged experiments, also long pulses are needed. So we implemented a delay line which take 20% from the main pulse energy before compressor, using a beam-splitter. This pulse travels on the optical table, directed by seven mirrors, in the so called delay line. The total optical path is adjustable and is comparable with the optical path length of the pulses going through the compressor. In the experimental chamber, the pulses coming from the delay line and from the compressor are transformed in focal lines. In order to focus the pulses from the delay line, we use two cylindrical lenses, first one with a focal length of 1000mm and the second one with a focal length of 300mm. For the pulses from compressor, we use a tilted spherical mirror with focal length of 457 mm. The ray-tracing design for the long and short pulses reaching the target is shown in fig. 1. The focal line generated with the spherical mirror was characterized with an adapted CCD from a webcam, using a microscope objective. The focal length generated at 22.5 degrees is 3.2 mm long and less than 20 micron in width, as shown in fig. 2.1 and 2.2. [3]

We also developed a far field monitor in vacuum for the ultrashort pulses, in order to secure the positioning of the pulses on the needed place on the target.

Having all these instruments, laser produced plasma experiments will be performed starting this spring.

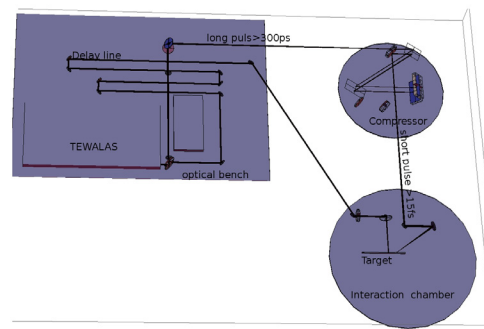


Fig. 1. X-ray Laser set-up at TEWALAS facility.



Fig. 2.1 Line focus length.



Fig. 2.2 Line focus width.

Journal: [1] D. Ursescu, L. Ionel, R. Dabu, R. Banici, Multiple ultra-short pulses generation for collinear pump-probe experiment, JOAM, 2010

Journal: [2] D. URSESCU et al., TEWALAS 20TW femtosecond laser, JOAM, 2010

Journal: [3] L. Ionel, R. Banici, L. Rusen, R. Ungureanu, O. Manta, R. Dabu, D. Ursescu, New X-Ray Laser Pumping method and experiments planning at TEWALAS, Journal of intense pulsed laser and applications in advanced physics, 2011

Posters

Visible and near UV light production by type-I non-critical phase matching second harmonic generation in $Y_{1-x}R_xCa_4O(BO_3)_3$ ($R = Lu, Sc$): crystal growth and nonlinear characterization

ACHIM, Alexandru¹, GHEORGHE, Lucian¹, VOICU, Flavius¹, LOISEAU, Pascal² and AKA, Gérard²

¹National Institute R&D for Laser, Plasma and Radiation Physics, Laboratory of Solid-State Quantum Electronics, P.O. Box MG 36, 077125, Bucharest-Magurele, Romania

²Ecole Nationale Supérieure de Chimie de Paris, LCMCP, CNRS-UMR 7574, 11 rue Pierre et Marie Curie, 75005 Paris, France

Keywords: crystal growth, nonlinear optical materials, non-critical phase matching, second harmonic generation.

In recent years, there has been a growing demand for specific visible and ultraviolet laser sources in medicine, industrial processing, remote sensing, laser printing, optical displays, and other areas. At this time, the availability of laser frequencies in the visible and UV is limited by laser materials and pump sources. Frequency conversion of solid-state lasers operating in the near infrared range by nonlinear optical (NLO) crystals has become the most available method to obtain shorter wavelength lasers with high beam stability, low cost and compactness. Thus, the reliance on nonlinear methods of frequency generation demonstrates the need for new nonlinear harmonic crystals with the ability to frequency convert a wide variety of laser wavelengths.

$YCa_4O(BO_3)_3$ (YCOB) has attracted great attention as a new NLO crystal for frequency generation since its earliest development [1]. YCOB is a congruent melting non linear material allowing the growth of large dimensions and high optical quality crystals to be used as frequency converters in solid-state laser systems [1-3]. Our previous researches [4] showed that in YCOB crystal, the Y^{3+} ions can be partially substituted by smaller radius ions Sc^{3+} or Lu^{3+} ($r_{Lu} = 0.861 \text{ \AA}$, $r_{Sc} = 0.745 \text{ \AA}$, $r_Y = 0.9 \text{ \AA}$) in order to tune the chemical composition of the crystal. By changing the compositional parameter x of $Y_{1-x}R_xCa_4O(BO_3)_3$ ($R = Lu, Sc$) crystals, their optical birefringence can be controlled in order to perform non-critical phase matching (NCPM) second harmonic generation (SHG) of specific near infrared laser emission wavelengths shorter than phase matching cutoff wavelength of YCOB crystal (724 nm along Y axis and 832 nm along Z axis at room temperature [2]). For biaxial crystals like YCOB family compounds, NCPM is the phase matching along one principal axis of the crystal, and for frequency conversion applications, NCPM is advantageous because of its large angular acceptance and because it eliminates walk-off between fundamental and harmonic radiations which leads to the highest efficiency.

As is shown in Figure 1, the value of NCPM wavelength decrease with increasing of compositional parameter x and decreasing of R^{3+} cations radius ($r_{Lu} = 0.861 \text{ \AA}$, $r_{Sc} = 0.75 \text{ \AA}$).

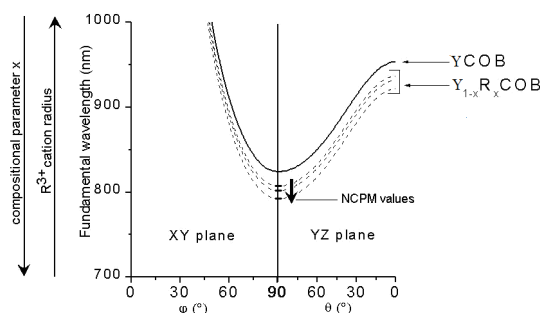


Figure 1. Adjustment of the type-I NCPM for SHG along Y axis in $Y_{1-x}R_xCa_4O(BO_3)_3$ crystals.

Five new nonlinear crystals of $Y_{1-x}Lu_xCa_4O(BO_3)_3$ and $Y_{1-x}Sc_xCa_4O(BO_3)_3$, with $x = 0.19, 0.29, 0.39$ and $x = 0.07, 0.11$, respectively, of good quality with no cracks and bubbles have been grown by Czochralski method, and their NCPM properties were investigated. We have demonstrated that efficient room temperature type-I NCPM SHG of any wavelength from 692.6 - 724 nm and 791.4 - 832 nm spectral ranges, can be achieved in $Y_{1-x}R_xCa_4O(BO_3)_3$ crystals by tuning the composition. This result has very important implications for many of today's tunable solid state lasers (Ti: Sapphire, Cr: LiSAF, Cr: LiCAF, Alexandrite) and laser diodes (AlGaAs, AlGaInP) with emission in these spectral ranges, in order to obtain specific blue and/or near UV laser emissions.

References

- [1] M. Iwai et al., "Crystal growth and optical characterization of rare-earth (Re) calcium oxyborate $ReCa_4O(BO_3)_3$ ($Re = Y$ or Gd) as new nonlinear optical material", *Jpn. J. Appl. Phys.* **36**, 1997, p. L276.
- [2] D. Vivien et al., "Crystal growth and optical properties of rare earth calcium oxoborates", *J. Cryst. Growth* **237-239**, 2002, p. 621.
- [3] Y. Fei et al., "Large-aperture YCOB crystal growth for frequency conversion in the high average power laser system", *J. Cryst. Growth* **290**, 2006, p. 301.
- [4] L. Gheorghe et al., "Synthesis and X-ray investigations of new $Y_{1-x}R_xCa_4O(BO_3)_3$ ($R = Sc, Lu$) nonlinear materials", *Optoelectron. Adv. Mater. - Rapid Commun.* **4**, 2010, p. 318.

Two-dimensional photonic crystals produced by femtosecond laser ablation on TiO₂ films

Anghel, Iulia¹, Jipa, Florin¹, Zamfirescu, Marian¹, Preda, Liliana², and Rizea Adrian³

¹ National Institute for Laser, Plasma and Radiation Physics, Atomistilor 409, 077125 Magurele, Romania

² Faculty of Applied Sciences, Politehnica University of Bucharest, Splaiul Independentei 313, 060042 Bucharest, Romania

³ S.C. PROOPTICA S.A, Gh. Petrascu 67, 745081, Bucharest, Romania

Keywords: photonic crystal, photonic bandgap, FDTD method, femtosecond laser ablation

Photonic structures were experimentally and theoretically studied on TiO₂ films. Periodical structures with hexagonal symmetry were produced by laser ablation. The samples were precisely processed by tightly focusing a femtosecond laser beam with 200 fs pulse duration, 775 nm wavelength, energy of hundreds of nJ per pulse, and repetition rate of 2 kHz. Dedicated software was realized and used for precisely positioning of the sample with resolution of tens of nanometers.

Figure 1 represents a photonic crystal structure produced by femtosecond laser ablation on TiO₂ films. Holes with diameter of about 1.6 μm and period of about 2 μm are made in a TiO₂ slab with refractive index of 2.4.

Numerical simulation of the photonic structure revealed photonic bandgaps around telecommunication wavelength at 1.55 μm . We studied the modification of the photonic bandgaps with variation of the radius of the holes, caused by limited laser processing accuracy. Figure 2 shows the evolution of the bandgap for a variation of the holes radius of about 5%. Δ represents the ratio between the radius of the holes and lattice period.

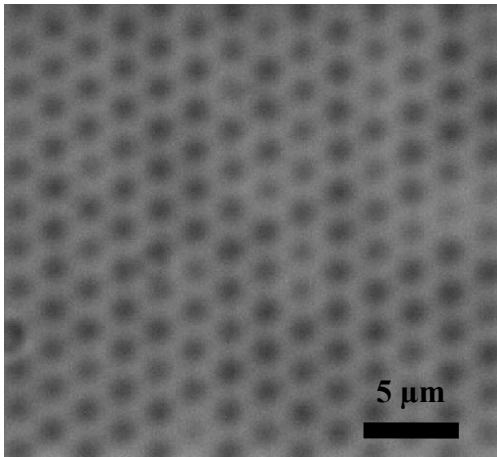


Figure 1. Photonic crystal structure produced by femtosecond laser ablation on TiO₂ films

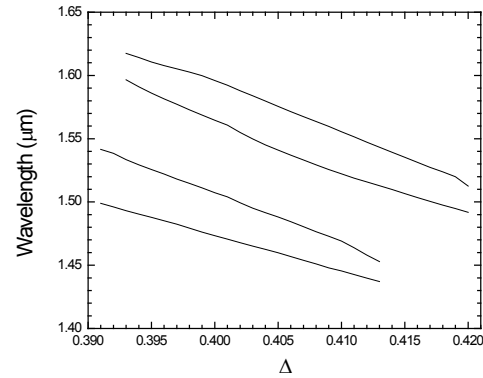


Figure 2. Variation of the minima and maxima of the central wavelength for a TiO₂ periodical structure with the ratio between the holes radius and lattice period.

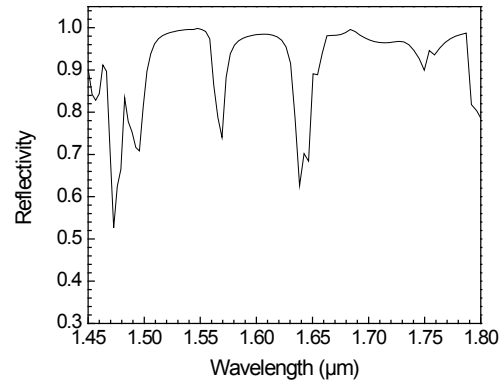


Figure 3 Calculated reflectivity spectrum of periodically structured TiO₂ film.

By Finite-difference time-domain algorithm (FDTD) the reflectivity spectrum was calculated in order to be compared with the experimental measurements.

Book: J. Joannopoulos et al, Photonic Crystals - Molding the Flow of Light 2nd Ed - Prince Ton, 2008.

Comparison of CALIPSO measurements with ground-bases measurements in Magurele, Rumania

Andreea Boscornea¹, Sabina Stefan,² and Doina Nicolae²

¹Department of Physics, University of Bucharest, Magurele, P.O.Box: MG-11 , Rumania

²INOE 2000, Magurele, P.O.Box: MG-11 , Rumania

Keywords: CALIPSO, LIDAR, AOD, Aerosol.

Aerosol are still one of the major sources of uncertainty in the assessment of climate change (IPCC-REPORT, 2007).

The vertical distribution of aerosol play an important role for the retrieval of radiative forcing of aerosol. The CALIPSO satellite is on the orbit since 2006 and determines vertically resolved aerosol and cloud properties

A validation of this measurements is needed in order to assess their accuracy and uncertainty. We try to validate the two measurement types, comparing different aerosol types.

In this paper, a comparison between ground-based and space-borne measurements at Magurele, Bucharest (inland station), Rumania for different aerosol measurements is done.

We compare the particle's optical depth obtained by CALIOP (Cloud-Aerosol Lidar with Orthogonal Polarization - instrument onboard the CALIPSO satellite, fig 1.) with the AOD - aerosol optical depth determined from the AERONET (Aerosol Robotic Network, fig 2.) Sun Photometer.

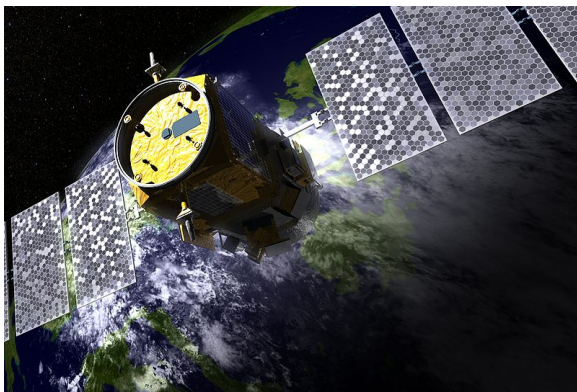


Figure 1. CALIPSO (Cloud-Aerosol Lidar and Infrared Pathfinder Satellite Observations), NASA

This comparison between the two measurement types has to deal with the problem of spatial and temporal matching of observations (Wagner *et al.*, 2009). We only use the data from overpasses near the ground site for our analysis.

We analyse more than 3 years of satellite measurements (June 2007- May 2010) over the ground station in Magurele (44°21'N 26°1'E).



Figure 2. Sun Photometer AERONET NASA

Journal: IPCC-Report, Climate Change – Synthesis Report, 2007

Winker D, W. H. Hunt, Initial performance assessment of CALIOP, *Geophysical Research Letters*, 2007, 34

Wagner F, Ana Maria Silva, Comparison of CALIPSO measurements with ground-bases measurements, *Proceedings of the 8th International Symposium on Tropospheric Profiling*, 2009

Web site: AERONET <http://aeronet.gsfc.nasa.gov/>

CALIPSO: <http://eosweb.larc.nasa.gov/>

Acknowledgments:

“The CALIPSO data were obtained from the NASA Langley Research Center Atmospheric Science Data Center.”

For the AERONET data we thanks the (RADO Project/ PI N. Nicolae) for its effort in establishing and maintaining (INOE 2000) sites.

ILA software for diffractive optics applications

Narcis Cernescu, Florin Garoi, Cristian Udrea, Tiberius Vasile

National Institute for Laser, Plasma and Radiation Physics, Atomistilor 409, 077125, Magurele, Romania

Keywords: Fourier, Gerchberg-Saxton, Profilometer

The concept of computer aided physics (e.g. optics) is applied more and more extensively within the laboratory practice, both in education and research. There are three arguments that lead to this evolution:

- didactic simulation and modeling of physics experiments;
- processing of experimental data;
- automation of experiments and command from a distance.

A software has been realized in order to meet the research applications of ILA group. It is a link between the process of mathematical understanding of optics notions and practical application. A good (mathematical) understanding of diffraction phenomenon is also important for this project.

The application is conceived using Net Framework 3.5 and Visual C#, allowing the user to interactively simulate experiments, record data and process this data for specific tasks. The program is in MSI format, which increases its utility and emphasizes the flexibility it was realized with.

Diffraction simulation permits to simulate both Fresnel and Fraunhofer diffraction. Images in .bmp format, with a 128 x 128 pixels resolution, showing the intensity profile of a wavefront are to be used. The near field (Fresnel) and far field (Fraunhofer) diffraction images are obtained in the same format.



Figure 1. Object and its Fourier pattern.

Phase retrieval of a wavefront is possible by accessing the Gerchberg-Saxton pictogram from Application submenu. This procedure uses an implementation of the Gerchberg-Saxton algorithm. The software interface will allow the user to load two images (in .bmp format, 128 x 128 pixels resolution) representing the optical field intensity in two diffraction planes.



Figure 2. Screenshot from the "Gerchberg-Saxton" result.

Profilometer is a submenu that allows for the intensity profile to be realized in 3D format. The image is in .bmp format and has a resolution of 100 x 100 pixels. It can be loaded by user or it can be taken by a CCD camera.

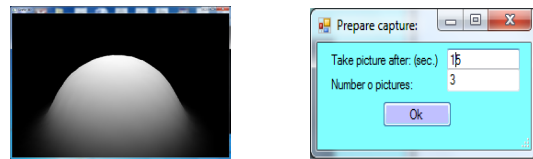


Figure 3. 3D intensity and CCD options

For precision measurements in a controlled medium (e.g. temperature, vibrations), an automated working procedure is imposed. The program has a series of methods to communicate efficiently with the computer. For example, by using the CCD Options menu, someone can use the CCD camera with the available options.

Someone can adjust the snapshot time interval as well as the number of pictures to be taken in the specified time interval. This is useful in a measuring chain, as is the case with the phase retrieval using Gerchberg-Saxton algorithm.

Book: Leonid Yaroslavsky, Murray Eden, "Fundamentals of digital optics", Birkhauser, 1996, 81-92-104p

Laser Direct Writing and Mask Lithographic produced Polymeric Integrated Optics

Heßke, Andre¹ and Koch, Alexander W.¹

¹Institute for Measurement Systems and Sensor Technology, Technische Universität München, Theresienstr. 90/N5, 80333 Munich, Germany

Keywords: integrated optics, laser direct writing, mask lithography, Ormocer[®].

The interest in integrated optics is continuously increasing. It is easy to produce, uses cheap materials, and enables the miniaturisation of optical components. In our laboratory we focus on manufacturing step-index-waveguide-like structures. To this end, we developed two different processes to provide several waveguides in polymeric integrated optics: (1) a line-writing UV-laser assembly and (2) a (direct contact) mask lithographic setup. Both are photochemical processes and use different stacked polymer layers (Ormocer[®]), which shall be structured.

The way of coating the polymers on substrates in both processes is basically the same. We are cleaning the substrates with a H₂SO₄-H₂O₂-dissolution, flushing with 100% isopropanol and blowing with air. By this way the best adhesive contact with the spincoated cladding polymer (Ormoclad[®]) and the used float glass substrate is produced. After UV-floodlighten and developing this layer the core polymer (Ormocore[®]) is spincoated. To construct waveguides in the core layer we can use one of the two following structuring processes. The waveguide is finished when a second coating layer surrounds the core. By blending the Ormocore[®] and Ormoclad[®] polymers for the core layer it is possible to modulate its refractive index. Akin values of the refractive indices of core and cladding are leading to larger singlemode waveguide diameters (Bludau, 1998). So an 8 µm core can be produced as singlemode at 1550 nm. Also a mixture of 2:3 to 1:2 of Ormocore[®] to Ormoclad[®] reduced a dewetting effect of the core and cladding layer.

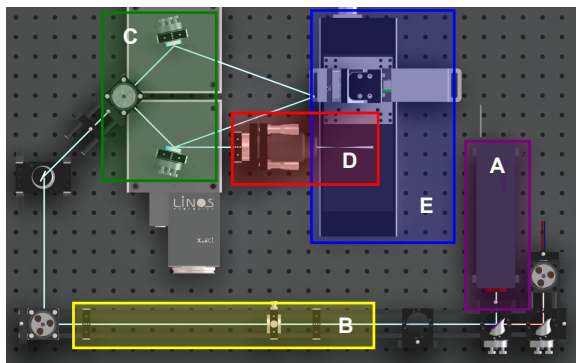


Figure 1. Laser direct writing setup. (A) UV-diode-laser, (B) mode filter, (C) ray guiding mirrors, (D) beam focussing telescope, (E) x-y-z-stage.

The laser direct writing setup (Fig. 1) is characterized by a focused singlemode diode laser with a wavelength of 365 nm and an intensity of 10 mW. The UV-beam is mode filtered and reflected to a focussing telescope. The 0.5 µm spot is positioned to an x-y-z-stage whereat the substrate is fixed. With a scanning speed of 4 mm/s waveguides can be written. A speed of 100 mm/s is reported in Wang (2009). The waveguide's width is set by an overexposure of the core polymer by tuning the laser intensity and the backside reflection of the substrate. Based on an accuracy of 3 µm only linear forms can be written in an acceptable precision. Round forms will result in rippled sidewalls and a high loss.

Another way to structure waveguides into the core layer is to use floodlight and a shadowing lithographic chrome mask (Fig. 2). We developed an easy-to-use exposure construction at which an UV-LED-array of 365 nm and 600 mW radiates the core layer through a mask. The mask includes several designs and delivers high reproducible waveguides. The dimensions of them depend on the exposure dose, the illuminating time, the mask gaps and the mask distance. To examine the resolution of the used core polymer different grating areas are used. We derive that the height of the core layer determines the minimal structure dimension in x-y-direction and so multi- and singlemode waveguides are produceable.

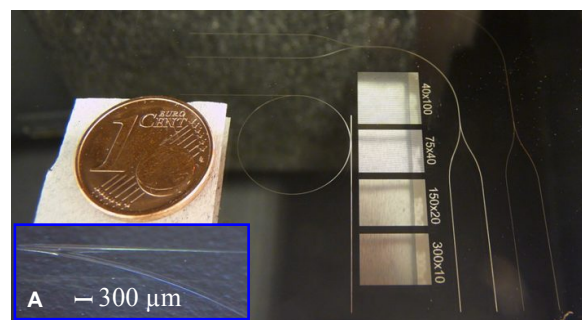


Figure 2. Lithographic chrome mask with several couplers and gratings. (A) 80 µm multimode-coupler.

Bludau, W., *Lichtwellenleiter in Sensorik und optischer Nachrichtentechnik*, 1998, 3-540-63848-2.

Wang, S., *Polymer optical channel waveguide components fabricated by using a laser-direct writing*

Luminescence properties of Eu-doped $\text{La}_3(\text{Ga}_{1-x}\text{Al}_x)_5.5\text{Nb}_{0.5}\text{O}_{14}$ nano-powders synthesized by a citrate sol-gel method

Matei, Cristina, Georgescu, Serban, Voiculescu, Ana-Maria, Toma, Octavian, Nastase, Silviu

National Institute for Laser, Plasma and Radiation Physics, 409 Atomistilor Street,
Magurele, Jud. Ilfov, 077125, Romania

Keywords: Langanite, Nanopowder, Sol-gel, Eu^{3+} , Luminescence

The search of new and efficient phosphors for solid-state lighting is a problem of great interest in present. The rare earth doped phosphors are efficient, but the matching between the emission of the LED and the narrow absorption lines of the phosphor remains an open problem.

A solution could be the use of partially disordered crystals as hosts for rare-earth ions showing wider absorption lines (Georgescu *et al.*, 2009, Georgescu *et al.*, 2010 (a)). Such hosts could be the crystals from the langasite family (generic - LGX), namely langasite (LGS - $\text{La}_3\text{Ga}_5\text{SiO}_{14}$), langanite (LGN - $\text{La}_3\text{Ga}_{5.5}\text{Nb}_{0.5}\text{O}_{14}$) and langatate (LGT - $\text{La}_3\text{Ga}_{5.5}\text{Ta}_{0.5}\text{O}_{14}$).

Eu-doped langanite nanopowders with gallium partially substituted by aluminum ($\text{La}_3\text{Ga}_{5.5-x}\text{Al}_x\text{Nb}_{0.5}\text{O}_{14}$) were prepared by a citrate sol-gel method and annealed in air at various temperatures between 700°C and 1100°C. Substituting 10% at. gallium by aluminum, for annealing temperatures up to 900°C, only the langanite phase is observed. For higher annealing temperatures, very small quantities of langanite transforms in perovskite $\text{La}(\text{Ga},\text{Al})\text{O}_3$ and, possibly, in $\beta\text{-Ga}_2\text{O}_3$, as evidenced in XRD and luminescence spectra. For the substitution of 20% at. gallium by aluminum, a significant part of LGN phase transforms in other phases, mainly perovskite, affecting dramatically the shape of the luminescence spectra. The phase transformation due to the thermal treatments is also evidenced in the shape and position of the charge transfer band. The reddish color of the powders due to color centers associated to oxygen defects intensifies with increasing annealing temperature. For the powders with 10% at. aluminum, a clear correlation between the area of the Eu^{3+} absorption bands (extracted from the diffuse reflectance spectra) and the integral luminescence was observed.

In Fig. 1 are given the XRD patterns of $(\text{La}_{0.97}\text{Eu}_{0.03})_3(\text{Ga}_{0.90}\text{Al}_{0.10})_{5.5}\text{Nb}_{0.5}\text{O}_{14}$ powders annealed at 700°C, 800°C, 900°C, 1000°C, and 1100°C.

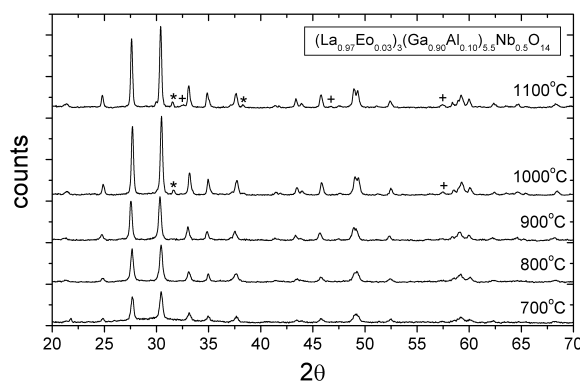


Fig. 1. XRD patterns for $(\text{La}_{0.97}\text{Eu}_{0.03})_3(\text{Ga}_{0.90}\text{Al}_{0.10})_{5.5}\text{Nb}_{0.5}\text{O}_{14}$ nanopowders annealed for five hours in air at temperatures between 700°C and 1100°C.

Besides the diffraction lines belonging to the langanite phase, other diffraction lines are observed for higher annealing temperatures (1000°C and 1100°C). In contrast with 'pure' langanite (Georgescu *et al.*, 2010 (b)), the intensity of the 'foreign' lines is much reduced.

(Georgescu *et al.*, 2009) S. Georgescu, A. M. Voiculescu, O. Toma, C. Tiseanu, L. Gheorghe, A. Achim, C. Matei, Eu-doped langasite, langatate and langanite - possible new red phosphors, *Optoelectron. Adv. Mater.*, 2009, 1379-1382.

(Georgescu *et al.*, 2010 (a)) S. Georgescu, A. M. Voiculescu, O. Toma, L. Gheorghe, A. Achim, C. Matei, S. Hau, Luminescence efficiency of europium-doped LGS, LGT and LGN crystals, *Optoelectron. Adv. Mater.*, 2010, 1937-1941.

(Georgescu *et al.*, 2010 (b)) S. Georgescu, A. M. Voiculescu, O. Toma, S. Nastase, C. Matei, M. Osiac, Luminescence of Eu-doped langanite nanopowders synthesized by a citrate sol-gel method, *J. Alloys Comp.*, 2010, 470-474.

Breit- Pauli R -matrix fine structure splitting calculation in the Ar III ion

Andreea Mihailescu, Vasile Pais, Olimpia Budriga and Viorica Stancalie

Laser Department, National Institute for Laser, Plasma and Radiation Physics, Atomistilor 409, 077125, Bucharest, Romania

Keywords: atomic data, R -matrix approximation, energy levels, collision strengths.

Argon is an important species for tokamak plasma studies, being used to radiatively cool the divertor and as potential means of mitigating plasma disruptions (Whyte et al. 2002). In addition, emission lines from Ar^{2+} can be detected in various astrophysical objects. The $3s^23p^4(^1D_2) \rightarrow 3s^23p^4(^3P_{1,2})$ and $3s^23p^4(^1S_0) \rightarrow 3s^23p^4(^1D_2)$ transitions of Ar III emit strongly in planetary nebulae (Aller and Keyes 1987; Perez-Montero et al. 2007). These lines have been used for spectral diagnostics purposes in astrophysical studies (Keenan and McCann 1990; Keenan and Conlon 1993).

For a good modeling of emission in laboratory as well as in astrophysical plasmas, there is, thus, a demanding need for accurate knowledge of atomic processes. Atomic data for near neutral systems present a challenge due to the low accuracy of perturbative methods for these systems. In order to obtain reliable theoretical data, we rely on non-perturbative methods such as the R -Matrix. For Ar^{2+} there is only little data available in the literature (Johnson and Kingston 1990 and Galavis et al. 1998).

In this work, we make use of the R -matrix Breit-Pauli approximation (Berrington et al. 1995) to calculate fine structure splitting in Ar III ion. This method includes relativistic effects in the Breit-Pauli approximation (Scott and Burke 1980, Scott and Taylor 1982). Incorporating relativistic corrections (spin-orbit, Darwin and mass) in the close coupling R -matrix method yields a large number of fine structure transition probabilities with higher accuracy. We use the package of codes RMATRIX1 to derive the energy levels within the Ar III ion. We have considered all possible bound levels for $0 \leq J \leq 7$ with $n < 4$, $l \leq n-1$, $0 \leq L \leq 9$, and $(2S+1) = 1, 3, 5$, even and odd parities. The levels are obtained as the eigenvalues of the Breit-Pauli Hamiltonian and labeled by the total angular momentum and parity, i.e. $J\pi$. A selection of data is shown in Table 1. A comparison with the available listed NIST levels is also provided, showing a good agreement.

Also reported, are collision data (collision strengths) in the case of electron impact excitation. The modeling is performed with the aid of code FARM. The flexible asymptotic R -matrix package is used for treatment of scattering in the external region of the configuration space, where exchange effects may be neglected.

The calculations have been performed over a colliding electron energy range of up to 10 Ry.

Table 1. Comparison between theoretical energy levels calculated with the R -matrix method and the levels published by NIST.

	Config.	Term	J	Level NIST (Ry)	Level R-matrix (Ry)
1.	$3s^23p^4$	3P	2	0.0	0.00
2.	$3s^23p^4$	3P	1	0.01013488	0.00923
3.	$3s^23p^4$	3P	0	0.01430898	0.01319
4.	$3s^23p^4$	1D	2	0.12766855	0.14479
5.	$3s^23p^4$	1S	0	0.30313958	0.31672
6.	$3s 3p^5$	$^3P^\circ$	2	1.03702609	1.03703
7.	$3s 3p^5$	$^3P^\circ$	1	1.04611045	1.04534
8.	$3s 3p^5$	$^3P^\circ$	0	1.05094608	1.04964
9.	$3s 3p^5$	$^1P^\circ$	1	1.31242797	1.35403
10.	$3s^23p^3(^4S^\circ)3d$	$^5D^\circ$	1	1.32029353	1.36557

References:

- Whyte D. G., Jernigan T. C, Humphreys D. A. et. al., Phys. Rev. Letts., 2002, vol. 89, pp. 055001.
 Aller L. H. and Keyes C. D., The Astrophysical Journal Supplement Series., 1987, vol. 65, pp. 405.
 Perez-Montero E., Hagele G.F., Contini T., and Diaz A., Mon. Not. R. Astron. Soc., 2007, vol. 381, pp. 125.
 Keenan F.P and McCann S.M., J. Phys. B., 1990, vol. 23, pp. L423.
 Keenan F.P. and Conlon E.S., The Astrophysical Journal., 1993, vol. 410, pp. 426.
 Johnson C.T., Kingston A.E., J. Phys. B: At. Mol. Opt. Phys., 1990, vol. 23, pp. 3393.
 Galavis M.E., Mendoza C., Zeipen C.J., A&A. Suppl. Ser, 1998, vol. 133, pp. 245.
 Berrington K.A., Eissner W.B., Norrington P.H., Comput. Phys. Commun., 1995, vol. 92, pp. 290.

Studies on molecular aggregates in quinazoline derivatives solutions by exploring methods

Andra Militaru¹, Sandrine Alibert², A. Mahamoud², V. Damian¹, Mihaela Filipescu¹, Monica Enculescu³, J. M. Pagès², M. L. Pascu¹

¹National Institute for Laser, Plasma and Radiation Physics, 077125, Magurele, Romania

²UMR-MD1, Faculté de Pharmacie, Université Méditerranée, IFR88, Marseille, France

³National Institute of Material Physics, 077125, Magurele, Romania

Keywords: quinazoline derivatives, aggregates, optical microscopy, electron microscopy, atomic force microscopy

Quinazolines and quinazoline derivatives are an important group of compounds which have a variety of pharmaceutical properties; a class of quinazoline derivatives was designed and developed at UMR-MD1 (Marseille, France) to fight the multidrug resistance of antibiotics acquired by bacteria.

During stability studies performed on the quinazoline derivative BG1188 (and presented in the oral exposure “Stability properties of medicines solutions: spectral evidence and wire-like formations”), aggregation phenomena took place that produced precipitates in the form of thin wires, of different dimensions (lengths and diameters) and shapes observed initially with the naked eye.

The BG1188 solutions were prepared in ultrapure de-ionized water, in distilled water and in dimethyl sulfoxide (DMSO). The concentration range was: 10^{-6} M to 2×10^{-3} M. The solutions were kept in dark; two cases were studied: samples kept at 4°C and samples kept at room temperature (22°C).

The wire-like formations are produced gradually, starting from the first hours after solutions preparation. These were observed in all samples regardless of the solvent, concentration or the conditions in which the solutions were kept.

Because the computed degree of polymerization was 1.018, these precipitates can not be polymers. For the studied range of concentrations, at all times, BG1188 was present in solution only in monomer form. An explanation could be that the BG1188 molecules organize themselves to form micro-crystallites or precipitates and an approximate number of molecules contributing to these wire-like formations may be in the range 10^{15} - 10^{16} molecules. This number was calculated from the difference in the absorption spectra of BG1188 10^{-3} M solutions in ultrapure water recorded immediately after preparation and at 4 months after preparation.

At later stages, these wires mould into aggregates/clusters. The images of the aggregates which are shown in Fig.1 were obtained using an optical microscope working in reflection, transmission or epifluorescence. The pixel dimension on the probe varies from 1.08µm for 5X objective to 0.05 µm for 100X objective.

Electron microscopy investigations revealed that the precipitates are built from spherical, micrometric formations which develop connections leading to the wire-like shapes and are very stable with temperature.

From optical microscopy and electron microscopy images two types of aggregates could be described. The first type of aggregates looks like a transparent, light color, long wire which seems to have the same width for all its length. The second type of observed wire-like formations looks like a chain of dark colored spheres/balls, which apparently contain dry material.

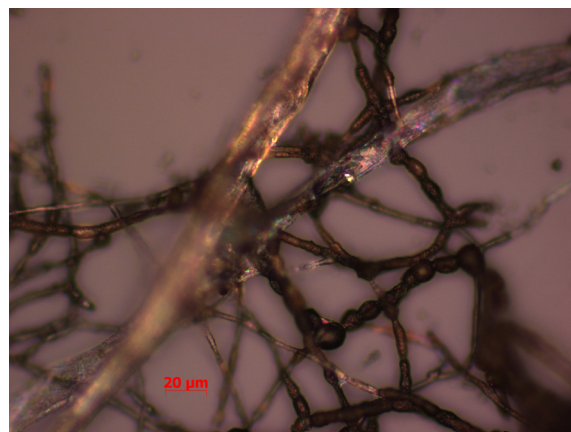


Figure 1. 50X optical microscopy image of cluster of aggregates: BG1188 in ultrapure water at 5×10^{-4} M.

Further studies were conducted using atomic force microscopy: the width of the considered wire-like aggregates was 3–4µm and their height/thickness was about 1 – 2 µm.

The appearance like a chain of dark colored spheres/balls of some formations was also confirmed by the longitudinal profile of an aggregate. The diameter of a sphere appears to be about 3 µm.

It remains to better understand the mechanisms of wire formation.

Acknowledgements: The authors belonging to the NILPRP acknowledge the financing of the project by Rom. ANCS project 41-018/2007 and Program LAPLAS 3, PN 09 39/2009. Authors acknowledge the COST network BM0701 – ATENS support in carrying out this work.

Structure and morphology of InN thin films grown by PLD: The impact of nitrogen plasma flow vs. pressure and substrate temperature

Nedelcea Anca, F. Stokker-Cheregi,
A Moldovan., V. Ion, R Birjega., M.Dinescu

*INFLPR - National Institute for Laser, Plasma and Radiation Physics,
Magurele RO-077125, Bucharest, Romania*

Keywords: InN, thin films, RF-PLD

While the optical and electronic properties of InN and related III-nitride alloys make them an interesting choice for device applications ranging from LEDs covering the infrared-ultraviolet spectrum to terahertz emitters, the successful growth of InN-based commercial-grade materials is met with serious challenges. Significant effort is being dedicated by the growers in overcoming issues related to the lattice mismatch with popular substrates, the relatively low-temperature dissociation of InN with respect to that of other III-nitrides (GaN, AlN), and the consequent low diffusion length of In. While plasma assisted pulsed laser deposition (PLD) offers several advantages (e.g. high kinetic energies of ablated species) over traditional epitaxial growth techniques (MBE, CVD) for the obtaining of InN, the interplay between nitrogen plasma flow and pressure has not been properly documented in the case of the former. This work provides insight on how the balance between flow and pressure of the reactive nitrogen plasma used for the growth of InN by PLD influences the structural and morphological properties of the resulting thin films, as revealed by X-ray diffraction and scanning electron microscopy analysis, respectively.

Temperature dependence was also studied.

The depositions have been done using a set-up described in Fig. 1. In Fig. 2 a photo of installation during thin films deposition is presented.

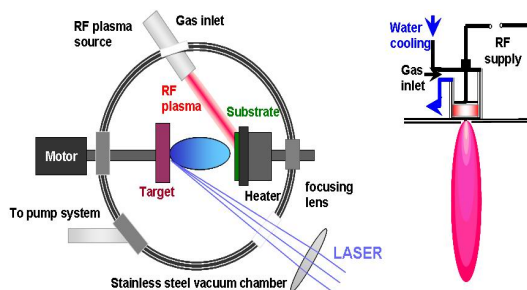


Fig.1 Schematic of the RF-PLD setup



Fig.2 Close-up on the InN thin film deposition

The set up contains: the laser, a reaction chamber, target, collector and a RF plasma source. The ablated material from the In metallic target is condensed on a substrate and thus the thin film is formed; the process takes place in nitrogen gas flow. PLD technique has some important advantages:

a. Thin films of complex chemical composition can be produced from a bulk target, preserving its stoichiometry [1].

b. Nitrides or oxides can be obtained starting from simple metallic target and working in nitrogen or oxygen reactive atmosphere.

c. The atoms and ions in the plume have a kinetic and internal excitation energy that initially may exceed thermal energy by more than two orders of magnitude. At the arrival at the substrate these non-thermal atoms and ions may have an appropriate excess energy which increases the sticking and nucleation rate as well as the surface mobility.

d. PLD is a “pulsed” process by which the number of particles arriving at the substrate can be controlled precisely with the number of pulses and the fluence. This means that a layer-by-layer growth can be achieved by adjusting the number of arriving atoms to the number of atoms in a monolayer, and thus highly perfect surfaces and interfaces in sandwich-systems can be produced.

The addition of the radiofrequency beam increases the reactivity on the growth area (on the substrate), as it supplies excited and ionized nitrogen species.

[1] J. Schou, “Physical aspects of the pulsed laser deposition technique: The stoichiometric transfer of material from target to film”, Applied Surface Science 255 (2009) 5191–5198

Study of the SiO₂/Si Nanoparticle luminescence

Nistorescu Alexandru¹, Sima Cornelia², Nicolae Ionut², Octavian Toma², Anca Maria Voiculescu²,
Constantin Grigoriu², Georgescu Serban²

¹Faculty of Physics, University of Bucharest, Atomistilor 405, 077125, Magurele, Romania

²National Institute for Laser, Plasma and Radiation Physics, Atomistilor 409, 077125, Magurele, Romania

Keywords: Nanoparticles, Photoluminescence, Silicon-Silicon Dioxide

The main purpose of this work is to study SiO₂/Si nanocluster luminescence.

The clusters consisted of spherical nanoparticles with a crystalline silicon core, coated with an amorphous silicon dioxide layer. The synthesis of silicon nanoparticles was performed by pulsed laser ablation technique, by irradiating a silicon target in an ambient gas, such as argon or helium. The particle size distribution was a lognormal function; the nanoparticles had dimensions less than 10 nm, with the arithmetic mean value of 4.9 nm.

The work focused on study of the SiO₂/Si particle photoluminescence as a function of temperature. Particles were excited by a He-Cd laser beam, at 325 nm (in ultraviolet). The investigations were carried out in the temperature range of 10-300 K. The nanoparticle photoluminescence exhibited emission form visible to middle infrared. The luminescence spectrum has two peaks, one in visible and another one (more intense) in IR, around 700 nm.

The study revealed that by decreasing of the temperature, the spectrum shifted toward UV wavelengths, and the emission intensity is increasing. The luminescence observed by naked eye in day-light was changing from red to orange.

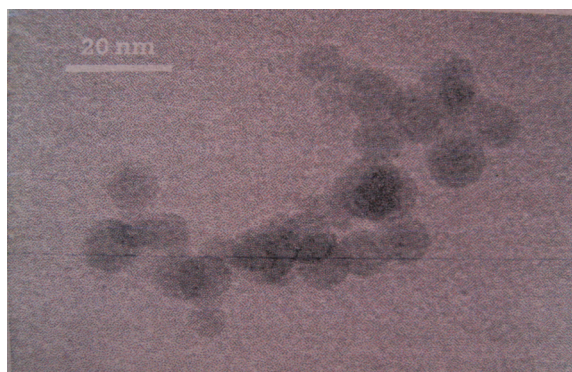


Figure 1. Typical TEM image of a SiO₂/Si nanoparticle cluster.

Journal: C. Grigoriu, Y. Kuroki, I. Nicolae, X. Zhu
M. Hirai, H. Suematsu, M. Takata, K. Yatsui,
Photo and Cathodoluminescence of Si/SiO₂
Nanoparticles Produced by Laser Ablation,
Journal of Optoelectronics and Advance
Materials Vol. 7, No. 6, December 2005, p 2979-
2984 .

Micro elements fabrication using e-beam lithography for laser applications

Păiuș Diana - Petronela, Mihăilescu Mona *

SC OPTOELECTRONICA SA, 409 Atomistilor Str. , Magurele, Romania

*Politehnica University from Bucharest, 313 Splaiul Independentei, Bucharest, Romania

Keywords: micro lens, Fresnel lens, reticles, micro particles, e-beam lithography.

Microelements for laser application need great accuracy and dimensions in micrometers range. These requirements are satisfied in technological processes using masks fabricated with electron beam lithography followed by UV pattern transfer and sequential chemical etching.

Our company developed these technological processes to fabricate several micro components with different applications:

- micro lens;
- Fresnel lens;
- reticles;
- grids;
- resolution targets;
- diffractive optical elements;
- micro particles.

The minimum resolution in masks fabrication is of 600 nm and microelements have the following transversal dimensions: microlens diameter 100-300 μm , Fresnel lens steps 10-30 μm , reticles width line 2-10 μm , diffractive optical elements pitch 1-2 μm .

To fabricate the micro-optic elements, we need two wafers as follows: one wafer (W1) is a borosilicate glass (coated with Cr and electronoresist) on which will be produced the masks by e-beam lithography and one wafer (W2) is a borosilicate glass (coated with Cr and photoresist) in which will be fabricated the microelements. W2 plate consists of 2,54 mm thick polished borosilicate glass, covered with thin film Cr+CrO₂ and 400-600 nm photoresist layer deposited by spinning at 1500 rpm and dried at 80°C at IR radiation.

Electron beam lithography (e-beam lithography) is a lithographic process that uses a focused beam of electrons to scan point to point large surfaces (170x170 mm) and to form desired

patterns across it. In the initial process, a thin film from sensitive polymer (called electronoresist) is exposed by e-beam. In the second process electronoresist is selectively removed in the exposed regions (process called developing). In the third step, Cr layer is etched after the same pattern.

The mask pattern from W1 is recorded on W2 using UV radiation. The photoresist from W2 is developed and removed in the exposed area, followed by the chemical removal of Cr+CrO₂ after mask pattern, chemical etching of the glass from W2 where it is not covered by Cr+CrO₂ and total chemical removal of photoresist and Cr+CrO₂.

The purpose is to create very small structures in the resist that can subsequently be transferred to the substrate material, by etching. Our study is focused to find the proper parameters of e-beam exposing dose for each optical element fabrication .

Book: P.Rai-Choudhury, Handbook of Microlithography, Micromachining and Microfabrication – Volume 1: Microlithography, 1997.

Journal:

1. Y. Sarov, I. Kostic, P. Hrkut, L. Matay, Fabrication of diffraction gratings for microfluidic analysis, Bulg. J. Phys. **29** (2002) 17–29.
2. S.F. Abd Rahman, Fabrication of nano and micrometer structures using electron beam and optical mixed lithography process, Int. J. Nanoelectronics and Materials 4 (2011) 49-58.

Modified Fresnel rhomb with collinear input and output beams

Anca Maria Beldiceanu¹, George Nemeş²

¹ProOptica, RO-745081, Bucharest, Romania, <http://www.prooptica.ro>, anca.beldiceanu@prooptica.ro

²ASTiGMAT™, Santa Clara, CA 95050, USA, <http://astigmat-us.com>; gnemes@astigmat-us.com

Keywords: modified Fresnel rhomb, quarter-wave retarder, achromatic retarder, polarization control.

Classical Fresnel rhombs (better called Fresnel parallelograms) are quarter-wave retarders with relatively good achromaticity for wide spectral ranges. For example, a BK7 glass Fresnel rhomb designed for an ideal 90.0° phase shift at 585 nm, has about 89.4° and 92.0° of phase shift at the extremes of the visible spectrum [1]. Their working principle is based on the relative phase shift between the p- and the s-polarized light components subjected to two total internal reflections in a transparent, homogeneous optical material, normally BK7 glass, or fused silica. The geometry involved in the design uses normal incidence for the collimated input and output beams. The result is an optical component displacing the beam from input to output [1].

We present a modified design for the Fresnel rhomb, resulting in a device with a collinear input and output beams. Instead, the incidence on the input and on the output surfaces are no more normal. The design is conceived for a nominal wavelength of 1064 nm (Nd:YAG laser beam) and for the most used optical material, BK7 glass. A first physical model of the new optic was manufactured and measured to verify the principle.

The theoretical behavior (retardation) of the physical model for different laser wavelengths is calculated, for the device with the nominal geometrical sizes. Experimental (polarimetric) results of polarized light measurements for several wavelengths, including the 633 nm (HeNe laser beam) are presented and compared to the theoretical results. Some optimizing criteria and applications for future physical models are discussed, implying mainly a specific refractive index and the quality requirements for the glass to be used.

References:

[1] J.M. Bennett, H.E. Bennett, Polarization, in *Handbook of Optics*, W.G. Driscoll, W. Vaughan, eds., McGraw-Hill, New York, 1978, Ch. 10, pp. 10-120.

Spectroscopical determination of photophysical parameters for non-fluorescent Phthalocyanine compounds, further laser excitation in the Soret band.

Pascu, M.L.¹, Staicu, Angela¹, Nuta, Alexandrina², Pascu, A.¹, Smarandache, Adriana¹

¹National Institute for Laser, Plasma and Radiation Physics, Magurele, 077125, Bucharest, Romania. ²National Institute for Research & Development in Chemistry and Petrochemistry, 060021, Bucharest, Romania.

Keywords: Phthalocyanines, photophysics, singlet oxygen, triplet states.

Phthalocyanines, a rich class of chemical compounds are structurally related to the porphyrins. Their catalytic, photoconductive, photovoltaic and photosensitizing properties have propelled them into different applications. One of them, based on the photosensitization capability of the phthalocyanine molecules is the Photodynamic therapy (PDT), a relatively new treatment modality recently accepted as clinical therapy to treat malignant and premalignant dysplasias, but also for other diseases such as psoriasis, age-related macular degeneration and other diseases. The key element of the therapy is the generation of a large number of active molecular species (mainly singlet oxygen) following the primary light activation of the photosensitizer compound – phthalocyanines e.g.

Measurement of the photophysical properties involved in or associated with the sequence of photophysical and photochemical molecular processes climaxing with generation of active species singlet oxygen is important in evaluating the photosensitizing capabilities of the analysed photosensitisers.

The paper reports the methods & the equipment applied as well as the experimental results obtained in measuring non-fluorescent photosensitisers - metallated phthalocyanines with diamagnetic metals, in regard to:

- the energy "deposited" in the triplet states of the photosensitiser molecules (triplet states which are populated by Intersystem Crossing after laser excitation in Soret band)
- the Quantum Yield of generating singlet oxygen active species by laser excited phthalocyanine, and
- the life-time of the population of active species (singlet oxygen) generated by the laser excited phthalocyanines (via triplet - triplet excitation transfer).

All the performed measurements were based on spectroscopic measurement methods, further the laser excitation of phthalocyanine molecules at Soret absorption band. In order to avoid the intense dimerization of the phthalocyanines, which take place in aqueous media, the chosen solvent was DMSO.

In order to measure the energy "deposited" in the triplet states of phthalocyanines further their laser excitation, time-resolved optoacoustical spectroscopy (TR-LIOAS) of the phosphorescence emission ($\lambda = 1270$ nm) of singlet oxygen generated has been employed.

To measure the singlet oxygen Quantum Yield via laser excited phthalocyanines, the intensity of the singlet oxygen phosphorescence generated by phthalocyanines was measured immediately after the laser excitation pulse, and compared with the singlet oxygen phosphorescence generated in quite identical conditions by a compound whose Quantum Yield of singlet oxygen is known.

The life-time of the population of singlet oxygen species generated by the laser excited phthalocyanines was measured by time-resolved spectroscopy of the phosphorescence of singlet oxygen.

Literature.

1. S. Kimel, B. J. Tromberg, W. G. Roberts, M. W. Berns, Singlet oxygen generation of porphyrins, chlorins and phthalocyanines, *Photochemistry and Photobiology*, 50, 2, pp. 175–183, 1989.

2. Ana Jimenez-Banzo, Santi Nonell, Johan Hofkens, Cristina Flors, Singlet Oxygen Photosensitization by EGFP and its Chromophore HBDI, *Biophysical Journal*, 94 January 2008, 168–172

3. Nonell, S., S. Braslavsky, Time-resolved singlet oxygen Detection, *Methods Enzymol.* 319:37–49, 2000.

Acknowledgements. Financial support for this work was provided by Romanian Ministry of Education, Research and Innovation, National Centre for Programme Management, under contract 61-023/ 2007.

Time resolved fluorescence spectroscopy used in the assessment of drinking water quality

Puiu Adriana*, Sporea Dan, Stancalie Andrei

Laser Metrology and Standardization Laboratory,
National Institute for Laser, Plasma and Radiation Physics,
Magurele, P.O.Box MG-36, 077125 ROMANIA
*adriana.puiu@inflpr.ro

Keywords: time resolved fluorescence, water quality, dissolved organic matter

The growth of the global population combined with industrialization and urbanization puts continued stress on our environment. Thus, the problem of water quality is certainly important in our days because of industry wastes released in the environment, inhabitant's lifestyle, the leakage of pipes, infiltration of the groundwater, etc. In the present work we aimed to assess the quality of drinking water by mean of the time-resolved emission spectroscopy (TRES). Currently, Heterotrophic Plate Counts (HPC) is used for monitoring overall water quality. The existing laboratory chemical-based analysis has several drawbacks: the process is labour intensive, is sensitive to errors during performance of the tests and the results are generally not available for two to four days. Some results indicating the usefulness of fluorescence spectroscopy for the assessment of water quality are already reported in the literature, but only few scientific papers discuss about the employment of time resolved fluorescence [1], [2], [3]. Simultaneous measurement of fluorescence spectra and the fluorescence decay are useful for the interpretation of fluorescence data in complex systems. While normal fluorescence spectroscopy is useful as a highly selective and sensitive non-invasive probe, better chemical information can be gained from the same experiment by exploiting the time-dependent nature of fluorescence. On the other hand, emission spectra tend to be broad and this results in a limited specificity.

In this paper we report on the application of the TRES method in evaluating the properties of Magurele city tap water and some commercial, bottled water from different natural springs in Romania. An example of acquired time resolved fluorescence spectra for a sample of drinking water is reported in Fig. 1.

The presence of some pollutants (e.g. dissolved organic matter – DOM, disinfection by-products – DBPs etc.) leaves a specific fluorescence signature, thus allowing for their identification in water. In addition, increased analytical power can be obtained by measuring both wavelength and lifetime of fluorescent emission. The apparatus employed for the present experimental work was a custom made

PicoQuant – Fluorescent Lifetime System. Excitation source was a xenon flashlamp emitting 400 ns broad flashes at up to 300 Hz repetition rate.

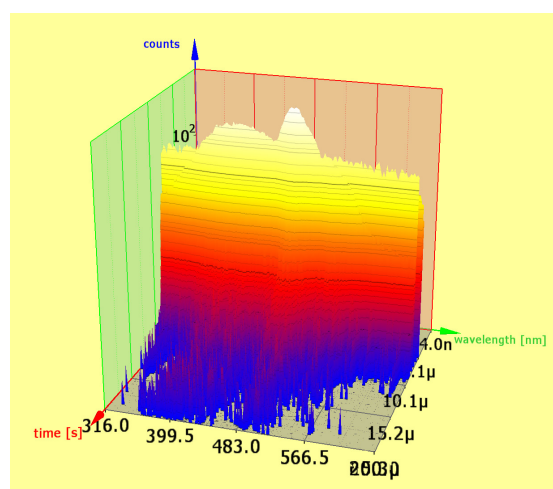


Fig. 1 Example of a 3D plot of time-resolved fluorescence spectra obtained from a commercial, bottled water sample excited at 295 nm.

References

- [1] U. Wachsmuth, M. Niederkrüger, G. Marowsky, N. Konradt, and H.-P. Rohns, Monitoring of Dissolved Organic Carbon (DOC) in a Water Treatment Process by UV-Laser Induced Fluorescence, *Advanced Environmental Monitoring*, Y.J. Kim and U. Platt (eds.), Springer 2008, p. 282-294.
- [2] Kl.-H Mittenzwey, R. Reuter, Correlations between COD, DOC, UV₂₅₄ and fluorescence of inland waters measured in the laboratory, *EARSeL Advances in Remote Sensing*, Vol. 3, No. 3 – VII, 1995, p. 57-65.
- [3] R. Niessner, W. Robers and A. Krupp, A new analytical concept: remote laser-induced and time-resolved fluorescence (LIF) of PAH's in aerosols or water, *Fresenius' Journal of Analytical Chemistry*, Vol. 333, No. 7, 1989, p. 708-709.

Ceilometer validation *via* satellite measurements

R. C. Radulescu^{1,2}, Ioana Ungureanu¹ and Sabina Stefan¹

¹University of Bucharest, Faculty of Physics, P.O.BOX MG-11, Bucharest, Romania

²National Research and Development of Optoelectronics, INOE2000, 409 Atomistilor Street, Magurele, Ilfov, Romania

Keywords: clouds, ceilometer, satellite

The ceilometer Vaisala CL31 (Figure 1), a mini-lidar installed at Faculty of Physics (Magurele, 44.35N;26.03E) was used for making continuous observations of the clouds and atmospheric boundary layer (ABL).



Figure 1. Ceilometer CL-31

The aim of this work is to validate the ceilometer's data. The validation of the ceilometer's data involved the comparison of the ceilometer's measurements with satellite data. Therefore, we processed both the Ceilometer's retrievals with Lab-View software and as for the satellite images we used MODIS because of its higher spatial resolution. In the satellite case, the algorithm determines the height of the clouds using the atmospheric standard model after the type of pixel has been determined (through use of neural networks). Two data sets from 2010, in the case of the representative months for winter (January) and for summer (July) were analysed.

In Figure 2, one can observe three cloud types in an image obtained from the ceilometer for 24 hours on 14.01.2010 and on 10.07.2010. For the same day, satellite images confirm the cloud cover over Magurele. The frequency of appearance of different types of clouds in winter has shown small differences between satellite data and the ceilometer's data (not shown here).

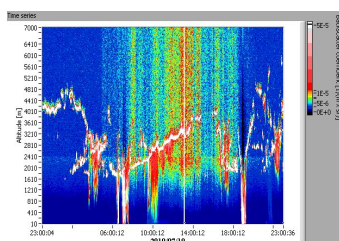
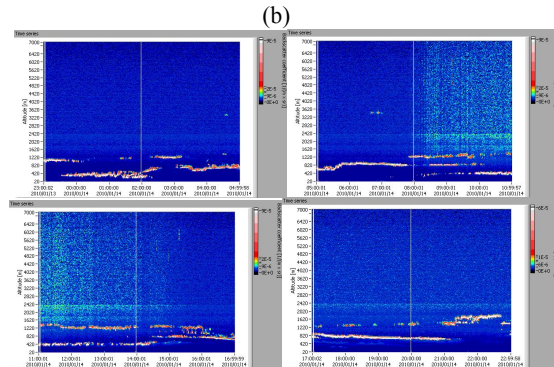


Figure 2. A 24-h period of ceilometer's echo intensity observations at 10 July 2010 (a) and 14 January 2010 (b)



The cloud albedo was also used for comparison. The clouds' albedo was determined, using satellite products and computed using the ceilometer's data for winter's days. The comparisons between the cloud's albedo obtained from the two types of data are represented in Figure 3.

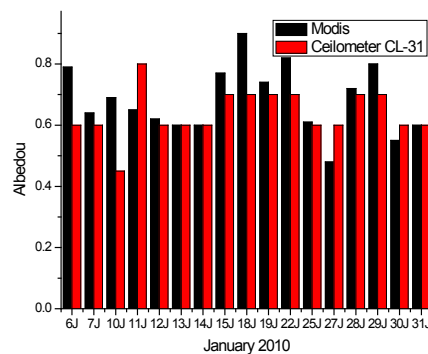


Figure 3. Comparison between the satellite and ceilometer's cloud albedo data

Selected references

1. S. Stefan, G. Iorga, Effects of aerosol on the optical properties of clouds, Proceedings of the 14th International Conference on Clouds and Precipitation, Bologna, Italy, 18-23 July, 2004 pp
2. Iorga G., S. Stefan, Romanian Reports in Physics, vol 57, No 3, 383-393 (2005)
3. Menzel, Frey, Baum, 2010: Cloud Top Properties and Cloud Phase - Algorithm Theoretical Basis Document
4. <http://modis-atmos.gsfc.nasa.gov/>

Acknowledgements

This work was supported by grant no. STVES 115266 from Norway through the Norwegian Cooperation Programme for Economic Growth and Sustainable Development in Romania.

Excimer Laser Micromachining of PMMA

Vasile Sava¹, Sorin Stanescu², Mircea Udrea³

¹University of Bucharest, Faculty of Physics, Bucharest, Romania

²„Politehnica” University of Bucharest, Biomedical Engineering Centre

³ NIPLR (National Institute for Laser, Plasma and Radiation Physics), Bucharest, Romania

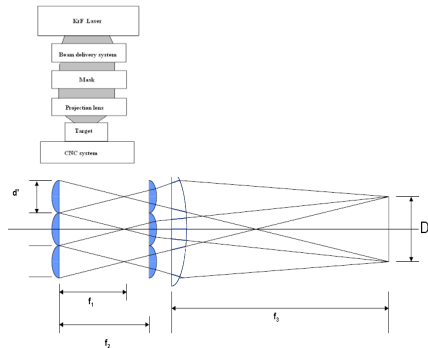
Keywords: excimer laser, PMMA, MEMS manufacturing, optical systems.

ABSTRACT

This paper describes the experimental results in micro-machining of PMMA which were performed by using a 248 nm excimer laser, beam homogenizers, mask image, and a projection lens. The optical system is composed by two beam homogenizers of different focal lengths, a condenser lens that takes and reshapes the laser beam, the field lens that collimates the beam, the mask that defines the image and the projection lens. The aim of this study is to optimize the machining of PMMA – (Polymethyl methacrylate) with excimer laser in order to get an accurate processing. Some devices which were manufactured are presented.

Experimental setup:

Here are presented some results of laser micro machining with a excimer laser Compex 205 and an optical system for reshaping the laser beam, a mask and a plano-convex projection lens. The tests were performed using a fluency between $0,7\text{J}/\text{cm}^2$ and $2\text{J}/\text{cm}^2$ with a total number of shots between 100 and 550.



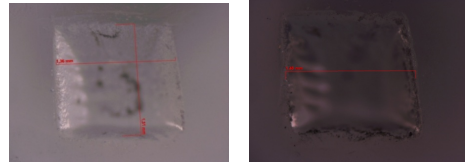
Pic. 1 The schematics of the optical system used

Results:

We made several tests varying the energy, total pulse number and measuring the angle between the channel wall and target surface, the increasing of the channel width at the entrance and at the bottom for different energy fluency.



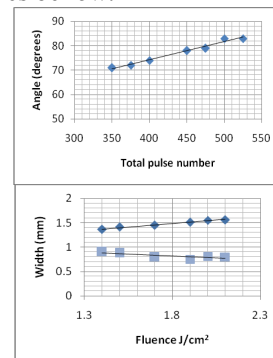
Pic.2 Some result of total pulse number influence for angle between channel wall and entrance surface. The tests were made for a fixed fluency of $2\text{J}/\text{cm}^2$, 3Hz and a total number of pulses between 300 and 550.



Pic.3 Results of energy fluence over the size of laser spot at the surface target of PMMA. The tests were made with a repetition rate of 1Hz, the same total pulse number and a fluency between $1,2\text{J}/\text{cm}^2$ and $2,5\text{J}/\text{cm}^2$

Discussions:

The influence of the total pulse number over the quality of the channel for a fixed fluency and frequency and the influence of the laser fluency over the width variation of the channel can be seen in the graphics below:



a) b)

Pic.4 a) Evolution of the angle between channel wall angle and surface entrance b) the evolution of the upside and bottom side channel width with the laser fluency

Other results:

Using the results obtained above we made some other tests, one of them was to make a small wheel device in PMMA and other to drill channels, 2 cm long. This was made by using a wheel mask (Pic.5a) and a circular mask for drilling the channels (Pic.5b), using the same optical system.



a.) b) Pic.5 a,b) The results of cutting a photovoltaic cell point by point with a circular mask and a slot mask c) wheel made directly with the mask

References:

[1] S. Kiipcr, M. Stuke, Appl. Phys. A **49**, 211 (1989).

Nanoparticles obtained in liquid medium with Nd:YAG laser

Cristian Udrea, Victor Damian, Ileana Apostol

National Institute for Laser, Plasma and Radiation Physics, Magurele, 077125, Bucuresti, Romania
Department of Lasers, Magurele, 077125, Bucuresti, Romania

Keywords: Nd:YAG laser, nanoparticles, laser ablation

Intense pulsed laser has been used to obtain nano-scale materials from bulk metals of interest (in this case, aluminum). The physical process used in the following case, for producing nanoparticles, is laser ablation in liquid environment.

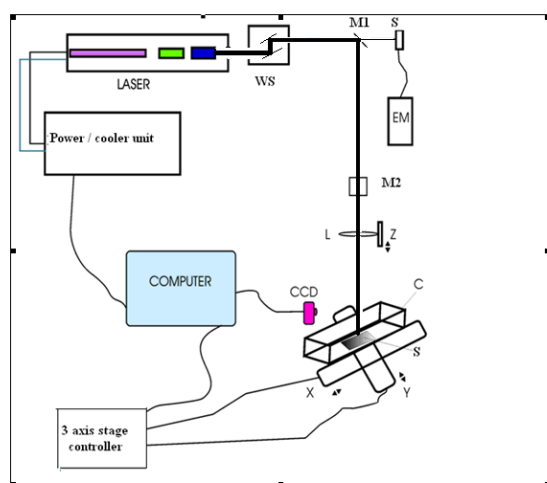


Figure 1. Experimental setup for nanoparticles production (Laser: Nd:YAG; WS: wavelength selector; M1,M2: mirrors; S: energy meter sensor; EM: energy meter; L: lens; C: cuvette fill with water, S: aluminum sample)

The laser source used for ablation is a Nd:YAG (Continuum Surelite II), with operational wavelength, in this case, of 355 nm (third harmonic). The laser pulse is directed over the probe with two mirrors (M1 and M2) and focused with a 250 mm focal length lens L (Fig. 1).

We have analyzed the main parameters which influence the nanoparticles production and process reproducibility related with the morphology of the laser ablated surface.

Laser ablated surface was microscopically analyzed after each sequence or irradiation pulses. The surface morphology and crater profile permitted us to select the best irradiation conditions for laser-surface coupling. Also permitted us to evidence that the stability and reproducibility of the irradiation conditions is important for the reproducibility of the obtained nanoparticles diameter distribution.

We have monitored the laser energy, with the energy meter (EM), which passes through M1 mirror in order to analyze the laser emission stability

(which is 4 %) and also the laser energy incident on the target surface.

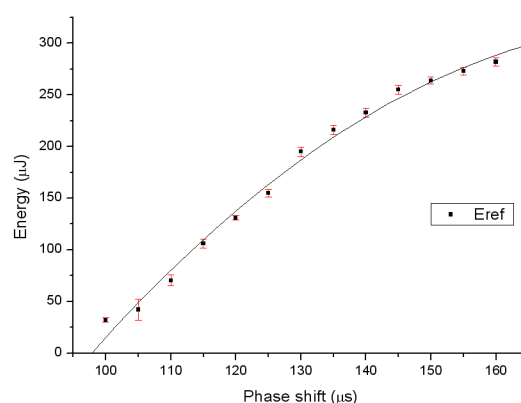


Figure 2. Energy stability of the Surelite II laser at the wavelength of 355 nm

In the figure 2 we have represented the energy from EM with respect to phase shift (time delay between flash lamp trigger and Pockels cell)

The research regarding determination of the laser fluence and intensity in order to obtain nanoparticles from laser ablation in liquid medium was realized on aluminum targets. The liquid medium, in our case, is pure water.

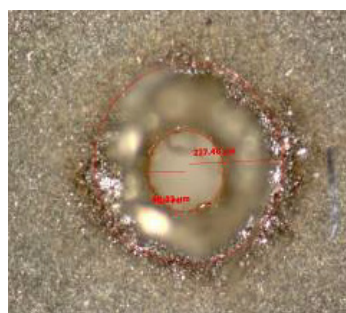


Figure 3. Microscope image of a crater situated on the aluminum target surface

The microscope image of the irradiation crater for ablation of the aluminium sample surface is given in Fig. 3. The irradiation conditions were: incident energy of 26.5 mJ, corresponding to a fluence of 20.8 J/cm², and 180 pulses. The crater radius was 227 μm, and a depth of 18 μm.

Synchronous detection technique for optical transmission imaging of biological objects

Karen Vardanyan, Anna Khachaturova, Sargis Varzhapetyan, Anahit Badalyan, Svetlana Shmavonyan, and
Aram Papoyan

Institute for Physical Research, NAS of Armenia, Ashtarak-2, 0203 Armenia
vardanyankaren@gmail.com

We present technique and initial results of optical screening and imaging of highly scattering and/or absorbing media, including biological objects. The method relies on scanning a weak modulated laser beam across the tested object followed by highly-sensitive lock-in detection, PC-acquisition and data processing. Modulation of laser beam amplitude is synchronized with

computer-controlled scanning step and subsequent synchronous detection followed by online data processing allowing to enhance the spatial resolution and significantly reduce the overall variation of the transmitted signal. The preliminary studies have shown principal applicability of the suggested technique for medical diagnostics, biology, quality control and homeland security.

VCSEL in Interferometry: a Comparison to Edge Emitting Diode Lasers Regarding their Applicability in Speckle-Interferometry

Bodendorfer, Thomas¹, Heßke Andre¹, Koch, Alexander W.¹

¹Institute for Measurement Systems and Sensor Technology, Technische Universität München, Theresienstraße 90/N5, 80333, Munich Germany

Keywords: VCSEL, Speckle-Interferometry.

Speckle-Interferometry (SI) is a powerful tool for fast, robust and noncontact measurements of deformation (Koch et al., 1998), vibration (Løkberg & Høgmoen, 1976), roughness (Goodman, 1975) or shape (Purde et al., 2005). One of the key components in SI is the used light source (Bodendorfer & Koch, 2010). There are different requirements for the light source: (1) the emitted light has to be highly coherent; (2) the output power has to be above a certain limit to guarantee a good illumination of the specimen depending on the used camera chip; (3) the beam profile has to be as homogeneous as possible; (4) the light source has to feature a high wavelength stability.

Typical light sources in SI are gas lasers (e.g. argon ion laser, helium neon laser, etc.), which meet all of the named requirements. Due to large size, temperature control and high costs these types of laser can often not be used as an illumination source.

Standard edge emitting diode lasers are a smaller and cheaper alternative, although they cannot satisfy all named requirements as good as gas lasers. This often leads to a decrease of resolution, due to low intensity, poor beam quality or instability in wavelength.

Vertical cavity surface emitting lasers (VCSEL, see Figure 1) are a promising light source for SI: they are small, have a homogeneous beam profile and a low wavelength dependency on temperature. Furthermore, the operation current is very low compared to standard diode lasers (< 10 mA).



Figure 1. Picture of a red (670 nm) single mode VCSEL.

VCSELs are often used as pumping lasers or in applications like spectroscopy (Affolderbach et al., 1999).

To our knowledge there has not been an investigation about the potential of VCSELs for Speckle-Interferometry. Here VCSELs could be an alternative to diode lasers due to good beam quality, large coherence length and high wavelength stability.

VCSELs are commercially available in the visible and infrared range of spectrum of light. In both cases they can be produced as single element or as an array of individual VCSELs.

Next to a general comparison of edge emitting diode lasers and VCSELs, measurements using both are shown in this work. The results are compared with respect to resolution, stability and complexity. In conclusion we provide an estimate under which circumstances VCSELs may be preferred over edge emitting laser diodes in SI.

Koch, A.W., Rupprecht, M.W., Toedter, O., Gäusler, G., *Optische Meßtechnik an technischen Oberflächen*, 1998, 102, ISBN 3816913725

Løkberg, O., Høgmoen, K., *Vibration phase mapping using electronic speckle pattern interferometry*, *Applied Optics*, 1976, 2701

Goodman, J., *Dependence of Image Speckle Contrast on Surface Roughness*, *Optical Communications*, 1975, volume 14, 324

Purde, A., Werth, N., Meixner, A., Koch, A.W., *ESPI for contouring of surfaces with discontinuities*, *Proceedings of SPIE*, 2005, volume 5856, 525

Bodendorfer, T., Koch, A.W., *Resolution limit of Mach-Zehnder two-wavelength phase-shifting speckle interferometer*, *Proceedings of SPIE*, 2010, volume 7387

Affolderbach, C., Nagel, A., Knappe, S., Jung, C., Wiedenmann, D., Wynands, R., *Nonlinear spectroscopy with a vertical-cavity surface-emitting laser (VCSEL)*, *Applied Physics B: Lasers and Optics*, 1999, volume 70, 407

Radiation induced changes in Fiber Bragg Grating under gamma-ray irradiation

Dan Sporea¹, Andrei Stancalie¹, Daniel Negut², Adriana Puiu¹, Adelina Sporea¹

¹ Department of Laser Metrology, National Institute for Laser, Plasma & Radiation Physics, Atomistilor 409, Magurele, P.O.Box MG-36, 077125 ROMANIA

² Horia Hulubei National Institute of Physics and Nuclear Engineering, Atomistilor 407, Magurele, P.O. Box MG-6, 077125 ROMANIA

Keywords: fibre Bragg grating sensors, ultrafast optics, high temperature sensors.

Fibre Bragg Gratings (FBG) are widely used in many optical systems as band filters, dispersion compensators, in-fibre sensors or fibre grating lasers and amplifiers (Othonos, 1997, and references herein). It was also already pointed out (Krebber et al., 2006) their sensitivity to radiation exposure. The principle of fibre grating is in core refractive index modulation. The Bragg grating resonance, which is the centre wavelength of light back reflected from a Bragg grating, depends on the effective index of refraction of the core and the periodicity of the grating. A shift in the Bragg wavelength (BWS) due to thermal expansion changes the index of refraction. When FBGs are used as radiation sensors the most obvious and best-known effect is an increase of fibre attenuation. Since the radiation-induced attenuation strongly depends on the wavelength of the transmitted light, the FBG dosimeter sensitivity to temperature is usual measured by the shift of the Bragg wavelength with temperature. This shift can be used to calculate the corresponding refractive index changes. The paper presents results from a series of experimentally investigations on FBG dependence of temperature and Gamma radiation dose. All the experiments were conducted in a comparatively manner, using two FBGs, one providing the standard indication. Before using, the fibres were carefully cleaned and calibrated with the aid of Memmert Oven system. They were subject of a number of heating cycles in the range of 20-60 Celsius degrees.

The influence of gamma ray dose on the changes in Bragg wavelength shift was carefully monitored. The response of the irradiated fibres have been recorded and analyzed with respect to the wavelength Bragg shift, the signal to noise ratio and the full transmission spectrum. Finally, these data, collected from a series of experiments, can be used when comparing with the initial measurements, to test the FBG's history, i.e. the Fibre Bragg Gratings can recover after Gamma-ray irradiation or the effect is permanent. After exposure to Gamma-ray radiation with the measurement of the BWS, the fibre is heated. The changes in measured Bragg peak shift during heating cycles gives an indication of the fibre sensitivity to the radiation dose.

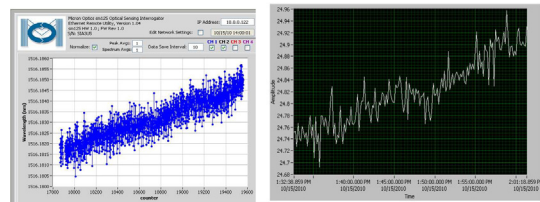


Fig.1. Time dependence of the BWS (left) corresponding to time dependence of the temperature (right).

The FBG spectra are characterized on-line in transmission, during irradiation or heating. The spectra were recorded using SM125 Optical Sensing Interrogator of Type Micron OpticsX25, that operates very stably (based on Fabry-Perrot interferometer) and achieves very high wavelength resolution. Irradiation with different dose rates was made at a ⁶⁰Co γ -source by varying the distance between the source and FBG. The signal averaging time during the irradiation was limited so that the dose error can be estimated.

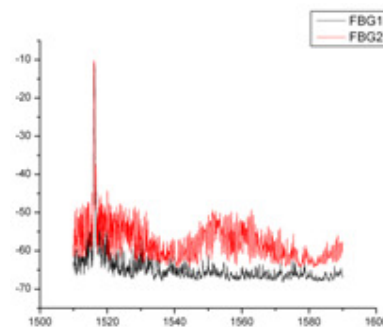


Fig2 The response of the irradiated sensor compared with the second one out of irradiation range.

References Krebber, K., Henschel, H., Weinand, U., "Fibre Bragg gratings as high dose radiation sensors?" *Meas. Sci. Technol.* **17**(2006) 1095-1102. Othonos, A., "Fibre Bragg gratings" *Rev. Sci. Instrum.* **68** (1997) 4309 -4341.

Upconversion luminescence of langanite powders doped with erbium and ytterbium

Voiculescu Ana-Maria¹, Georgescu Serban¹, Matei Cristina¹, Toma Octavian¹,
Nastase Silviu¹, Birjega Ruxandra¹

¹ National Institute for Laser, Plasma and Radiation Physics, 409 Atomistilor Street,
Magurele, Jud. Ilfov, 077125, Romania

Keywords: upconversion, langanite, sol-gel method, Er³⁺, Yb³⁺.

The use of upconversion materials for efficient conversion of infrared radiation into visible light presents a great interest. This phenomenon has applications in several areas, such as upconversion lasing, fluorescent labels for biological samples, two-photon fluorescence imaging, etc. The phenomenon of upconversion is also useful for the detection of infrared radiation by changing it to the visible range, where detectors are more efficient. Among the multitude of upconversion mechanisms, excited-state absorption (ESA) and energy transfer are the most efficient upconversion processes. Yb-Er, Yb-Tm and Yb-Ho are the usual rare-earth pairs for efficient upconversion. Er³⁺ ion is an ideal candidate for this purpose due to its many resonances between its energy levels. Codoping of Yb³⁺ as a sensitizer can yield a substantial improvement in upconversion efficiency due to the efficient energy transfer between the sensitizer and the emitter.

In this paper we present preliminary data concerning synthesis and characterization of Er, Yb-doped langanite-LGT obtained by solid-phase reaction. The intensity of the upconversion-pumped luminescence (transitions $^4S_{3/2} \rightarrow ^4I_{15/2}$, $^4F_{9/2} \rightarrow ^4I_{15/2}$) recommends this material as a potential upconversion phosphor.

The crystals from the langanite family are partially disordered. That may promote energy transfer processes.

Using solid phase synthesis, LGT powder doped with Yb³⁺ and LGT powder doped with Yb³⁺ and Er³⁺ were obtained. In preparation we used stoichiometric formulas $(La_{0.97}Yb_{0.03})_3Ga_{5.5}Ta_{0.5}O_{14}$ and $(La_{0.96}Yb_{0.03}Er_{0.01})_3Ga_{5.5}Ta_{0.5}O_{14}$ with the following oxides as raw materials: La₂O₃, Ga₂O₃, Ta₂O₅, and Er₂O₃, Yb₂O₃. The mixture was homogenized by grinding and heated in air at 1350°C for 36 hours.

These materials were characterized by X-ray diffraction and optical spectroscopy (absorption, diffuse reflectance and luminescence).

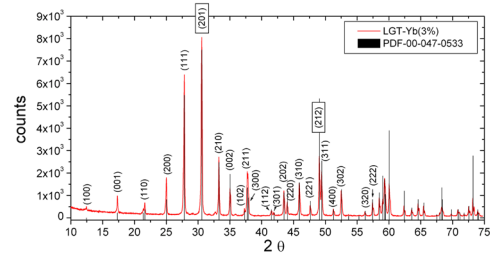


Fig. 1. XRD pattern of the LGT:Yb (3%) sample.

In the XRD pattern of the LGT:Yb (3%) sample, only the diffraction lines of the LGT phase were observed (Fig. 1).

The diffuse reflectance spectra of Yb³⁺ in LGT (transformed with Kubelka-Munk equation) were compared with the absorption spectrum obtained for LGT diluted with KBr powder, achieving comparable results. Absorption spectrum of Yb³⁺ in LGT is wide, from this point of view, the material is suitable for upconversion-pumped phosphor.

The Er³⁺ emission spectrum was obtained for the pumping of Yb³⁺ at 936 nm.

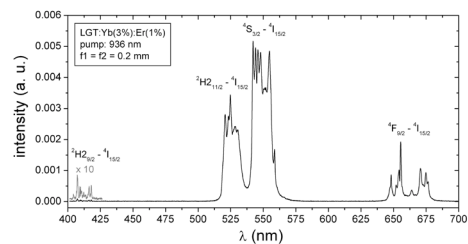


Fig. 2. Luminescence spectrum of LGT:Yb (3%): Er (1%) pumped at 936 nm.

Surface Nano-metrology

Roughness: a new paradigm

Mihaela BOJAN, Iuliana IORDACHE, Florin GAROI, Dan APOSTOL

Roughness can be measured with angstrom sensitivity for many years. (See Tolansky S, Microstructure of surface using interferometry, Ed. Eduard Arnold, London, 1968). Connected to nanometrology (metrology for nano science and nano technology) the roughness paradigm must be changed. Referring to Fig 1. , the three axis define the geometry of a macroscopic system (lateral dimensions or 2D, axial or normal to the surface z, and finally the roughness dimension R_a)

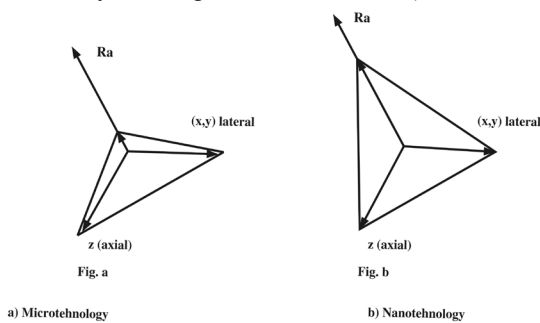


Fig.1

For the macroscopic systems lateral and axial dimensions are very large as compared to roughness (Fig.1a). At nano scale objects the roughness could be comparable with the other geometrical dimensions (Fig.1b). To understand this statement and the necessity of a new paradigm see Fig2.

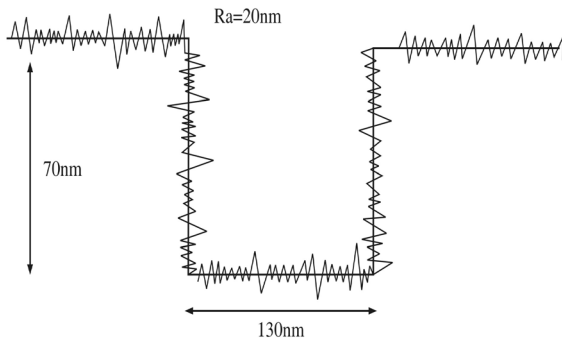
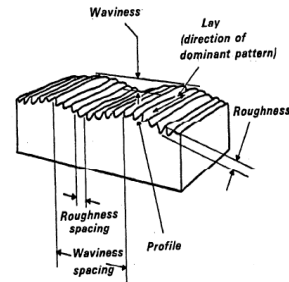


Fig.2 Step-height measurement.

The ideal inspection technique for surface roughness measurement (indeed, for measurements of almost any parameter) would be truly contactless, objective, reproducible, and ideally assess the full necessary area, at least, a statistically significant fraction of it.

The stylus instruments are the most popular between scientists!

A force measuring instrument (Atomic Force Microscope) is used to investigate the roughness at nanometric scale.

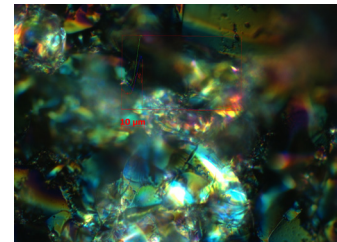


Waviness Lay Roughness

Paradigm means instruments and measuring technology:

Instruments:

- Stylus
- White light interferometry (Zygo, Wyko,)
- Lateral shear interferometry (Zeiss microscopy)
- AFM
- Confocal
- SNOM
- Digital holography
- Scattering
- DIC microscopy
- TIC microscopy



Viscosity Measurement of Synthetic Oils by means of Laser Induced Fluorescence

Wiesent, Benjamin R.¹, Dorigo, Daniel G.¹, Jülich, Florian¹, Şimşek, Özlem¹, and Koch, Alexander W.¹

¹Institute for Measurement Systems and Sensor Technology, Technische Universität München, Theresienstr. 90 / N5, D-80333, Munich

Keywords: oil analysis, laser induced fluorescence, viscosity,

The viscosity of lubricants is one of the most important properties. This parameter has to be adopted to the specific operation conditions where the lubricant is used. Pure oils can be divided into mineral and synthetic oils. Especially for high quality applications synthetic oils are more and more accepted despite of their higher price.

During the hydrocracking step at the lube refining process, crude oils are converted to more desirable species (Pirro & Wessol, 2001). During this process the viscosity of the synthetic lubricant is adjusted by the length of its hydrocarbon chains. The most common unit for kinematic viscosity is reported in centistokes (cSt) or as SI unit square millimetres per second (mm²/s) (Cresham & Totten, 2009). The viscosity of oil is temperature dependent. Therefore, the viscosity of oil is generally given at two temperatures, 40 °C and 100 °C.

We used laser induced fluorescence (LIF) with deep UV excitation and a fiber optic probe to measure viscosity levels of fresh oil samples. Three types of synthetic oils each with seven different viscosity levels in the range of 32 to 320 cSt were measured. The used setup is illustrated in Figure 1.

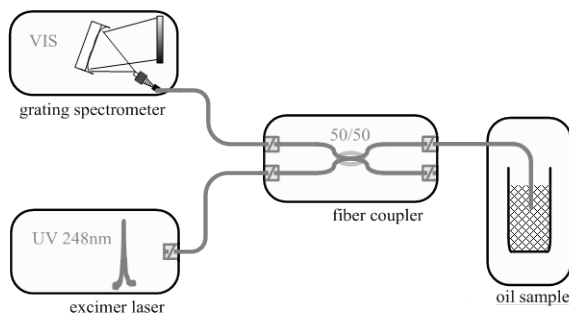


Figure 1.: Measurement setup.

An excimer laser at 248 nm wavelength was coupled to a 200 µm core diameter low-OH fiber. The excitation light propagates via a 3 dB coupler and a measurement probe into the oil sample. The deep UV excitation induces fluorescence directly in front of the fiber tip. This characteristic fluorescence spectrum is captured by the same fiber tip probe and guided back to the VIS grating spectrometer where it is interrogated. This setup allows a quick sample handling and a simple cleaning process for the reusable probe. Compared to methods based on IR-spectroscopy a much lower instrumentation and handling effort was achieved.

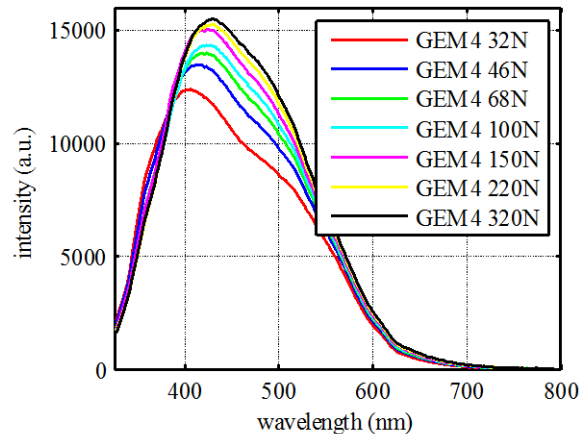


Figure 2.: Fluorescence of synthetic oil Klüber Gem 4 at different viscosity levels.

As an example we illustrate in Figure 2 the measured fluorescence signal of the seven different viscosity steps of the synthetic gear oil Klüber GEM 4.

The different viscosities can be distinguished by their fluorescence intensities between 400 and 500 nm. All three oils were measured and their fluorescence spectra show characteristic features which allow a clear classification of the fresh oil viscosity levels. This setup can also be constructed very cost effective using a deep UV 250 nm LED and a low resolution VIS grating spectrometer. Also in-situ measurement of oil viscosity gets possible by this setup.

Cresham, R. M., & Totten, G. E. (2009). *Lubrication & Maintenance of Industrial Machinery*. (R. M. Cresham & G. E. Totten, Eds.) New York: CRC Press Taylor & Francis Group.

Pirro, D. M., & Wessol, A. A. (2001). *Lubrication fundamentals* (2nd ed.). New York: Marcel Dekker Inc.

Biocompatible thin films grown on Ti_6Al_4V substrates by PLD

Ana-Maria Niculescu^{1,2}

¹Politehnica University of Bucharest, Faculty of Material Engineering and Science, 313 Splaiul Independentei, section JA, RO-060042, Bucharest, Romania

²INFPLR - National Institute for Laser, Plasma and Radiation Physics, Department of lasers, 409 Atomistilor st., Magurele RO-077125, Bucharest, Romania

Keywords: thin films, PLD, prosthetics.

This paper presents some data obtained during the deposition and analysis of biocompatible thin films on Ti alloy by pulsed laser deposition (PLD).

The deposited samples were thermally processed for six hours at 400 °C, in water vapor atmosphere, after which were investigated by X-ray diffraction (XRD), scanning electron microscopy (SEM), and atomic force microscopy (AFM). These investigations revealed that structural and crystalline characteristics of the sample (substrate and thin film) improved after the thermal treatment.

XRD analysis on the thin films shown a hexagonal structure; the lattice indexes were determined, and a mean value of 38 nm was identified for the crystalline grain.

SEM and AFM images of the samples surface identified small cracks after the thermal treatment of the sample; the presence of different sized droplets was also evidenced at the surface of the samples, prior and after the thermal treatment.

In agreement with data available in the literature, such a biocompatible coating improves the proliferation speed of cells and, thus bringing an improvement to the quality of the sedimentation, and to the prosthetic quality of the sample.

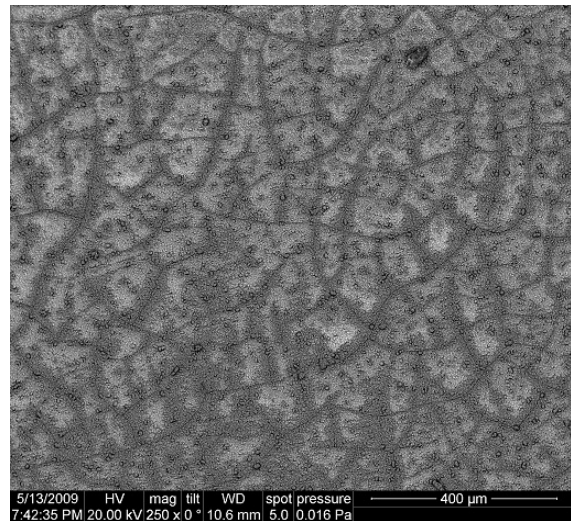


Figure 1. SEM image of a biocompatible thin film deposited by PLD on Ti_6Al_4V .

Books: R.W. Eason, Pulsed Laser Deposition of Thin Films, John Wiley & Sons, New York, 2007;

Journals: J. Schou, "Physical aspects of the pulsed laser deposition technique: The stoichiometric transfer of material from target to film", Applied Surface Science 255 (2009) 5191–5198.

Methods to generate compound micro- and nano-droplets individually or at large scale

Viorel Nastasa¹, Reinhart Miller², Vincent Pradines², Thodoris Karapanthios³, Kostas Samaras³,
Mihai Lucian Pascu¹

¹National Institute for Laser, Plasma and Radiation Physics, Laser Department, Magurele, Ilfov, Bucharest, Romania.

²Max Planck Institute for Colloids and Interfaces, Potsdam Germany

³Department of Chemistry, Aristotle University of Thessaloniki, Greece

Keywords: micro-droplets, nano-droplets, emulsions, DST, Vancomycin, Vitamin A

There is currently significant interest in fighting the multiple resistance to treatment (MDR) using drugs, developed by bacteria and malignant tumors. One of the alternatives to the existing medicines and treatment procedures in fighting MDR is strengthening the effects of cytostatics by improving their delivery methods. Such a method is represented by the generation, transport and use of micro/nano-droplets which contain medicines. This approach can reduce the medicines consumption by generating micro-droplets which contain drugs incorporated in solvents substances; the micro-/nano-droplets can favor a faster delivery to the targets and a higher drug concentration in them.

This paper reports first, results concerning the generation of single micro-droplets containing an inner core (medicine solution in water) and a thin layer of oily liquid covering it. We have generated and measured stratified micro-droplets, each of them containing a solution of Vancomycin in ultrapure water as a core and a surrounding layer of Vitamin A in sunflower oil; the micro-droplets generation was made using a double capillary system.

Secondly, micro-/nano-droplets were produced by mixing two immiscible solutions in particular conditions (high rotating speed and/or high pressure difference). For this we have studied the generation of emulsions of vitamin A diluted in sunflower oil and a solution of Tween 80 surfactant in distilled water. The concentration of surfactant in water was, typically, $4 \cdot 10^{-5}$ M. We have studied the dependence of the droplets dimensions in emulsion on the mixing rotation speed, agitation time and components ratio.

The droplets diameters were measured using a light scattering method. It is found that at appreciably high energy input (high rotation speed, large pressure drop) and relatively small oil/water ratio, droplets diameters smaller than 100 nm were obtained.

Emulsions are the dispersions of an immiscible or partially miscible liquid (dispersed phase) in

another liquid (continuous phase). These liquids are immiscible or are mutually only slightly soluble. The dispersed phase is present in the form of droplets in the continuous phase. Usually, in order to stabilize the dispersed phase against coalescence, the presence of a surfactant is essential as the droplets are thermodynamically metastable. An emulsion is characterized by the mean size and the size distribution of the droplets, characteristics that can be controlled by a proper choice of the dispersing apparatus and the process conditions [1].

Interest in nano/submicron droplets dimensions in emulsions recently increased in the pharmaceutical, cosmetic and food domains, in parallel with the development of more performing emulsification technologies. Droplets with diameters lower than 1 μ m can be used as transport vectors of medicines for therapeutic applications such as parenteral, oral, ophthalmic or transdermal delivery systems. They allow that substances poorly soluble in water- but oil-soluble, such as vitamins or drugs to be incorporated in a lipophilic phase, so that the increase of their local bioavailability takes place; this also stabilizes components sensitive to enzymatic degradation, allows a slower, controlled release of components to the targets over a prolonged period of time and reduces the side effects of drugs. Based on small particles use in systemic treatments, one predicts that micro/nano-emulsions uptake improves efficiency of lipophilic substances.

References:

[1] V. Nastasaa, K. Samaras, I.R. Andrei, M.L. Pascu, T. Karapantsios "Study of the formation of micro and nano-droplets containing immiscible solutions" Colloids and Surfaces A: Physicochem. Eng. Aspects 382 (2011) 246–250

Experimental analysis of chaotic coupling of two lasers with external optical feedback

Andrei, Ionut-Relu¹, Ticos, Catalin-Mihai¹, Popescu, George Viorel¹, Bulinski, Mircea² and Pascu, Mihail-Lucian^{1,2}

¹ National Institute for Laser, Plasma and Radiation Physics, Department of Lasers, str. Atomistilor 409, 077125, Magurele, Romania

² University of Bucharest, Faculty of Physics, str. Atomistilor 405, 077125, Magurele, Romania

Keywords: laser diode, optical feedback, chaos synchronization

A semiconductor laser (SL) displays chaotic behavior when subjected to optical feedback from an external reflector. This configuration is known as external-cavity semiconductor laser (ECSL). One of the most intensely studied issues on the chaotic dynamics of ECSL is the regime of low-frequency fluctuations (LFF), manifested as a cyclic dropout almost to zero of the output light intensity evidenced when a typical ECSL with weak optical feedback operates slightly above the lasing threshold.

Coupling of two chaotic lasers can result in total synchronization of their nonlinear output and has shown great promise in achieving secure communications encoded with chaos between these types of optical systems. Different configurations, such as delayed optoelectronic feedback or coherent optical injection have been suggested for the synchronization of two semiconductor lasers. The coupling between the lasers is accomplished in a unidirectional or bidirectional fashion, leading to different kinds of synchronization phenomena.

In the present work we aimed to experimentally evaluate the synchronization quality of two semiconductor lasers emitting in visible in conditions of optical feedback provided of unselective external reflectors, such as mirrors. The synchronization quality is analyzed with respect to the different experimental conditions, such as injection current, laser temperature, and external cavity length.

The experimental setup used is schematically shown in Figure 1.

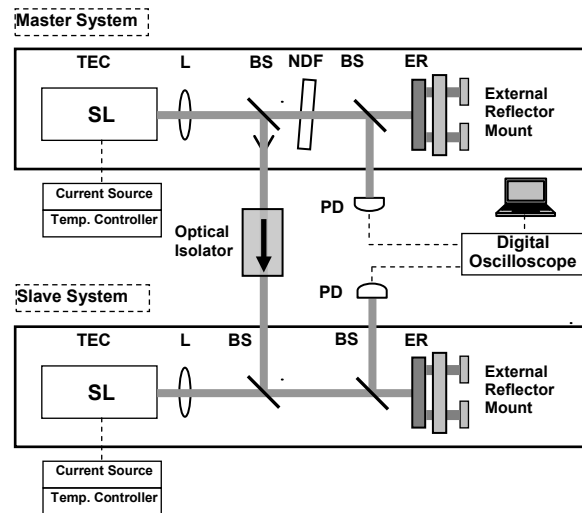


Figure 1. Experimental setup of two coupled chaotic lasers (master and slave systems): TEC, SL mount with thermo-electric cooler; L, collimation system; BS, beamsplitter; NDF, neutral density filter; ER, external optical reflector; PD, photo-detector; the external cavity length is around of 30 cm.

Acknowledgments. This work was supported by the National Centre for the Management of Programs (CNMP) under contract no. 72-219 within the PNCDI2 program and by the National Authority for Scientific Research (ANCS) under contract Nucleu-LAPLAS 2010.

References: Vincente R, Mirasso C R and Fischer I, *Opt. Lett.* 32 403 (2007).

Y. Takiguchi, Y. Liu, and J. Ohtsubo, *Opt. Lett.* 23, 1369 (1998).

E. Klein, R. Mislovaty, I. Kanter, and W. Kinzel, *Phys. Rev. E* 72, 016214 (2005).

Einat Klein and all, *Phys. Rev. E* 73, 066214 (2006)

Comparison of the experimental techniques used to obtain foams out of medicines solutions

Smarandache, Adriana¹, Nastasa, Viorel¹, Militaru, Andra¹, Staicu, Angela¹, Trelles, Mario², Moreno-Moraga, Javier³, Pascu, Mihail-Lucian¹

¹Department of Lasers, National Institute for Lasers, Plasma and Radiation Physics, Magurele, Romania

²Instituto Médico Vilafortuny/Fundacion Antoni de Gimbernat, Cambrils, Spain

³Instituto Medico Laser, Madrid, Spain

Keywords: pharmaceuticals, foam generation, drops, laser, Raman spectroscopy.

Several foam production technologies have been developed in recent years with the aim of enhancing and/or facilitating topical drug delivery. Our study is focused on the following two classes: drug-specific topical foams and new methods for foam generation.

The reissue of an active agent already marketed in the liquid form as a topical foam is signalled for Polidocanol, the active agent in the commercially drug Aetoxisclerol. This is one efficient medicine in the sclerotherapy of small veins. Clinical observations proved that foam sclerotherapy is preferable to the use of the liquid sclerosing substances. Detergent-like sclerosing agents can be transformed into a fine-bubbled foam by special techniques, named after those who used these methods for the first time: Monfreux, Tessari, Sadoun, Frullini etc.

Clinical experimental results prove that the exposure of tissues impregnated with foaming Polidocanol to laser radiation emitted at 1.06 μm improves the efficiency of the treatment (M. Trelles & al., 2005).

Previous absorption studies on Aetoxisclerol solution (A. Smarandache & al., 2010) before and after Nd:YAG 1.06 μm laser irradiation have not shown important spectral modifications of it. We supposed that the clinical positive results are mainly due to photoinduced processes of the primary photoacceptors. The effect of the laser light may be enhanced if the Polidocanol is introduced as foam since then the light scattering in the tissue becomes more important and the overall absorption of the laser beam becomes larger. It is important to investigate the scattering involved in the laser irradiation process of Polidocanol foam samples.

Using the Tessari method (two disposable syringes connected to a three-way stopcock) we produced foam by mixing Aetoxisclerol 2% solution and atmospheric air; the mixture ratio was 1:4. This batch is passed between the two syringes about 40 times. The resulting foam is stable for 5-6 min.

A 10 mm optical cell containing foam sample was introduced into a Raman spectroscopy system. The laser radiation used to excite the Raman emission is the second harmonic of a pulsed Nd:YAG laser (Continuum, Excel Technology), model

Surelite II with 10Hz frequency, 6ns pulse duration and 350 mJ energy at 532 nm. The detection (Princeton Instruments & Acton Research) is made by a spectrograph (Spectra PRO 750, Acton Research) and ICCD camera (Princeton Instruments). The obtained Raman spectra are discussed.

Concerning the new methods for foam generation, in recent works, pulsed laser submicron foam formation has been demonstrated (S. Gaspard & al., 2007). This process has been observed, indeed, during an irradiation session made on droplets of Vancomicine HCl in our lab. We used an experimental set-up for droplet irradiation consists of a tunable laser source (Panther EX OPO SURELITE pumped with a Nd:YAG Laser, range 410 – 710 nm), a droplets generator (Microlab ML500C Hamilton), an investigation system (Ocean Optics Spectrometer - range 250 – 1100nm, optical resolution 0.02 nm, integration time 3.8 ms; FASTCAM 1024PCI Photron – max. frame rate 120000 fps) and a number of optical components (Neutral filters, Telescope, Lenses, Digital Shutter System 845HP Newport). We investigated the behavior of Vancomycin HCl drops whose volume was 10 μl . The sample was exposed to 266 nm wavelength laser radiation, with 3.6 mJ beam energy. The recorded LIF spectra indicate a decrease with the irradiation time. The appearance of small bubbles was detected. They are discussed the mechanisms involved in this behavior.

References:

1. M. A. Trelles, I. Allones, X. Alvarez, M. Vélez, C. Buill, R. Luna, O. Trelles, Medical Laser Application 20, 255 (2005).
2. A. Smarandache & al., Measurement of the modification of Polidocanol absorption spectra after exposure to NIR laser radiation, JOAM, 12 (2010), 1942-1945;
3. S. Gaspard & al., Submicron foaming in gelatine by nanosecond and femtosecond pulsed laser irradiation, Applied Surface Science 253 (2007), 6420-6424.

Acknowledgements: This research was supported by: ANCS, project LAPLAS 3-PN 09 33 and COST Action BM0701 (ATENS).

Optical properties for the biocompatible polymers obtained by matrix assisted pulsed laser deposition (MAPLE)

Valentin Ion¹, Irina Alexandra Paun², Antoniu Moldovan¹, Anca Nedelcea¹ and Maria Dinescu¹

¹National Institute for Laser, Plasma and Radiation Physics, RO-077125, Magurele, Bucharest, Romania

²Faculty of Applied Sciences, University Politehnica of Bucharest, RO-060042, Romania

Keywords: spectroscopic ellipsometry, biocompatible polymers, MAPLE

In recent years, the use of biocompatible polymers for medical applications has been extensively investigated. In particular, films of biocompatible polymers (like Polyethylene glycol (PEG) and Poly (lactide-co-glycolide) (PLGA)) offer promising perspectives for controlled drug delivery implants. When these implants are designed for intraocular applications, the wavelength dependence of the optical constants of the polymeric films is of critical importance for their proper functionality. Despite the relevance of the issue, reports on the optical characteristics of polymeric films are limited. In this work, we use spectroscopic ellipsometry (SE) for determining the optical properties of PEG and PLGA growth as thin films by matrix assisted pulsed laser evaporation (MAPLE). The dependences of the optical properties of the films on the characteristics of the two polymers under study are discussed. Furthermore, the obtained results are validated by two independent techniques (atomic force microscopy and UV-Vis spectrophotometry) [3,4].

Measurements were performed in the (400–800) nm spectral range, at angles of incidence 60° and 70° . The optical model consisted of 4 layers: a Si substrate, a SiO₂ layer, a polymer layer and a rough layer. The latter takes into account the roughness of the surfaces, being composed by polymeric material and air [1]. The values for the bulk dielectric functions of Si and SiO₂ substrates were obtained from literature [2]. For determining the optical properties and the thickness of the films, a standard fitting procedure, consisting of two steps, was performed. In the first step, the experimental data were fitted in the (600–800) nm spectral range. In this range the films are non-absorbing, as indicated by ultraviolet-visible (UV-vis) spectro-photometry; in consequence, the Cauchy model was used for the fit. From the fitting, the films thicknesses were obtained. Subsequently, the thicknesses were fixed and the fitting was extended to the whole measured spectral range (fig 1). As a result, the preliminary optical constants were obtained [3]. Next, for obtaining the final values of the optical constants of the films (refractive indices and extinction coefficients), a second step was performed. The whole measured spectral range was fitted with oscillators, using the thicknesses and the preliminary optical constants determined in the first step. We tried different fitting procedures, the best fit being

obtained with two Gaussian oscillators [4]. This is probably due to the fact that our films consist of two different materials/polymers.

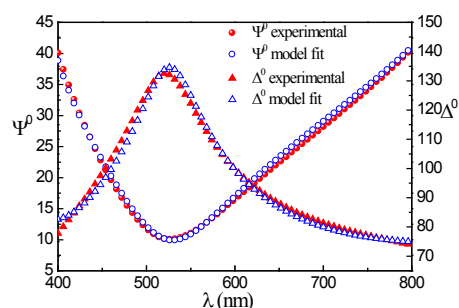


Fig 1. Comparison between fit predictions and experimental measurements.

In all, our findings indicate spectroscopic ellipsometry as suitable technique for determining the optical properties for thin films of biocompatible polymers deposited by MAPLE.

Acknowledgements

This work was supported by CNCIS-UEFISCSU, project number PN II-RU code PD 146/2010 financing contract number 140/09.08.2010 and by the project e-LFT 73 EU/2010

Bibliography:

- [1] H. Fujiwara, Spectroscopic Ellipsometry Principles and Applications, Maruzen Co. Ltd., Tokyo, Japan, 2007.
- [2] C.M. Herzinger, B. Johs, W.A. McGahan, J.A. Woollam, W. Paulson, Ellipsometric determination of optical constants for silicon and thermally grown silicon dioxide via a multi-sample, multi-wavelength, multi-angle investigation, J. Appl. Phys. 83 (615) (1998) 3323–3336.
- [3] Irina Alexandra Paun, Valentin Ion, Antoniu Moldovan, and Maria Dinescu, Thin films of polymer blends for controlled drug delivery deposited by matrix-assisted pulsed laser evaporation, APPLIED PHYSICS LETTERS 96, 243702 (2010).
- [4] Irina Alexandra Paun, Valentin Ion, Antoniu Moldovan, Maria Dinescu, Thin films of polymer blends deposited by matrix-assisted pulsed laser evaporation: Effects of blending ratios, Applied Surface Science, Volume 257, Issue 12, 1 April 2011, Pages 5259-5264.

Participants list

Achim	Alexandru	alexandru.achim@inflpr.ro	Romania
Achim	Cristina Mihaela	cristina.achim@inflpr.ro	Romania
Aleksandrov	Veselin	ahearer_@abv.bg	Bulgaria
Alexandru	Zorila	alexandru.zorila@inflpr.ro	Romania
Andrei	Ionut -Relu	ionut.andrei@inflpr.ro	Romania
Banita	Stefan George	banita.stefan@inflpr.ro	Romania
Bojan	Mihaela Eleonora	mihaela.bojan@inflpr.ro	Romania
Boni	Mihai	mihai.boni@inflpr.ro	Romania
Boscornea	Andreea	boscornea.a@gmail.com	Romania
Bratu	Ana-Maria	ana.magureanu@inflpr.ro	Romania
Budriga	Olimpia	olimpia.budriga@inflpr.ro	Romania
Chitu	Catalin	catalinchitumail@yahoo.com	Romania
Chuchumishev	Danail Vladimirov	danail.ch@gmail.com	Bulgaria
Dorigo	Daniel	d.dorigo@tum.de	Germany
Fazacas	Andreea	antifoton@gmail.com	Romania
Goldner-Constantinescu	Catalin-Daniel	catalin@nipne.ro	Romania
Heßke	Andre	a.hesske@tum.de	Germany
Ion	Valentin	valentin.ion@inflpr.ro	Romania
Iulia	Anghel	iulia.anghel@inflpr.ro	Romania
Jipa	Florin Cosmin	florin.jipa@inflpr.ro	Romania
Kamil	Kamil	tatuško@gmail.com	Poland
Karnowski	Karol	karnow@fizyka.umk.pl	Poland
Kolenderska	Sylwia	sylwkol@wp.pl	Poland

Kraszewski	Maciej	kraszewski.maciej@gmail.com	Poland
Manta	Ovidiu	ovidiu.manta@inflpr.ro	Romania Republic of
Mantashyan	Paytsar	paytsar.mantashyan@gmail.com	Armenia
Matei	Consuela Elena	consuela.matei@inflpr.ro	Romania
Matei	Cristina	cristina.matei@inflpr.ro	Romania
Mihailescu	Andreea	andreea.mihailescu@inflpr.ro	Romania
Militaru	Andra Cristina	andra.militaru@inflpr.ro	Romania
Narcis-Sorin	Cernescu	narcis.cernescu@inflpr.ro	Romania
Nastasa	Viorel	viorel.nastasa@inflpr.ro	Romania
Neagu	Liviu	liviu.neagu@inflpr	Romania
Niculescu	Ana Maria	ani.niculescu@yahoo.com	Romania
Nistorescu	Alexandru Ion	alexnistorescu@yahoo.com	Romania
Oreshkov	Bozhidar	b.oreshkov@gmail.com	Bulgaria
Păiuș	Diana-Petronela	diana_paius@yahoo.com	Romania
Patachia	Mihai Virgil	mihai.patachia@inflpr.ro	Romania
Petrus	Mioara	mioara.petrus@inflpr.ro	Romania
Popescu	Silviu Teodor	silviutpopescu@gmail.com	Romania
Puiu	Adriana	adriana.puiu@inflpr.ro	Romania
Radu	Catalina	catalina.radu@inflpr.ro	Romania
Rădulescu	Răzvan-Cosmin	razvan@inoe.inoe.ro	Romania
Rusen	Laurentiu Nicolae	laurentiu.rusen@inflpr.ro	Romania
Salamu	Gabriela	gabriela.salamu@inflpr.ro	Romania
Sava	Vasile	sava_vas@yahoo.com	Romania
Stancalie	Andrei Octavian	andrei.stancalie@inflpr.ro	Romania
Stancu	Radu Florin	radu_florin_stancu@yahoo.com	Romania

Udrea	Cristian	cristian.udrea@inflpr.ro	Romania
Ungurenu	Georgian Razvan	razvan.ungurenu@inflpr.ro	Romania
Vardanyan	Karen	Vardanyankaren@gmail.com	Armenia
Voiculescu	Ana-Maria	ana.voiculescu@inflpr.ro	Romania
Wiesent	Benjamin Reinhard	b.wiesent@tum.de	Germany